The Dissertation Committee for Michael August Chirillo certifies that this is the approved version of the following dissertation:

Coordinated Structural Plasticity across Synapses in the Adult Hippocampus

Committee:

Kristen M. Harris, Supervisor

Mark F. Bear

Laura L. Colgin

Nace L. Golding

Kimberly F. Raab-Graham

Coordinated Structural Plasticity across Synapses in the Adult Hippocampus

by

Michael August Chirillo, B.Music; M.Music

Dissertation

Presented to the Faculty of the Graduate School of

The University of Texas at Austin

in Partial Fulfillment

of the Requirements

for the Degree of

Doctor of Philosophy

The University of Texas at Austin

May, 2015

Dedication

To Jennifer N. Bourne and Mikayla S. Waters,

because they filled my experience as a doctoral student with laughter.

Coordinated Structural Plasticity across Synapses in the Adult Hippocampus

Michael August Chirillo, Ph.D.

The University of Texas at Austin, 2015

Supervisor: Kristen M. Harris

Neural circuitry is determined primarily by trillions of synaptic junctions that link cells in the nervous system. Understanding how the structure of the synapse influences its function has been a central goal of cellular neuroscience since synapses were first recognized more than a century ago. Long-term potentiation (LTP), a long lasting enhancement of synaptic efficacy, is a well-characterized cellular correlate of learning and memory that results in dramatic structural remodeling of the synapse. Research has focused heavily on the postsynaptic structural remodeling that occurs to support LTP, but concomitant presynaptic and subcellular remodeling during LTP has been left largely unexplored. To address these questions, three-dimensional reconstructions from serial section electron microscopy of presynaptic boutons, vesicle pools, and dendritic smooth endoplasmic reticulum (SER) in hippocampal area CA1 were created and quantified. The data presented in this dissertation demonstrate that coordinated structural plasticity occurs at both pre- and postsynaptic sides of adult hippocampal synapses by 2 hours during LTP induced with theta burst stimulation. Presynaptically, the number of presynaptic boutons correlated perfectly with fewer dendritic spines during LTP that were previously reported,

suggesting that synaptic units act as cohesive structures. Vesicle pools were mobilized and vesicle transport packets were moved into boutons or were released in transit. Dendritic SER is a ubiquitous intracellular membranous network involved in calcium signaling and protein modification. The complexity of SER influences the movement of diffusible membrane cargo. SER was dramatically remodeled during LTP, redistributing from the shaft of the dendrite into spines and becoming highly complex near synapses that were largest during LTP. As a preliminary investigation into how normal mechanisms of structural plasticity described in this dissertation might go awry under conditions of synaptic pathology, three-dimensional reconstructions of CA1 synaptic ultrastructure in a mouse model of Fragile X, which is known to express exaggerated mGluR-dependent long-term depression (LTD), were created and quantified. Synaptic ultrastructure was similar with that of the wild-type mouse, suggesting that structural malformation in FX might be confined to development or to other brain regions.

Table of Contents

Chapter 1: Introduction

The transfer of information in the nervous system occurs primarily across microscopic junctions between neurons called synapses. Synapses are not static structures of the nervous system landscape; they can be created and eliminated, strengthened and weakened. This flexible nature of the synapse is known as synaptic plasticity. Plastic changes at the synapse influence the transfer of information from one neuron to the next and can lead to the modification of large-scale neural circuits. As such, synaptic plasticity is intensely investigated as a cellular mechanism underlying learning and memory. Understanding how the structure of the synapse influences its function and how this might go awry during pathology has therefore been a central goal of cellular neuroscience since the infancy of the field.

One form of synaptic plasticity known as long-term potentiation (LTP) induces dramatic structural remodeling of synapses (Bosch and Hayashi, 2012; Bourne and Harris, 2007; 2008; Meyer et al., 2014; Yuste and Bonhoeffer, 2001). One region of the brain implicated in learning and memory is the hippocampus (Jeneson and Squire, 2012; Morris et al., 2003; Morris, 2007; Preston and Eichenbaum, 2013) and an investigation into the underlying subcellular and synaptic remodeling associated with LTP in the adult hippocampus forms the majority of this work. Before delving into the studies presented in this dissertation, I consider the anatomy of the synapses in question, early studies on synaptic plasticity, the distinct nature of plasticity in the adult animal, and the behavioral relevance of the topic.

1.1 Anatomical Considerations

The Hippocampus and Area CA1

In rodents, the hippocampus is a large, C-shaped structure lying deep to the neocortex. It stretches rostrodorsally from septal nuclei, around the thalamus, and caudoventrally into the temporal lobe. Relative to humans, the hippocampus in rodents makes up a large percentage of total brain volume. This makes it fairly easy to access the region experimentally. Additionally, the hippocampus has a relatively simple and highly organized laminar structure, which has encouraged its use as a model system researchers use to study the structure and function of synapses (Amaral and Lavenex, 2007). Consensus on what anatomically constitutes the hippocampus is, however, hardly universal. More broadly the term *hippocampal formation* has been used to signify an area of the brain that is composed of five main parts: the dentate gyrus, area CA3, area CA1, the subiculum, and the entorhinal cortex. For this dissertation, the term *hippocampus* refers specifically to the structure including the dentate gyrus, area CA3, area CA1, and the subiculum.

Santiago Ramón y Cajal noted early on that the vast majority of hippocampal input arrives from the entorhinal cortex. Entorhinal efferents form connections on molecular layer dendrites of dentate gyrus granule cells. These entorhinal efferents make up the famous perforant path as they course through ("perforate") the subiculum and fissure of the hippocampus. Dentate gyrus granule cells send unmyelinated axons (mossy fibers) distally to form synapses with proximal CA3 pyramidal cell dendrites in a layer of CA3 called stratum lucidum (*lucidum*, as the unmyelinated axons appear translucent in the sectioned hippocampus). CA3 pyramidal cells then send axons to form connections with

pyramidal cells in area CA1. This so-called "trisynaptic circuit" (entorhinal cortex → dentate gyrus → CA3 → CA1) was highlighted early on when researchers believed the majority of hippocampal output was directed to subcortical regions of the brain (Andersen et al., 1971). It is now know that most hippocampal output is directed back to the entorhinal cortex. CA1-entorhinal cortex connections close a large hippocampal processing loop (**Fig. 1.1**). Multimodal information from higher order cortical areas is projected to the entorhinal cortex, which relays that information into the loop. That information is integrated and processed in the hippocampus and the output is returned to the entorhinal cortex. The entorhinal cortex projects the processed information back to higher order cortical areas (Schultz and Engelhardt, 2014).

The connections between and within the subfields of the hippocampus are themselves more complex than the trisynaptic circuit would lead one to believe. For example, area CA1 forms a variety of connections within and beyond the hippocampal formation[1]. Area CA1 has a neatly structured lamellar organization and its connections are spatially restricted (**Fig. 1.2**). The principal cells of area CA1 are pyramidal cells, which line up in a layer known as the pyramidal cell layer. These cells send axons to synapse with subicular and entorhinal cortical cells. In fact, area CA1 is the dominant hippocampal subfield projecting to the entorhinal cortex (Naber et al., 2001). The basilar dendrites of CA1 pyramidal cells project into stratum oriens and apical dendrites project into stratum

---

[1] CA1 receives a number of neuromodulatory inputs such as cholinergic inputs from the septum, noradrenergic inputs from locus coeruleus, serotonergic inputs from raphae nuclei, and dopaminergic inputs from ventral tagmental area. A vast community of researchers is keen on investigating how these inputs modulate the activity of CA1 pyramidal cells.
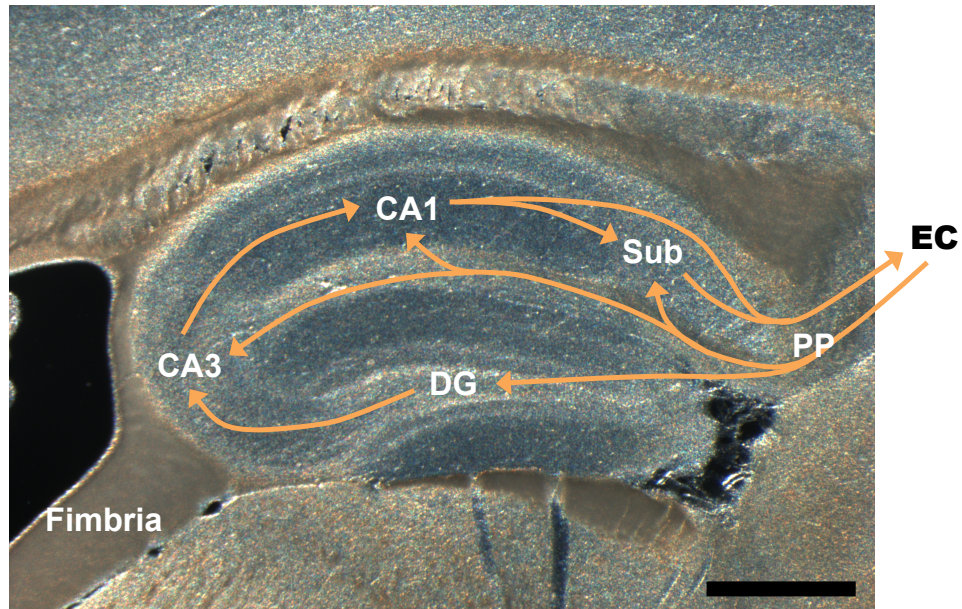
Figure 1.1: The hippocampal processing loop. 70-µm thick transverse section through the middle of an adult mouse hippocampus. A schematized diagram of information flow with the entorhinal cortex (EC) is superimposed. Information from the EC is passed into the hippocampus via the perforant path (PP) to the dentate gyrus (DG), which relays that information to area CA3. Area CA3 passes that information to area CA1, which is the predominant hippocampal output back to the EC. CA1 also projects to the subiculum (Sub), which itself also sends output to the EC. The EC also sends direct inputs to areas CA1 and CA3 via perforant path fibers coursing through stratum lacunosum-moleculare. The synapses investigated in this dissertation are those made by CA3 pyramidal cell axons with CA1 pyramidal cell dendrites in CA1 stratum radiatum (see Fig. 1.2). Scale bar = 0.5 mm.
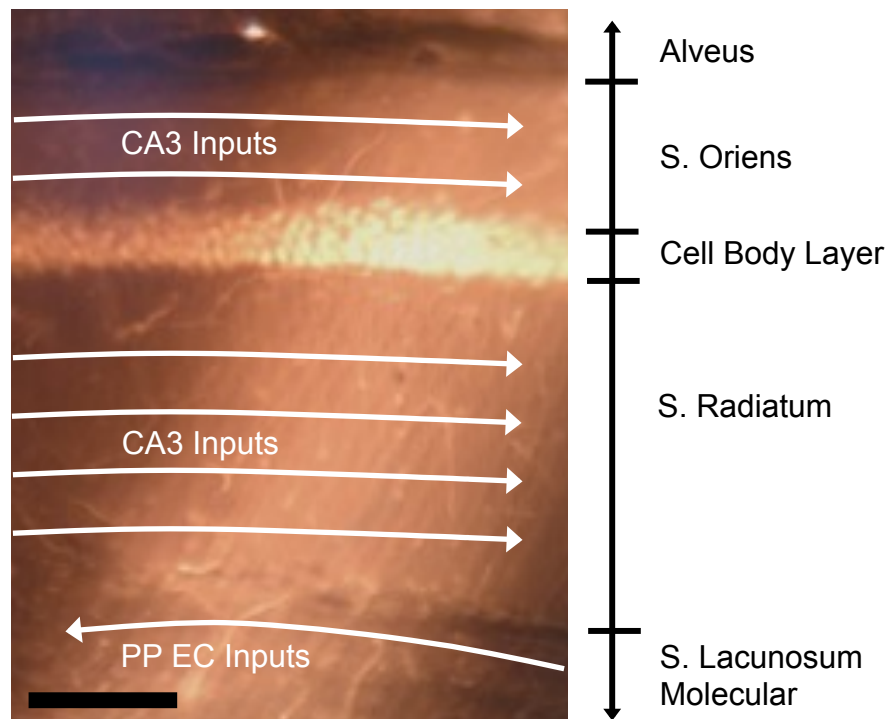
Figure 1.2: Hippocampal area CA1 of an adult mouse. Area CA1 in a 70-µm thick transverse hippocampal section from an adult mouse embedded in epoxy resin reveals the various layers of this hippocampal subfield. The cell bodies of CA1 pyramidal cells line up in a layer known at the cell body layer, which appears translucent in transverse hippocampal slices. These cells project dendrites into stratum oriens, radiatum, and lacunosum moleculare. CA1 pyramidal cells receive direct entorhinal (EC) inputs on their distal most dendrites via perforant path (PP) fibers in stratum lacunosum moleculare and indirect entorhinal inputs from area CA3 in stratum radiatum and stratum oriens. The structure of CA3-CA1 synaptic connections in stratum radiatum is investigated in this work. Scale bar = 100 µm.

radiatum. Radial oblique branches from the apical dendrite create an elaborate dendritic arbor in stratum radiatum. Furthermore, the dentate gyrus is not the only subfield of the hippocampus to receive direct entorhinal inputs. A distally located apical tuft of dendritic branches reaches into stratum lacunosum moleculare, where incoming entorhinal connections are formed. Thus, CA1 cells receive both direct and indirect (via dentate gyrus and CA3) input from the entorhinal cortex. Ipsilateral and contralateral CA3 pyramidal cells send axons that form synapses with CA1 dendrites in stratum oriens and stratum radiatum. Axons from ipsilateral CA3 pyramidal cells are known as Schaffer collaterals[2], while those from contralateral CA3 pyramidal cells are simple known as commissural fibers. Thus, *Schaffer collateral-commissural fibers* is a more appropriate term when referring to axons coursing through stratum radiatum of CA1. The synapses these fibers make with CA1 pyramidal cell dendrites are the focus of this dissertation and, in favor of a more anatomical description, will be referred to simply as CA3-CA1 synapses.

Synaptic Structure

By the end of the nineteenth-century, several leading anatomists, including Ramón y Cajal, had rejected the notion of direct "protoplasmic" continuity between neurons, a theory championed most notably by Camillo Golgi. The debate between "neuron" and "reticular" theories of neuroanatomy would not be definitively settled, however, until after the advent of the electron microscope (Harris and Weinberg, 2012). First developed in Germany in the 1930s by Ernst Ruska and Max Knoll, electron microscopy (EM) allows visualization of structures

---

[2] These collaterals are named after the Hungarian neuroanatomist Károly Schaffer.

whose size falls well below the resolution of conventional light microscopy. With an electron microscope, anatomists could, for the first time, "see" synapses. Thanks in large part to the contributions of Keith Porter and George Palade (both of whom will reappear later in this dissertation), the first high-quality EM images of neuronal tissue and first descriptions of synapses appeared in the 1950s (De Robertis and Bennett, 1955; Palay, 1956; Palay and Palade, 1955). We now know the synapses they saw can be either chemical or electrical depending on their mode of signal transduction. Electrical synapses form direct connections between neurons via gap junctions, which allow propagation of electrical signals from one neuron to the next. Chemical synapses, on the other hand, require an intermediate chemical signal between pre- and postsynaptic neurons. At chemical synapses, an electrical signal from the presynaptic neuron is converted to a chemical signal. This chemical intermediate is passed to the postsynaptic neuron and reconverted into an electrical signal. The focus of this dissertation is on the plasticity of axodendritic chemical synapses in stratum radiatum of hippocampal area CA1. Chemical synapses will from this point on be referred to simply as synapses.

A synapse is formed at the close apposition of plasma membranes of two discrete cells[3] (**Fig. 1.3**). The majority of excitatory synaptic connections in the central nervous system form between a presynaptic terminal (or bouton) and the head of short, roughly 1-µm long dendritic protrusions known as dendritic spines

---

[3] Even though synaptic junctions typify neural tissue, non-traditional synapses occur between non-neuronal cells as well. Most famously, the immunological synapse is a transient synapse formed between T lymphocytes and antigen-presenting target cells (Grakoui et al., 1999). Ongoing investigations into immunological synapses promise to generate findings that might illuminate the function of their more rostral cousins in the central nervous system (Dustin, 2012; Dustin and Colman, 2002).
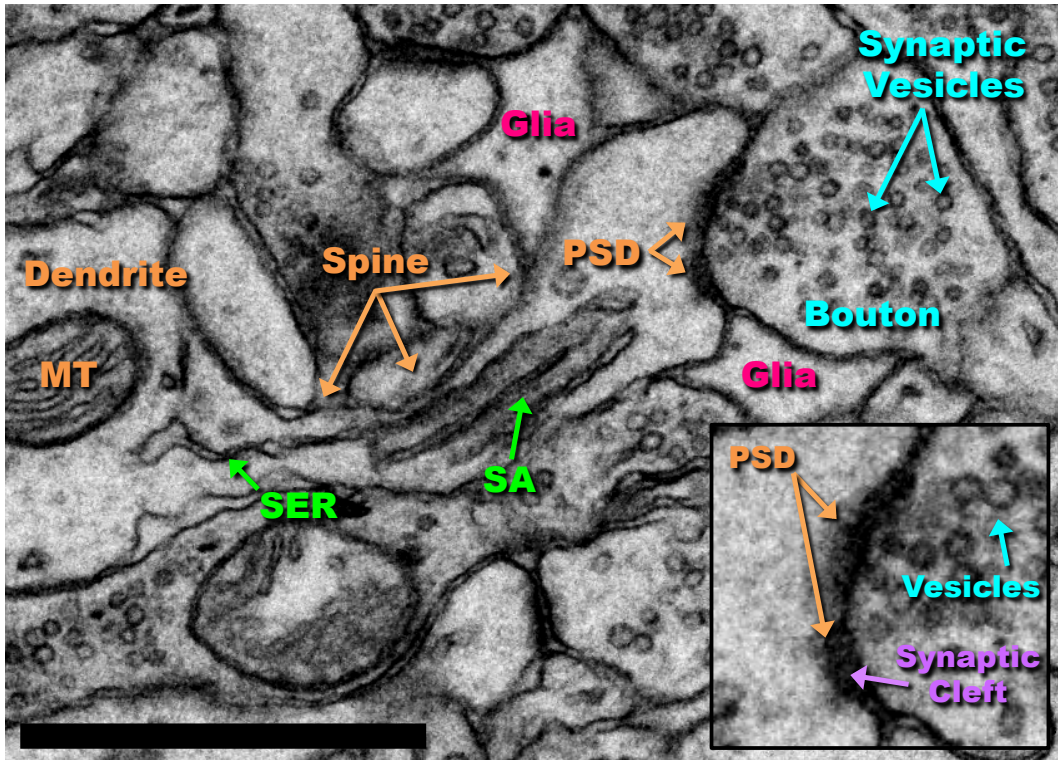
Figure 1.3: CA3-CA1 synapse in an adult rat. Example electron micrograph of an excitatory CA3-CA1 synapse in stratum radiatum of hippocampal area CA1 fixed in vivo from a 77-day-old adult rat. Inset shows magnified view of the synapse. The dendritic shaft can be seen on the left with a cross-sectioned mitochondrion (MT). Smooth endoplasmic reticulum (SER) can be seen entering the base of a large dendritic spine and forming an elaborate spine apparatus (SA), fold of SER stacked between densely staining material. The post-synaptic density (PSD) is a thickening along the postsynaptic membrane of the synapse where receptor, signaling, and scaffolding proteins congregate. The synaptic cleft is almost completely obscured by densely staining proteinaceous material. In the presynaptic bouton, pools of vesicles are readily visible. At this particular synapse, glia, identifiable by its relatively clear cytoplasm, comes into contact with both pre- and postsynaptic compartments. Scale bar = 1 μm.

(Harris and Kater, 1994). Dendritic spines can host a number of organelles, most notably polyribosomes, the cell's protein synthesis machinery, and smooth endoplasmic reticulum (SER), a membranous network that extends through the majority of the cell. (For more on SER, see Chapter 3.) In CA1 stratum radiatum, swellings along unmyelinated axons known as boutons (i.e., en passant boutons) originate predominately from CA3 pyramidal cells. These boutons host tens to hundreds of small synaptic vesicles, which are each ~35-55 nm in diameter, electron lucent on EM sections, and contain non-peptide neurotransmitters. At excitatory synapses (which are investigated in this dissertation), these vesicles primarily carry the neurotransmitter glutamate (Ottersen and Storm-Mathisen, 1984; Somogyi et al., 1986; Storm-Mathisen et al., 1983). Vesicles are docked along a specialized region of the presynaptic plasma membrane known as the "active zone". At the active zone, vesicles are primed for release upon arrival of an action potential (Landis et al., 1988; Phillips et al., 2001; Sudhof, 1995). Vesicles that are not docked along the plasma membrane make up the "reserve" pool of vesicles. (For more on presynaptic boutons and vesicles, see Chapter 2.)

Upon fusion of the vesicle with the presynaptic membrane, glutamate is released into the synaptic cleft, a ~20 nm-wide space[4] between the pre- and postsynaptic neuron. Glutamate diffuses across the cleft, where it binds to and activates postsynaptic glutamate receptors: the ionotropic glutamate receptors, AMPA (α-amino-3-hydroxy-5-methyl-4-isoxazolepropionic acid) and NMDA (*N*-Methyl-D-aspartate) receptors, and metabotropic glutamate receptors (mGluRs).

---

[4] This "space" is, in fact, not a space at all. The synaptic cleft is filled with extracellular proteins as well as unique synaptic proteins (Dityatev et al., 2010). Cryo-electron microscopy reveals a densely staining, complex web of material that fills the cleft (Lucić et al., 2005; Zuber et al., 2005).

These receptors congregate in the postsynaptic density (PSD), an electron dense thickening along the postsynaptic membrane. Whereas the number of NMDA receptors in the PSD is fairly constant from synapse to synapse, the number of AMPA receptors directly correlates with the size of the PSD (Nusser et al., 1998). Furthermore, the size of the PSD is perfectly correlated with the size of the active zone (Lisman and Harris, 1993). Thus, synaptic size has been used as an anatomical marker of synaptic strength. The PSD contains a host of scaffolding proteins, such as PSD95, Homer, and Shank, and a variety of signaling molecules, such as CaMKII (calcium/calmodulin-dependent protein kinase II), Ras, Rho, and other small GTPases, all of which seem arranged in a very organized manner (Chen et al., 2008b). Activation of glutamate receptors in the PSD leads to a net influx of positive ions into the postsynaptic compartment. This depolarization (excitatory postsynaptic potential [EPSP]) propagates with varying strength along the dendrite. Summation of synaptic potentials in the soma influences the firing of the cell. As explored below, inside the dendritic spine itself, the local depolarization generated by the synaptic potential can affect a variety of cellular processes that influence the function of the synapse.

1.2 Synaptic Plasticity

Early LTP/LTD Studies

Investigations into how memories are encoded in the brain have greatly enhanced our understanding of synaptic structure and function. In his 1949 book *The Organization of Behavior*, Canadian psychologist Donald O. Hebb proposed that learning and memory was encoded in the brain by a strengthening of synapses (Hebb, 1949). Experimental evidence supporting this hypothesis

would not come until decades later, when Tim Bliss and Terje Lømo demonstrated that repetition of brief, high-frequency stimulation of perforant path inputs resulted in a long-lasting increase in the efficacy of dentate gyrus granule cell synapses in rabbits (Bliss and Lomo, 1973). This phenomenon came to be known as LTP (after a brief stint as "long-lasting potentiation" or LLP). After the introduction of the acute hippocampal slice preparation (Skrede and Westgaard, 1971), LTP was shown to occur at both dentate gyrus-CA3 synapses and CA3-CA1 synapses (Schwartzkroin and Wester, 1975). Subsequent studies have shown that this form of synaptic strengthening is expressed not only at hippocampal synapses but throughout the brain (Bliss et al., 2007) and that LTP truly lives up to its moniker, lasting for weeks or even months in non-anesthetized animals (Abraham, 2003; Abraham et al., 2002).

Several molecular mechanisms underlying LTP induction were worked out in the 1980s, beginning with the finding that the specific NMDA receptor blocker D-AP5 (D-2-amino-5-phosphonopentanoic acid, also known as AP5 or APV) blocks the induction of LTP in area CA1 (Collingridge et al., 1983). Furthermore, LTP induction was also blocked by injection of calcium chelators into CA1 pyramidal cells (Lynch et al., 1983; Malenka et al., 1988). These two findings were fused together when researchers looked more closely at NMDA receptors. Curiously, these receptors were found to be both ligand- and voltage-gated. Several groups uncovered evidence of a magnesium block, which sits in the NMDA receptor pore. Sufficient depolarization is required to relieve the channel of this block (Ault et al., 1980; Mayer et al., 1984; Nowak et al., 1984). Subsequent studies showed postsynaptic depolarization can result from back-propagating action potentials (Debanne et al., 1998; Magee and Johnston, 1997;

Stuart and Sakmann, 1994) or locally generated dendritic spikes at more distal synapses along CA1 dendrites (Golding et al., 2002). In addition to sodium and potassium, NMDA receptors were also found to pass calcium (Ascher and Nowak, 1988; Jahr and Stevens, 1987; MacDermott et al., 1986). Thus, NMDA receptors were shown to function as coincident detectors at the synapse. These receptors could simultaneously detect postsynaptic depolarization (relief of the magnesium block) and presynaptic release (binding of glutamate). Upon activation, calcium influx through these channels acts as the initial trigger of LTP. These results were the first descriptions of an NMDA receptor-dependent LTP. While a variety of studies have documented distinct forms of LTP that do not depend on NMDA receptor activation (Johnston et al., 1992; Le Duigou and Kullmann, 2011; Wang et al., 1996), NMDA receptor-dependent LTP forms the basis of our understanding of the processes governing synaptic plasticity.

Though calcium enters dendritic spines primarily through NMDA receptors at CA3-CA1 synapses (Bloodgood and Sabatini, 2007; Sobczyk et al., 2005; Yuste et al., 1999), calcium can also enter dendritic spines through voltage-gated calcium channels and from internal calcium stores such as the SER or mitochondria (Higley and Sabatini, 2012). Calcium inside the spine acts on a wide variety of targets, which are able to modify the structure and function of the synapse. While a host of protein kinases, including protein kinases A (PKA) and C (PKC), are activated by calcium, one of calcium's most crucial targets (in terms of LTP) is CaMKII. CaMKII constitutes 2% of the entire PSD and is activated upon binding of calcium-loaded calmodulin (Byth, 2014; Lisman et al., 2002; Okamoto et al., 2009). In its inactive state, CaMKII binds filamentous actin and is kept at a distance from the PSD (Zhang et al., 2008). Once activated, CaMKII

autophosphorylates itself and remains active after intracellular levels of calcium return to unstimulated levels (Miller and Kennedy, 1986). CaMKII phosphorylates AMPA receptors leading to an increase in single current conductance (Barria et al., 1997; Mammen et al., 1997; McGlade-McCulloh et al., 1993) while activating other proteins that stabilize AMPA receptors in the PSD (Huganir and Nicoll, 2013). Perfusing cells with activated CaMKII results in increased AMPA receptor responses and LTP (Ehlers, 2000; Lisman et al., 2002; Malenka and Nicoll, 1999). Furthermore, NMDA receptor activation results in increased fluorescence of GFP-fused AMPA receptor subunits in dendritic spines (Shi et al., 1999). While it is clear that induction of LTP involves the insertion of AMPA receptors into the PSD, the steps linking CaMKII activation to AMPA receptor insertion are still murky. Indeed, there might be other kinase intermediates between the two, such as the Ras-MAPK (mitogen-activated protein kinase) pathway (Zhu et al., 2002). PKC might be another candidate kinase driving the insertion of AMPA receptors. The conventional PKC isoform is activated by calcium and diacylglycerol and PKC inhibitors have been found to impair LTP, while PKC loading into cells enhances LTP (Hu et al., 1987; Klann et al., 1991; Linden and Routtenberg, 1989; Sacktor et al., 1993). Thus, through its activation of a variety of kinases, calcium is necessary and crucial in the induction of LTP.

Many researchers refer to synaptic potentiation as LTP if the potentiation lasts for at least 30 minutes. This precludes those results, however, from applying to later LTP phases. Hippocampal LTP has been historically divided into multiple phases: short-term potentiation, early LTP, and late LTP. These stages are defined by pharmacological blockade of various biochemical mechanisms that support synaptic strengthening (Frey et al., 1993). Early on, Krug et al.

(1984) showed that infusion of the protein synthesis inhibitor anisomycin caused potentiated field recordings in the dentate gyrus of freely moving rats to return to baseline over several hours. Importantly, the baseline recordings were found to be unaffected by protein synthesis blockade. These results were soon replicated in area CA1 (Frey et al., 1988). Subsequent studies have demonstrated that LTP returns to baseline within an hour following the administration of broad spectrum kinase inhibitors (Lisman et al., 2002; Nguyen and Woo, 2003). CaMKII and PKC are two of the more important kinases rapidly activated during early LTP as discussed above. Interestingly, protein synthesis inhibitors such as anisomycin or transcription inhibitors such as actinomycin cause LTP to return to baseline in hours depending on the induction stimulus (Frey et al., 1988; Kang and Schuman, 1996; Kelleher et al., 2004a). By directly comparing translational and transcriptional blockade, Kelleher et al. (2004b) demonstrated that translation is required for 60-90 minutes and is followed by a longer-lasting phase, which is dependent on both translation and transcription. Slow-onset, late LTP can be induced with cAMP (cyclic adenosine monophosphate) analogues or BDNF (brain-derived neurotrophic factor) and these forms of plasticity are also dependent on protein translation and gene transcription (Kang and Schuman, 1996; Leal et al., 2014; Nguyen et al., 1994).

The amount of calcium influx into the dendritic spine has been shown to influence the magnitude and, interestingly, the direction of plasticity. Building upon the Bienenstock-Cooper-Munro (BCM) model, a theoretical framework describing plasticity in the developing visual cortex (Bienenstock et al., 1982; Cooper and Bear, 2012), Bear (1987) proposed that some threshold (analogous to BCM's modification threshold, θ_m) of calcium influx through NMDA receptors

should be sufficient to induce LTP, whereas input activity that results in less calcium influx should weaken the connection and cause an NMDA receptor-dependent form of LTD. Several years later, Dudek and Bear (1992) were able to reliably induce homosynaptic LTD in area CA1[5]. They showed higher and lower frequency stimulation induced LTP and LTD respectively, which produced a BCM-like curve. In support of this, calcium chelators were found to prevent the induction of LTD and reducing extracellular calcium shifts a high frequency stimulus from producing LTP to producing LTD (Mulkey and Malenka, 1992). In light of the fact that kinases are important in the induction of LTP, Lisman (1989) proposed that preferential activation of phosphatases, such as the calcium/calmodulin-dependent protein phosphatase calcineurin as well as protein phosphatase 1, by low levels of calcium might support the induction of LTD. Indeed, it is now well supported that induction of NMDA receptor-dependent LTD involves a variety of phosphatases (some of which have higher affinity for calcium than most kinases), which ultimately drive the removal of AMPA receptors from the PSD (Carroll et al., 2001; Lüscher and Malenka, 2012; Mulkey et al., 1994; 1993). Lisman's proposal forms our "classical" assumptions about LTP and LTD: LTP is produced upon large calcium influx into the spine, while LTD is produced upon modest calcium influx into the spine.

Another form of LTD involves the activation of mGluRs (Bashir et al., 1993; Oliet et al., 1997; Palmer et al., 1997; Stanton et al., 1991) and, in fact, this form of LTD seems to predominate in area CA1 of adult animals (Kemp et al.,

---

[5] Though Dudek and Bear (1992) were the first to demonstrate a reliably inducible form of LTD (900 pulses at 1 Hz), Dunwiddie and Lynch (1978) had demonstrated earlier that low frequency stimulation (100 pulses at 1 Hz) was able to induce LTD. They found, however, that their stimulation protocol was not reliable in inducing LTD.

2000). Interesting, mGluR-dependent LTD requires the rapid synthesis of locally translated proteins (Huber et al., 2000). The rapid protein synthesis requirement, however, has been shown not to exist in older rats (Moult et al., 2008) and in animals with pathologically increased levels of protein synthesis (Huber et al., 2002). One protein that is rapidly translated at the synapses following activation of mGluRs is Arc (Arg3.1, activity-regulated cytoskeleton-associated protein). Arc associates with endocytic machinery and causes AMPA receptor endocytosis (Chowdhury et al., 2006; Shepherd et al., 2006). Perhaps not surprisingly, $Arc^{-/-}$ mice show very little mGluR-LTD (Park et al., 2008) and very little depression of visual cortex synapses following monocular deprivation (McCurry et al., 2010).

Adult versus Developmental Synaptic Plasticity

Development of hippocampus-dependent behaviors is delayed relative to elemental conditioning and effector systems development (Dumas, 2005; Stanton, 2000). Perhaps not surprisingly, hippocampal synaptic plasticity is reported to be categorically different in adult and developing animals. In organotypic cultures, LTP induction reliability and magnitude decrease with maturation (Muller et al., 1993). In slice, LTP induction with tetanus begins promptly at P15 in the rat (Harris and Teyler, 1984; Jackson et al., 1993). With TBS, LTP induction begins three days earlier at P12 and, furthermore, TBS delivery between P8-11 prevents test-pulse induced depression that normally occurs in the developing hippocampus (Cao and Harris, 2012), which is known as "developmental LTP". While CaMKII seems to be of extreme importance for induction of synaptic potentiation, during the first postnatal week, CaMKII levels are surprisingly low (Kelly and Vernon, 1985). Using protein kinase inhibitors,

Yasuda et al. (2003) found that potentiation ("developmental LTP") in area CA1 in P7-8 hippocampal slices depends upon the activation of PKA. This was not true for slices from > P27 animals. Furthermore, CaMKII inhibitors had no effect on potentiation induced in slices from P7-8 animals but did block LTP induction in slice from > P27 animals. The group also measured miniature excitatory postsynaptic currents (mEPSCs) in slices and found that incubation with forskolin, which enhances presynaptic neurotransmitter release via adenylate cyclase activation (Chavez-Noriega and Stevens, 1994), caused an increase in mEPSC frequency in both younger and older slices but only induced an increase in mEPSC amplitude in younger slices. This is presumably reflective of an increase in AMPA receptors at synapses in younger slices and further supports the notion that PKA plays a larger role in inducing LTP in those slices. Another study has shown that PKA and CaMKII work in parallel during P14, an intermediate stage of development (Wikström et al., 2003). Thus, there is a developmental shift in signaling cascades that are activated downstream from NMDA receptors, which might persist in animals as old as P26.

Another developmental phenomenon that highlights the differences between adult and developmental plasticity is the "silent" synapse. Silent synapses lack AMPA receptors and do not contribute to dendritic depolarization unless NMDA receptors are activated. LTP-inducing stimulation is able to recruit AMPA receptors to "unsilence" these synapses (Isaac et al., 1995). Silent synapses are, however, more prevalent in neonatal rat hippocampus and their number declines steeply after P5-6 (Durand et al., 1996). Using fluorescent calcium dyes, Enoki et al. (2009) demonstrated that changes in presynaptic machinery contribute heavily to the expression of LTP at CA3-CA1 synapses in

animals older than 21-28 days old. The group proposed younger animals, unlike mature animals, might express LTP primarily through unsilencing of synapses, which is consistent with the developmental profile of silent synapses. (See *Section 2.1: Presynaptic Physiological Plasticity* for a brief description of the experiments in Enoki et al.)

Similarly, LTD has some as-of-yet uncovered developmental profile. As noted above, there does, however, appear to be a shift from NMDA receptor-dependent LTD predominating in young animals to mGluR-dependent LTD predominating in older animals (Kemp et al., 2000). Furthermore, with electrical stimulation, LTD is much more reliably induced in younger animals than it is in adult animals (Bliss et al., 2007; Collingridge et al., 2010). This has led some researchers to speculate that LTD might be a phenomenon that is involved in sculpting circuits during development only.

McCutcheon and Marinelli (2009) conducted a systematic review of 314 papers published on hippocampal LTP from 1997-2007 in the journals *Science*, *Nature*, *European Journal of Neuroscience*, and *Journal of Neuroscience*[6]. The researchers found that the definitions used by study authors to denote "young" and "adult" were dramatically varied, "adult" ranging from as young as postnatal day (P) 21 to P594 (18 months). They also found that investigators often pooled animals of vastly different ages, sometimes spanning critical developmental periods such as puberty. Sexual maturity is reached in female rats at ~P32-34 and in males at ~P45-48 (Lewis et al., 2002). Nearly two-thirds of all the papers investigated hippocampal LTP using in vitro methods were conducted on animals

---

[6] Specifically the group searched the PubMed database for the following keywords: ('hippocampus') and ('LTP' or 'long-term potentiation' or 'long term potentiation').

just reaching or younger than sexual maturity. This might call into question the results' applicability to plasticity in the adult mammal. Investigation into the mechanisms of plasticity in male rats older than P50 should give a better impression of those mechanisms that occur specifically in the adult mammalian brain.

Structural Plasticity of the Synapse

LTP and LTD are two mechanisms whereby synaptic strength is modified. What structural remodeling of the synapse is occurring to support these changes? Structural reorganization of the synapse is known as synaptic structural plasticity. While the synapse includes both pre- and postsynaptic compartments, the vast majority of research into structural plasticity has focused on dendritic spines changes (though see *Section 2.1 Presynaptic Structural Plasticity*). Indeed, spine numbers along a dendrite changes dramatically with hormonal status (Woolley et al., 1990), unfamiliar environments (Moser et al., 1994), blockade of neurotransmitter release (McKinney et al., 1999), and temperature (Kirov and Harris, 1999). Because of these dramatic changes in spine structure occurring with internal and external environmental manipulation, researchers have been attracted to uncovering how structural changes at the level of the synapse influence its function.

Some of the earliest proposals that suggested a change in spine dimensions might support the increase in synaptic efficacy following the induction of LTP came in the 70s. By cutting out spine profiles on EM images and weighing them, Van Harreveld and Fifková (1975) showed that spine profile cross-sectional area (indirectly measured by paper weight) increased in the dentate

gyrus only in the outer molecular layer, where tetanus had been delivered, and not in the inner molecular layer. By implanting electrodes into the angular bundle of rats to investigate synapse size on EM sections, Desmond and Levy (1986a; 1986b) demonstrated that LTP was associated with an increase in the size of the PSD. These early studies were followed by a cascade of others that, using a variety of techniques, show LTP is associated with an increase in spine or PSD size (Bourne and Harris, 2011a; Matsuzaki et al., 2004; Okamoto et al., 2004; Popov et al., 2004; Zhang et al., 2008). Ostroff et al. (2002) found that polyribosomes in dendritic spines increase 2 hours during LTP induced with tetanus. Interestingly, PSDs on spines with polyribosomes were found to be significantly larger suggesting that these organelles might provide protein translation necessary to expand synapses during LTP.

Other studies have shown that the number of spines increases following potentiation. Investigating the dynamics of dendritic spines in response to high frequency stimulation in hippocampal organotypic cultures transfected with GFP, Maletic-Savatic et al. (1999) observed the rapid outgrowth of filopodia-like structures, thin dendritic protrusions that are thought to be developmental precursors to dendritic spines (Fiala et al., 1998). Furthermore, a subset of these filopodia developed bulbous heads suggesting they were transitioning into becoming full-fledged spines (Maletic-Savatic et al., 1999). Engert and Bonhoeffer (1999) showed that bathing organotypic hippocampal neurons in a cadmium-containing solution suppressed synaptic transmission, but that local perfusion of a calcium-containing solution "activated" an area of the dendrite. By delivering high frequency stimulation, they observed the outgrowth of new spines in an area, which had calcium available to it. Unfortunately, both studies were

unable to definitively show that synapses actually existed on spines that appeared throughout the course of their experiments, but glutamate uncaging experiments have been used to show that these new spines are functionally relevant to the circuit (Kwon and Sabatini, 2011). It is thus tempting to take the above data and link LTP with an increase in the number of spines and the size of synapses. This, however, appears to be an oversimplification.

An early study on the structural effects of chemically induced LTP showed that the number of dendritic spines did not change, but that spines became long and thin (Hosokawa et al., 1995). This finding was corroborated by Matsuzaki et al. (2004) with a series of glutamate uncaging experiments. Furthermore, most studies have investigated structural plasticity using younger animals (< 30 days old). As with physiological plasticity, structural plasticity induced by LTP seems to be categorically different in mature animals. In mature animals, EM studies reveal synapse number and spine structure are stable following induction of LTP with tetanic stimulation (Sorra and Harris, 1998) or following chemically-induced LTP (Stewart et al., 2005). LTP induced with theta-burst stimulation (TBS), on the other hand, either causes the elimination of small thin spines or prevents a constitutive formation a small spines (Bell et al., 2014; Bourne and Harris, 2011a). Preliminary data supports the idea that spine outgrowth accompanies LTP induced with TBS in 15 day-old animals (D. Watson and K. Harris, in preparation). It seems reasonable to tentatively assume that younger animals most likely express hippocampal LTP through addition of new synaptic contacts, while mature animals express hippocampal LTP primarily through modifications of existing connections.

The structural remodeling of synapses that occurs after LTD induction has been far less studied, but researchers seem to reach greater consensus on the structural changes that support synaptic depression. Okamoto et al. (2004) tagged filamentous (F-) and globular (G-) actin with two different fluorescent proteins and observed an increase in F-actin and spine head sizes when tetanic stimulation was delivered near the dendrite. Interesting, delivery of low frequency stimulation reduced the F- to G-actin ratio as well as caused spine heads to shrink. The same year, Zhou et al. (2004) injected fluorescent dye into CA1 pyramidal cells and stimulated synapses through a glass electrode positioned near dendrites. Delivery of low frequency stimulation reduced the size of EPSPs measured somatically and also caused spine heads to shrink. Cofillin, an actin regulator that causes actin depolymerization, was inhibited by the infusion of p-coffilin. This prevented the spine head shrinkage observed with low frequency stimulation. Other studies have shown that spines retract during LTD (Nägerl et al., 2004) and that fluorescent pre- and postsynaptic marker colocalization decreases with LTD, both of which suggest synapses might be eliminated during LTD (Bastrikova et al., 2008). Thus, LTD appears to be associated with the shrinkage of spines and synapses.

Behavioral Relevance of Synaptic Plasticity

LTP and LTD are proposed to be necessary for both the encoding and retrieval of information and are thus thought to be two cellular mechanisms that mediate learning and memory (Bliss et al., 2007; Bourne and Harris, 2007; Malenka and Bear, 2004). This idea is frequently thrown into report introductions to imbue relevance into studying synaptic plasticity, but what evidence is there to

22

support this claim? Undoubtedly, one of the reasons this question is often investigated at hippocampal synapses is due to the most famous patient in neuroscience, H.M. (Henry Molaison, 1926-2008). H.M. suffered intractable seizures, the focus of which seemed to exist in his medial temporal lobes. Removal of a significant amount brain tissue from this region corrected H.M.'s seizures, but, for the rest of his life, H.M. suffered profound anterograde amnesia, an inability to form new memories (Scoville and Milner, 1957). Since the original descriptions of H.M., the hippocampus has come to be known as a crucial brain region for declarative memory, consciously recalled memory such as new facts and events. Thus, the report by Bliss and Lømo (Bliss and Lomo, 1973) that hippocampal synapses could act to store information via the strengthening of synapses has captivated scientists as a possible cellular mechanism of learning and memory. Frankly put, however, LTP and LTD are not memory. They are experimentally induced phenomena that involve unnatural synaptic activation. But the mechanisms that mediate synaptic plasticity might also be the same mechanisms that mediate learning and memory (Eichenbaum, 2008; Malenka and Bear, 2004). The pioneering early studies of Carol Barnes showed that LTP persistence in older animals was statistically correlated with rate of learning and spatial memory retention (Barnes, 1979; Barnes and McNaughton, 1985). A variety of researchers have subsequently investigated hippocampal LTP in the context of spatial learning. Early reports described an increase in dentate field EPSPs (fEPSPs) following exploration of novel environments (Green et al., 1990; Moser et al., 1993; Sharp et al., 1989).

Other groups have attempted to approach the question at the molecular level. Early on, Morris (1989) showed that APV blockade of NMDA receptors in

the dorsal hippocampus impaired learning in the now famous Morris water maze task. Though pharmacological blockade might have influenced a host of other signaling cascades, genetic techniques have supported the conclusions that NMDA receptor perturbation impairs learning. Using a Cre/loxP recombination system, Tsien et al. (1996a; 1996b) knocked out a specific NMDA receptor subunit in hippocampal area CA1. LTP was found to be normal in the dentate gyrus and neocortex, but severely impaired in CA1. These animals recapitulated the performance impairment in the Morris water maze that was observed a decade earlier. Interestingly, although cells in mice lacking normal CA1 NMDA receptors retain preference for position, place fields in these mice are highly abnormal (McHugh et al., 1996). A point mutation that blocks the ability of CaMKII to autophosphorylate also introduces profound deficits in water maze learning (Giese et al., 1998) and fluorescence studies have shown that learning induces the recruitment of newly synthesized AMPA receptors into spines (Matsuo et al., 2008). Thus, several of the biochemical steps necessary for the induction of LTP seem to be involved in some forms of learning and memory.

In perhaps one of the more compelling studies on the topic, Whitlock et al. (2006) used an inhibitory avoidance (IA) paradigm, a hippocampus-dependent task (Isaacson and Wickelgren, 1962), to investigate whether learning induced LTP. (Briefly, in this study IA involved animals learning that entry into one of two chambers caused delivery of a foot shock. Thereafter, they avoided the chamber associated with the shock and this served as a measure of memory.) The group found, as many who have investigated hippocampal learning report as well, that encoding of this task was dependent on the activation of NMDA receptors. They found that AMPA receptor phosphorylation at serine 831, which occurs during

LTP (Lee et al., 2000), and recruitment of AMPA receptors at synapses were increased in animals that had undergone IA training. By stimulating CA3-CA1 axons, the group measured fEPSPs in CA1 via a multielectrode recording array implanted into stratum radiatum before and after training. They observed an increase in fEPSP slope at only a subset of recording sites. Interestingly, at the sites that did show this LTP-like effect, subsequent induction of LTP was occluded. This study presented strong evidence to support the claim that learning induces LTP-like effects in hippocampal area CA1. Other electrophysiology studies since Whitlock et al. have supported their claims by demonstrating that other hippocampus-dependent tasks, such as trace eye-blink conditioning (Gruart et al., 2006) and novel object recognition (Clarke et al., 2010), involve the modulation of synaptic efficacy.

What evidence supports the role of LTD and depotentiation (LTP reversal) in learning and memory? Modeling of synaptic circuits suggests that the ability to encode experience depends on the ability to both strengthen and weaken synapses (Kemp and Manahan-Vaughan, 2007), but little is known about the contributions synaptic depression makes to hippocampal-dependent learning. mGluR activation produces robust LTD (Bashir et al., 1993; Oliet et al., 1997; Palmer et al., 1997; Stanton et al., 1991) and both antagonism and genetic deletion of mGluR5 results in impaired learning and extinction of hippocampus-dependent tasks in a radial arm maze or the Morris water maze (Lu et al., 1997; Manahan-Vaughan and Braunewell, 2005; Naie and Manahan-Vaughan, 2004; Xu et al., 2009). Manahan-Vaughan and colleagues have shown that LTD seems to be somehow important in environment and object novelty recognition (Kemp and Manahan-Vaughan, 2004; 2007; 2008; Manahan-Vaughan and Braunewell,

1999). In fact, delivering low frequency stimulation while animals explore novel objects placed in a hole-board facilitates LTD in CA1 and dentate gyrus. This was found to last up to 25 hours. Curiously, and somewhat confusingly, exploration of an empty hole-board facilitated LTP. Currently, the molecular steps linking LTD to learning and memory are vastly unexplored. Thus, while little evidence exists linking LTD with memory, these few tentative findings coupled with the many LTP-related molecular events associated with learning, back claims that synaptic plasticity serves as a mechanism whereby memories are encoded in the mammalian brain. It follows that understanding the cellular mechanisms that support synaptic plasticity should illuminate our understanding of learning and memory at the behavioral level.

1.3 Studies Presented in this Dissertation

In the subsequent chapters of this dissertation, I present studies I performed in the lab of Dr. Kristen Harris at the University of Texas at Austin (2011-2015). I used three-dimensional reconstructions of neuronal ultrastructure from serial section EM images to investigate synaptic structural remodeling associated with plasticity at CA3-CA1 synapses in adult rodents. Each chapter includes an independent introduction providing context and impetus that motivated each part of the study and, following the results, a discussion evaluating the implications of my findings. The final chapter of this dissertation considers future directions that might naturally lead from these studies.

As discussed above, LTP induces dramatic postsynaptic structural plasticity at CA3-CA1 synapses, synaptic plasticity (both physiological and structural) appears to be categorically distinct in adult and juvenile animals, and

LTP can be subdivided into various phases (early/late LTP). The studies in this dissertation are concerned with elucidating the structural mechanisms that support enduring LTP in the adult rodent hippocampus. Postsynaptic structural remodeling during LTP has been intensely investigated, but coincident presynaptic mechanisms are less clear. In Chapter 2 of this dissertation, I present an investigation into the presynaptic structural plasticity that occurs to support LTP in the adult rat. The underlying subcellular organelles that might coordinate plasticity during LTP have only recently garnered attention from researchers. In Chapter 3, I present evidence that supports the role of one organelle, SER, in coordinating plasticity along CA1 dendrites. Finally, it is of interest to uncover how normal mechanisms of plasticity might break down during pathology. Fragile X (FX) is the most commonly inherited form of autism and intellectual disability (Hagerman et al., 2010) and is proposed to be caused in part by aberrant synaptic signaling (Zoghbi and Bear, 2012). In Chapter 4, I present preliminary EM work investigating the synaptic structural deficits in the hippocampus of a mouse model of FX. Collectively, the findings in this dissertation demonstrate that structural plasticity is coordinated in pre- and postsynaptic compartments during LTP in the adult rodent hippocampus and provide a starting point from which to study how normal mechanisms of structural plasticity go awry during pathology.

Chapter 2: Presynaptic Structural Plasticity

2.1 Introduction

The locus of LTP induction at CA3-CA1 synapses is generally agreed upon by the scientific community to be postsynaptic. It involves the activation of postsynaptic NMDA receptors, a sufficient influx of calcium into the postsynaptic cytosol, and the activation of downstream signaling molecules, the most important of which seems to be CaMKII (Bliss and Collingridge, 2013; Kennedy, 2013). However, after nearly 50 years of LTP research, considerable controversy still surrounds the exact locus of LTP expression. While a select few researchers cling to the notion that LTP expression is a purely postsynaptic phenomenon, exclusively involving the insertion of AMPA receptors into the PSD (Granger and Nicoll, 2014; Kerchner and Nicoll, 2008), a wealth of studies from the early 1980s onwards has demonstrated a substantial presynaptic component to LTP expression at CA3-CA1 synapses (see below and MacDougall and Fine, 2014). Beyond the hippocampus, presynaptic forms of LTP have been observed at synapses throughout the brain including in the cerebellum (Bender et al., 2009; Salin et al., 1996), thalamus (Castro-Alamancos and Calcagnotto, 1999), amygdala (Humeau et al., 2003; Shaban et al., 2006; Shin et al., 2010; Tsvetkov et al., 2002), and visual cortex (Sarihi et al., 2012). Whether or not LTP expression is governed mainly or solely by one side of the synapse might be influenced by the age of the animal (Enoki et al., 2009; Isaac et al., 1995), synaptic receptor content present at the time of activity (MacDougall and Fine, 2014), anatomical location of the synapse (Dolphin et al., 1982), length of the experiments (MacDougall and Fine, 2014), and techniques employed to investigate the question at hand (Yang and Calakos, 2013). It is not the goal of

this chapter to wade into an argument for or against either camp of thinking. It is becoming increasingly clear, however, from the sheer volume of work published on synaptic plasticity, that LTP expression most likely involves mechanisms working in tandem on both sides of the synapse. Thus, it is of interest to use EM as a means of investigating what presynaptic ultrastructural remodeling might be occurring during LTP and how it might be coordinated with postsynaptic structural mechanisms to support physiological plasticity.

Presynaptic Physiological Plasticity

As Norway is the birthplace of LTP research, it is fitting that the earliest studies demonstrating a change in presynaptic activity during plasticity were also done in the Land of the Midnight Sun. Skrede and Malthe-Sørenssen (1981) working at the Norwegian Defense Research Establishment near Oslo monitored stimulus-evoked release of radioactive aspartate (D-[^{3}H] aspartate) as a proxy for endogenous glutamate release, by measuring levels of radioactivity in superfusate running over acute hippocampal slices. The group found that the release of D-[^{3}H] aspartate was significantly increased up to an hour after delivering tetanus to axons coursing through CA1 and interpreted these results as indicating an increase in neurotransmitter release during LTP. A year later across the North Sea, Timothy Bliss's group in the UK supported Skrede and Malthe-Sørenssen's findings by demonstrating an increase in neurotransmitter release during LTP in the dentate gyrus in vivo (Dolphin et al., 1982). Using similar tactics, the British group infused radioactive glutamine (^{3}H-glutamine) into the dentate gyrus of anesthetized rats. ^{3}H-glutamine is converted the ^{3}H-glutamate by glutaminase and the perfusate, collected via a push-pull cannula,

29

was measured for radioactivity. After inducing LTP with delivery of a 250 Hz stimulus for 0.5 s, release of ^{3}H-glutamate was elevated relative to control slices for more than an hour. Thus, even in the early days of LTP research, evidence was emerging that implicated plasticity of the presynaptic compartment in mediating an increase in synaptic strength.

Several studies have employed classical quantal analyses schemes that demonstrate an increase in the probability of release or increase in number of release sites without an increase in the response amplitude to a single quantum of neurotransmitter. In hippocampal dissociated cultures, Bekkers and Stevens (1990) induced LTP by repeatedly triggering action potentials in one neuron at 20 Hz for 2 s in a bath containing no magnesium. The group measured synaptic responses of a neighboring neuron pre- and post-tetanus delivery. While the average response amplitude was unchanged, they demonstrated that release probability had increased and the number of release sites remained stable. Work in dissociated culture was followed up with studies of CA3-CA1 synapses in acute hippocampal slice from P14-21 rats, which replicated their previous findings. Responses in this study were only measured up to 30 minutes post-tetanus. Malgaroli and Tsien (1992) demonstrated similar findings in cultured CA3-CA1 hippocampal neurons by inducing LTP with 30 s application of 50 μM glutamate and 0 mM magnesium to the bath. Quantal analyses have shown that after inducing LTP, previously "unreliable" synapses are recruited into the fray during synaptic stimulation (Stevens and Wang, 1994). Other studies employing quantal analyses have demonstrated that new synaptic sites are built to support LTP at CA3-CA1 synapses (Bolshakov et al., 1997) and that these sites come online at later phases during LTP (Sokolov et al., 2002).

Classical optical analyses suffer from that fact that minimal stimulation of afferents activates an unknown number of synapses at unknown sites along a neuron's dendritic arbor. This fact makes it difficult to interpret LTP-associated changes at individual synapses. Researchers monitoring calcium transients using fluorescent dyes have introduced the idea of optical quantal analyses by applying older mathematical techniques to monitor synaptic activity at single dendritic spines. Emptage et al. (1999) filled cells in areas CA1 and CA3 of organotypic slice cultures with Oregon Green 488 BAPTA-1, a high affinity calcium-sensitive dye, and demonstrated the ability to monitor calcium responses (excitatory postsynaptic calcium transients [EPSCaTs[7]]) in individual spines. A follow-up study by the same group monitored EPSCaTs 15 minutes before and up to 1 hour after inducing LTP with tetanic stimulation (Emptage et al., 2003). They found that the probability of EPSCaTs occurring increased from 0.11 to 0.44 30 minutes after inducing LTP. Several studies have argued that the probability of EPSCaTs occurring provides an estimate for the probability of presynaptic release (Emptage et al., 1999; Yuste and Denk, 1995; Yuste et al., 1999). Thus it follows that an increase in EPSCaTs observed after inducing LTP supports the idea that the probability of presynaptic release increases with LTP. Enoki et al. (2009) extended this optical analysis to explore what influence the activation of a single synapse has on somatically recorded EPSPs. Using hippocampal slices from P21-28 rats, which have fewer silent synapses than younger animals (Busetto et al., 2008; Durand et al., 1996; Kerchner and Nicoll, 2008), the group observed that somatically recorded EPSPs tended to be larger when an imaged

---

7 Pronounced *eps-kats*.

CA1 dendritic spine (presumably hosting a CA3-CA1 synapse) was active rather than inactive. They reasoned that the difference in somatically recorded EPSPs when they observed an EPSCaT in the imaged spine and when they did not would account for an average EPSP at the soma arising from the imaged synapse. The difference or "unitary" EPSP (i.e., the EPSP measured in the soma putatively from the activation of a single synapse) before and after LTP was found to be the same, lending more support to the notion that changes in release probability can contribute substantially to LTP at CA3-CA1 synapses. Interestingly, another study using this method suggested that "unsilencing" of silent synapses occurred via the postsynaptic insertion of AMPA receptors, but that subsequent rounds of LTP at those synapses occurred primarily via an increase in release probability (Ward et al., 2006), again supporting to the idea that both pre- and postsynaptic forms of LTP expression exist at individual synapses.

Quantal analyses rely on inferences of presynaptic activity from postsynaptic responses (be they measured somatically or by imaging calcium transients in dendritic spines). Studies employing fluorescent markers of the presynaptic vesicle pool have provided some of the most compelling evidence in support of presynaptic plasticity during LTP at CA3-CA1 synapses. FM1-43, a fluorescent, amphipathic molecule taken up by synaptic vesicles during endocytosis, destains during activity and can serve to measure release of neurotransmitter (Betz and Bewick, 1992; Cochilla et al., 1999; Ryan, 2001). Both chemically and electrically induced LTP are associated with an increase in FM1-43 destaining (Ahmed and Siegelbaum, 2009; Zakharenko et al., 2001; 2003), which suggests LTP is associated with an increase in neurotransmitter

release. Another class of fluorescent molecules used to investigate changes in presynaptic function during LTP are the pHluorins, pH-sensitive GFP mutant molecules that lose fluorescence as pH decreases. SynaptopHluorins, pHluorins fused with the presynaptic protein synaptobrevin, exploit the fact that the inside of synaptic vesicles is considerably more acidic (pH = ~5.7) than the surrounding cytosol and extracellular space (Miesenböck et al., 1998; Miesenböck, 2012). Upon exocytosis of synaptic vesicles, the pHluorin molecule is exposed to the more neutral extracellular space (pH = ~7.5), which causes it to suddenly fluoresce. Because it is an integral membrane protein, synaptopHluorin can be used to monitor vesicle dynamics over multiple rounds of endo- and exocytosis.

Another advantage to these molecules is that they are genetically encoded and mouse lines carrying the gene have been established (Araki et al., 2005; Li et al., 2005b; Tabares et al., 2007). Using acute hippocampal slices from mutant synaptopHluorin-expressing mice (8-12 weeks old), Bayazitov et al. (2007) monitored fluorescence changes at CA3-CA1 synapses to a 10 Hz (5 s) stimulus before and after the induction of LTP by 200 Hz tetanization. The group found that presynaptic function (as measured by peak fluorescence) and synaptic strength (field recordings) were both elevated up to 3 hours after inducing LTP. Curiously, although the field EPSP slope had reached its maximum by 30 minutes, changes in presynaptic function did not reach asymptote until roughly an hour after the induction of LTP. Using blockers of NMDA receptors and L-type voltage-gated calcium channels (L-VGCCs), the group demonstrated that activation of postsynaptic NMDA receptors is necessary to induce a rapid onset LTP, while activation of L-VGCCs contributes to the formation of a longer lasting component of LTP that correlated with their measure of presynaptic function.

This work generated the idea that changes in postsynaptic function occur rapidly to support LTP at CA3-CA1 synapses, while presynaptic changes, although slower to come online, support later phases of LTP.

Presynaptic Structural Plasticity in the Adult CNS

The vast majority of studies investigating structural plasticity have focused on postsynaptic remodeling following changes in the functional status of the synapse (Holtmaat and Svoboda, 2009). As outlined in this section, presynaptic structural plasticity is also, however, associated with dramatic changes in the presynaptic compartment. This form of plasticity seems to be somewhat conserved through evolution. Early investigations into the morphological correlate of long-term sensitization of the gill-withdrawal reflex in the sea slug *Aplysia californicus* found that trained animals had dramatic changes to presynaptic compartments, including more synaptic vesicles, presynaptic boutons, and axonal branches (Bailey and Chen, 1983; 1988a; 1988b). In the developing mammalian brain, structural remodeling of axons had been observed previously (Antonini and Stryker, 1993; Portera-Cailliau et al., 2005; Ruthazer et al., 2003). Portera-Cailliau et al. (2005) imaged axons in layer 1 of the neocortex of GFP-transgenic mice during the first three postnatal weeks. The group observed that axons exhibited growth and elimination at the same time, but that growth was overall more dominant during development. Axons from different types of cells displayed different forms of growth. Thalamocortical axons grew quickly in straight paths, while local axons of Cajal-Retzius interneurons grew more slowly with large growth cones coursing a tortuous path. It is clear from this work that different neuron types exhibit different forms of growth. Under more dramatic

conditions, axonal plasticity has been investigated during peripheral axotomy, which involves the disruption of motor neuron connections to muscle fibers and induces massive rearrangements of synaptic connections along damaged processes (for review see Coleman and Freeman, 2010; Neukomm and Freeman, 2014; Spejo and Oliveira, 2014). In adult neocortex, researchers had observed axonal growth in the CNS following lesions of peripheral sensory structures (Dancause et al., 2005; Darian-Smith and Gilbert, 1994; Florence et al., 1998), but it was not known whether axons were normally plastic in the adult CNS or if this was only induced by injury or peripheral sensory deprivation.

By observing presynaptic structures in vivo, De Paola et al. (2006) and Stettler et al. (2006) were the first studies to demonstrate definitively that CNS axons and boutons are dynamic in the non-perturbed adult brain. De Paola et al. monitored layer 1 and 2 axons through a cranial window above the somatosensory cortex of mature transgenic mice (> 2.5 months old) expressing cytoplasmic or membrane-bound GFP. The group followed axons for up to an impressive 9 months and found that, although the general geometry of the axonal arbor in these mice tended to remain stable, shorter side branches and distal axonal endings were highly dynamic, stretching and retracting up to ~150 µm during recording. Furthermore, although the arbors seemed to remain relatively intact, this was not so for boutons along those arbors. Some boutons were stable over the course of 9 months of imaging, while other boutons were observed disappearing or appearing. The survival rate of boutons was found to be dependent on the type of axon imaged; putative thalamocortical synapses were more stable than intracortical synapses. Stettler et al. used a different methodology and a different animal to demonstrate dynamic presynaptic

structures that persist into adulthood. This group injected a non-replicative adeno-associated virus carrying the gene for enhanced GFP in to the primary visual cortex of adult Macaque monkeys. Again, axonal arbors appeared to be stable in the adult Macaque, but terminal branches and boutons were observed coming and going, suggesting ongoing synaptogenesis and synaptic elimination in V1 of primates. In addition to the cortex, presynaptic terminals of cerebellar parallel fibers are dynamic in adult mice and become stabilized during the learning of motor tasks (Carrillo et al., 2013). Interestingly, it appears that the dynamic nature of axonal boutons, at least in mouse cortex, actually increases with age as demonstrated in a follow-up study using 22-24 month old mice (Grillo et al., 2013). This might be indicative of an inability to stabilize those structures in "elderly" animals. While these studies provide impressive data to support the claim that presynaptic structures are highly dynamic after development, they are restricted to the resolution of light and thus the structural remodeling occurring below that resolution had been left unexplored.

In classic studies on synaptic vesicle cycling, vesicles retrieved during recycling were thought to be reused exclusively at the same synapse (Ceccarelli et al., 1973; Heuser and Reese, 1973). Since those early studies, a variety of reports have shown that vesicle packets can be mobile at extrasynaptic sites in axons (Ahmari et al., 2000; Hopf et al., 2002; Krueger et al., 2003). These packets could potentially serve as a way to rapidly build synapses (Ahmari and Smith, 2002; Matteoli et al., 2004; Ziv and Garner, 2004). Furthermore, evidence of mobile vesicles beyond the synapse put into question the assumption that vesicles are restricted to recycling sites. To address whether or not recycling vesicles are restricted in this way, Darcy et al. (2006) used two FM dyes to

36

investigate movement of vesicles that had been endocytosed in cell culture. Vesicles from recycling pools were loaded with FM4-64 and putative synapses were identified where FM fluorescence was apposed to fluorescently tagged postsynaptic glutamate receptors. The group photo-bleached adjacent synapses and monitored the recovery of fluorescence in neighboring boutons, which suggested that recycling vesicles (filled with dye) were able to move through inter-bouton axonal regions to neighboring boutons. They subsequently stimulated axons and observed fluorescence decrease, which further supported the idea that these vesicles were fusion-competent at distant, non-native synaptic sites. As anatomical confirmation of the presence of these vesicles at distant boutons, the group used a photo-convertible form of FM1-43, which produces an electron dense product that can be analyzed at the level of the electron microscope. Densely stained vesicles were found on EM sections in distant boutons as well as docked along non-native active zones. Using similar techniques, a follow-up study by the same group found that vesicles in acute hippocampal slices from three-week old rats were also capable of moving to non-native synapses where they were also release competent (Staras et al., 2010). Vesicles in acute slices that moved to non-native synapses were extremely mobile and this mobility was found to be under the influence of BDNF. The subset of mobile recycling vesicles from multiple adjacent release sites was termed the vesicular "superpool" in Staras et al.

Bourne and Harris (2011) and the Current Study

Dr. Jennifer Bourne, a former postdoctoral researcher in the Harris lab, published a colossal study investigating the temporal aspects of postsynaptic

structural plasticity following the induction of LTP with TBS in area CA1 of adult (51-65 days old) rats (see Bourne and Harris, 2011a). A large portion of this dissertation forms an extension of her original work and a description of her findings is warranted. LTP was induced in hippocampal slices with TBS and tissue was fixed at 5 minutes, 30 minutes, or 2 hours after LTP induction. CA1 stratum radiatum tissue from the slices was subsequently prepared for electron microscopy (see Section 2.2 below for detailed methods). Interestingly, at 5 minutes during LTP, she uncovered an increase in the frequency of asymmetric shaft synapses and stubby spines, transitory postsynaptic structures that develop into spines or are eliminated (Engert and Bonhoeffer, 1999; Fiala et al., 1998; Maletic-Savatic et al., 1999). Non-synaptic filopodia were increased at 30 minutes. By 2 hours, the frequency of all "transitional" structures had returned to control levels. These results suggest that early LTP is associated with synaptogenesis and that by 2 hours, these structures are either eliminated or converted to mature spines. Furthermore, when typical spine types were categorized according to their size (by head diameter, small thin spines: < 0.45 µm, medium thin spines: > 0.45 µm, mushroom spines: > 0.6 µm), an interesting finding was uncovered. At 5 and 30 minutes, the frequency of these spine types during LTP did not differ from control levels. At 2 hours, however, while the frequency of medium thin and mushroom spines remained stable, there were significantly fewer small thin spines. Importantly, the study showed that synapse area on all remaining spines was increased at 2 hours during LTP, while at 5 and 30 minutes PSDs had not yet expanded. Inhibitory synapses showed the same pattern: there were fewer inhibitory synapses at 2 hours, but those remaining were larger than control conditions. Despite this dramatic remodeling of dendritic

spines and synapses during LTP, the total sum synaptic input hosted along a length of dendrite (excitatory or inhibitory) was the same during LTP as it was during control conditions. Thus, as synapses expanded during LTP, the summed input along the dendrite remained constant as small thin spines were eliminated or prevented from forming (in other words, fewer spines, larger synapses by 2 hours during LTP, **Fig. 2.1**). This work provided strong structural evidence promoting the idea that adult CA1 dendrites support a finite level of synaptic input and modifications of synaptic connections at one synapse can influence neighboring synapses. (An investigation into the dendritic resources that might shape synaptic coordination along dendrites during LTP is presented in Chapter 3 of this dissertation.)

The findings presented in this chapter of my dissertation seek to answer several questions that naturally follow from Bourne and Harris (2011) and previous studies investigating structural plasticity during LTP. The first obvious question is, what presynaptic structural arrangements are occurring to support LTP in tissue previously analyzed by Dr. Bourne for postsynaptic remodeling? Secondly, the majority of studies investigating hippocampal structural plasticity have investigated tissue that had undergone LTP for an hour or less. Because there are distinctive mechanisms in early and late phases of LTP (see *Section 1.2: Early LTP/LTD Studies*), it is of interest to consider presynaptic structural remodeling during both phases (30 minutes and 2 hours). Furthermore, to my knowledge, no study has investigated presynaptic structural plasticity using electron microscopy in unambiguously adult animals. While light microscopy has uncovered dynamic remodeling of axonal branches and boutons in adult mammals (De Paola et al., 2006; Grillo et al., 2013; Stettler et al., 2006), the
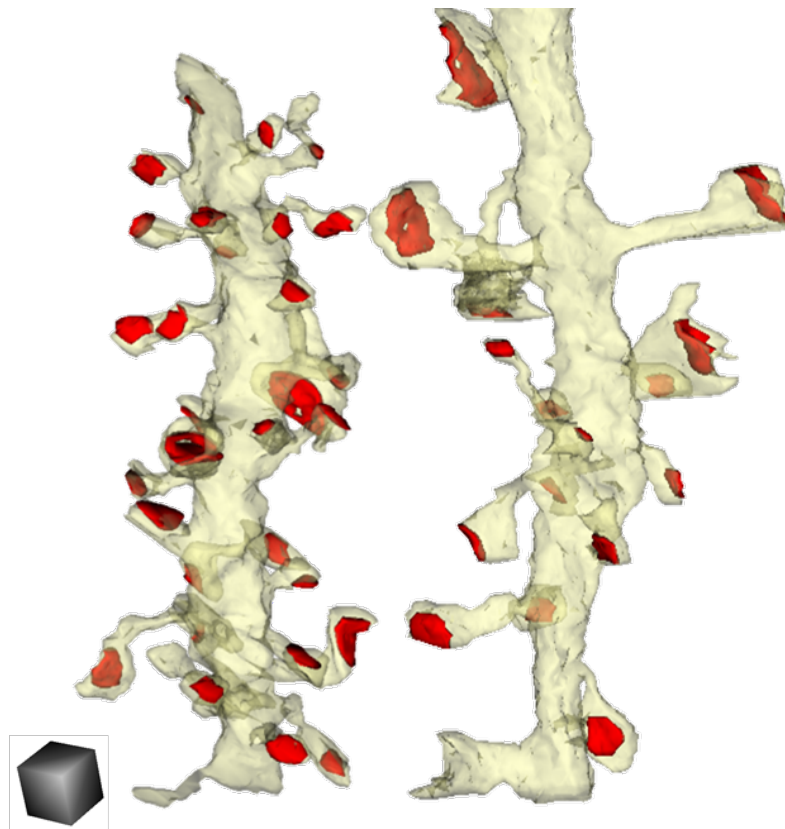
	Control	**LTP**
Synapses/µm:	4.69	2.70
Mean synapse size:	0.06 µm^2	0.11 µm^2
Σ Synaptic area/µm:	0.32 µm^2	0.32 µm^2

Figure 2.1: Total synaptic input along a dendrite conserved by 2 hours during LTP. Adapted from Bourne and Harris, 2011. Three-dimensional reconstruction of dendrites (yellow) with PSDs (red) from both control and LTP conditions from previous work in the Harris laboratory investigating postsynaptic structural remodeling during LTP. Despite dramatic differences in the number of synapses hosted along a dendritic segment during LTP, total synaptic input to the segment was conserved as synapses enlarged. Scale cube = 0.5 µm on each side.

underlying ultrastructural modifications that might occur fall well below the resolution of that technique. Finally, the vesicular superpool provides a mechanism whereby synapses along axons "share" recycling vesicles (Darcy et al., 2006; Staras et al., 2010). The dynamics of superpool vesicles might be altered during LTP and we were curious to investigate if we could uncover ultrastructural evidence of the vesicular superpool in our hippocampal tissue and whether or not those vesicles contributed to support LTP.

To consider these questions, we reconstructed axonal segments and boutons in three dimensions in hippocampal tissue from serial section electron micrographs that Dr. Bourne had previously analyzed for dendritic spines and synapses (Bourne and Harris, 2011a). We categorized and quantified bouton and vesicle types and searched for evidence of endocytosis. As outlined below, we uncovered a remarkably plastic presynaptic component of CA3-CA1 synapses. The presynaptic structural remodeling uncovered here appears to be coordinated with postsynaptic rearrangements previously described by Dr. Bourne. This study was done in conjunction with Dr. Bourne and was published in the Journal of Comparative Neurology in 2013 (see Bourne et al., 2013). Dr. Bourne performed the physiology experiments and processed the tissue for electron microscopy. Together, Dr. Bourne and I reconstructed presynaptic axons and boutons and analyzed the data. Dr. Bourne and I wrote the manuscript with Dr. Harris.

2.2 Methods

Hippocampal Dissections and Physiology

All methods were done in accordance with and approved by the Institutional Care and Use Committee of the University of Texas at Austin, which

follows the National Institutes of Health guidelines for the humane care and use of laboratory animals. For this study we used seven adult male Long Evans rats[8] aged 56-65 days old and weighing 263-361 g. In a large glass jar, a metal platform with nose hose was placed over cotton gauze, to which ~2 mL of the anesthetic halothane had been added. The jar was closed and the halothane was allowed to vaporize for 3-5 min. An animal was placed in the jar and, to guarantee it was completely unresponsive to external stimulus, it was removed only after it become unresponsive to a light toe pinch (~1 min). The animal was immediately decapitated and the hippocampus was removed. 400-μm thick slices from the middle third of the hippocampus were collected at room temperature (25 ºC) on a Stoelting tissue chopper (Wood Dale, Illinois). The slices were placed on nets in an interface chamber. The nets were over wells filled with artificial cerebrospinal fluid (aCSF: 116.4 mM NaCl, 5.4 mM KCl, 3.2 mM $CaCl_2$, 1.6 mM $MgSO_4$, 26.2 mM $NaHCO_3$, 1.0 mM NaH_2PO_4, 10 mM dextrose) that had been previously bubbled with carbogen (95% O_2, 5% CO_2) for at least 30 min. The slices were allowed to recover in vitro for ~3 hours at 32 ºC, a length of time necessary to allow synapse number to stabilize after trauma induced by cutting slices (Kirov et al., 1999)[9]. To control for the possibility that ultrastructural changes uncovered in this work might be a consequence of TBS delivery and not LTP, the NMDA receptor blocker APV (D-2-amino-5-phosphonopentanoic acid)

---

[8] For a study on the interesting effects of strain type on bidirectional plasticity in another region of the hippocampus, the dentate gyrus, see Bowden et al. (2011).

[9] Interestingly, several studies have shown that > 2-4 h of slice recovery is required to stabilize a variety of cellular processes that are thrown into disarray after dissection of neural tissue (Ho et al., 2004; Huber et al., 2001; Sajikumar et al., 2005; Whittingham et al., 1984). One study showed that an impressive 4-6 h of recovery after cutting slices is necessary to stabilize protein synthesis in hippocampal slices (Osterweil et al., 2010).

was used to prevent induction of LTP. For APV experiments, 50 μM APV in aCSF was added to the wells immediately after the slices had recovered.

After recovery, a glass recording electrode filled with 120 mM NaCl was placed in the middle of stratum radiatum in area CA1. Two concentric bipolar stimulating electrodes (100 μm diameter, Fred Haer, Brunswick, Maine) were placed on either side of the recording electrode separated by a distance of 600-800 μm (**Fig. 2.2a**) to guarantee stimulation of distinct populations of synapses (Ostroff et al., 2002; Sorra and Harris, 1998). Extracellular field potentials were recorded using IGOR (Wave Metrics, Lake Oswego, Oregon). The slope of the field excitatory postsynaptic potential (fEPSP) was measured over 400 μs at 170-250 μs after the stimulus artifact. We determined the responsiveness of the slice by performing an input/output curve. Stimulus intensity for set just below threshold for firing of a population spike. This stimulus intensity was then held constant for the remainder of the physiology experiments and baseline recordings were collected for each stimulating electrode with a test pulse every 2 min (offset by 30 s) for ~30 min. Theta-burst stimulation (TBS, 8 trains of 10 bursts at 5 Hz of 4 pulses at 100 Hz delivered 30 seconds apart), a protocol that mimics naturally occurring oscillations in the hippocampus (Buzsáki, 2002; Colgin, 2013; Hyman et al., 2003; Larson et al., 1986; Morgan and Teyler, 2001), was delivered to one stimulating electrode to induce LTP. The site of LTP induction (CA3 or subicular side of the recording electrode) was alternated between experiments. Synaptic responses after delivery of TBS were then monitored for 30 min or 2 hours (**Fig. 2.2b**).
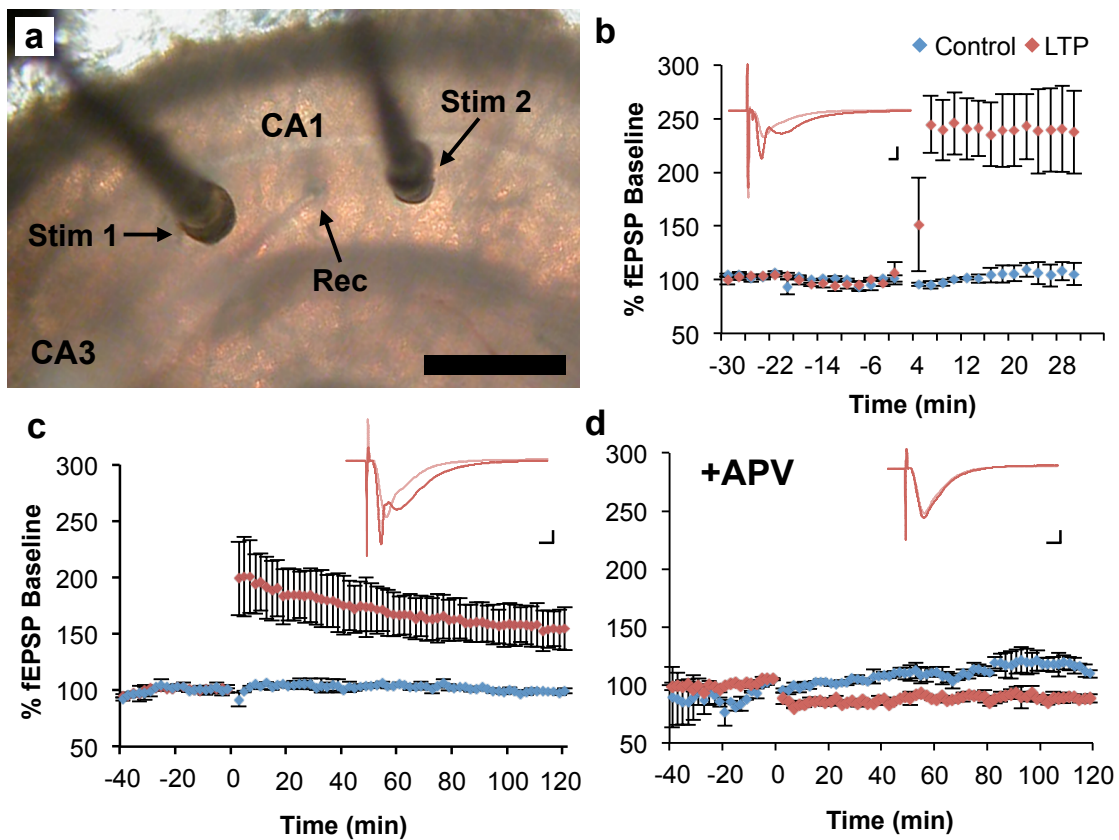
Figure 2.2: LTP induction in hippocampal area CA1 of adult rats. (a) Two stimulating electrodes (Stim 1 and 2) were positioned 600-800 μm apart on either side of a recording electrode (Rec) in the middle of stratum radiatum in hippocampal area CA1. Scale bar = 600 μm. Baseline responses were collected for ~40 min. TBS was delivered to one stimulating electrode to induce LTP while the other received control stimulation. Postsynaptic responses were monitored for (a) 30 minutes (3 slices from 3 animals) or (b) 2 hours (2 slices from 2 animals) post-TBS, after which the tissue was rapidly fixed (within 30 sec of last test pulse) and prepared for EM. (d) TBS delivered in the presence of APV did not produce LTP (2 slices from 2 animals). Insets show example averaged waveforms from responses to the stimulating electrode where LTP was induced before (pink) and after (red) receiving TBS. Scale bars = 5 mV/5 ms.

Fixation and Electron Microscopy

After the last test pulse, the electrodes were removed and the slice (still on its net) was turned into a mixed aldehyde fixative (6% glutaraldehyde and 2% paraformaldehyde in 0.1 M cacodylate buffer with 2 mM $CaCl_2$ and 4 mM $MgSO_4$). Penetration of the fixative into the middle of the tissue was enhanced by microwave irradiating the slice and fixative for 10 s while ensuring the slice did not reach greater than 35 ºC (Jensen and Harris, 1989). The slices were then kept in fixative overnight at room temperature and then embedded in 7% agarose and vibra-slices at 70 μm on a Leica WT 1000S vibratome (Leica, Nussloch, Germany) in cacodylate buffer. For each stimulation site, the vibra-slice containing the roughly 50-μm indentation of the stimulating electrode in its air surface along with two adjacent vibra-slices were kept to be further processing. The vibra-slices were processed for EM through 1% osmium and 1.5% potassium ferrocyanide mixture, 1% osmium alone, dehydrated through graded ethanols (50-100%) and propylene oxide, embedded in a plastic (LX112), and placed in a 60 ºC oven for 48 hours (Harris et al., 2006). Approximately 200 serial sections (each ~45 nm thick) were collected 150-200 μm lateral to the control and LTP electrodes at a depth of 120-150 μm from the air surface of the slice and were mounted on pioloform-coated slot grids (Synaptek, Ted Pella Inc., Redding, CA). Sections were counterstained with ethanolic uranyl acetate and Reynolds lead citrate. The serial sections and a calibration grid (Ted Pella Inc.) were then imaged on a JEOL 1230 transmission electron microscope (Peabody, MA) with a Gatan digital camera.

Three-dimensional Reconstructions

Each collection of serial section images (a "series") was coded with a random string of 5 letters so as to remain blind to condition. The series was imported into RECONSTRUCT™ (freely available at synapses.clm.utexas.edu) and aligned (Fiala, 2005; Fiala and Harris, 2001a). Actual section thickness was computed using the cylindrical diameters method by dividing the diameters of longitudinally sectioned mitochondria by the number of sections the mitochondria spanned (Fiala and Harris, 2001a). Dendrites and synapses had previously been traced in these series (Bourne and Harris, 2011a).

Statistical Analyses

Statistical analyses for this study were performed in Statistica (StatSoft, Tulsa, Oklahoma). A two-way ANOVA (factors: condition, slice) was used to ascertain whether the induction of LTP resulted in differences in frequency of bouton types at each time point. Hierarchical nested ANOVAs (hnANOVAs) were used to ascertain whether the induction of LTP resulted in changes in vesicle content per axonal bouton. For hnANOVAs, axon was nested in condition and experiment. Nested design was used to ensure none of our results were driven by a particular axon or experiment. To demonstrate differences from LTP at each time point, mean relative change (Δ mean ± standard error) is used in figures. This was calculated by subtracting individual measurements from the mean control value within each slice. Significance was set to $p < 0.05$ and asterisks in figures denote $p < 0.05$ (*), $p < 0.01$ (**), and $p < 0.001$ (***). Sample sizes are indicated in appropriate figure legends. For clarity, APV data is noted in the text.

2.3 Results

Sample Population of Axons and Boutons

We examined 772 excitatory boutons for the synaptic vesicle analyses. For a subset of those boutons, we reconstructed 192 axonal segments. Axons were identified as putatively excitatory (glutamatergic) by the presence of clear, round small synaptic vesicles opposed to a postsynaptic density (PSD) that was thickened (asymmetric). Boutons were classified according their number of postsynaptic partners. Single synaptic boutons (SSBs) had one post-synaptic partner, multi-synaptic boutons (MSBs) had two or more postsynaptic partners, and non-synaptic boutons (NSBs) were clusters of 10 or more vesicles along a length of axon with no postsynaptic partners (**Fig. 2.3**). At all times points and conditions, we found mitochondria present in ~50% of the analyzed population of boutons.

Bouton Types and Frequency

Our lab has previously shown that the number of smallest dendritic spines, those with a head diameter of less than 0.45 µm, was reduced by 33% 2 hours during TBS-induced LTP (Bourne and Harris, 2011a). Thus, it was of interest to investigate the corresponding presynaptic structural changes occurring during LTP. We reasoned that boutons would also be concomitantly reduced or there would be a shift in frequency of bouton types. To investigate the frequency of each type of bouton, we performed an unbiased three-dimensional volume (or "brick") analysis (Fiala and Harris, 2001b) by placing a 3.5 µm × 3.5 µm sampling frame on 50 serial sections of each series (**Fig. 2.4**) . All boutons falling within the sample frame or touching two inclusion lines (green) were included in the

47

analysis. Boutons falling outside the sample frame or touching two exclusion lines (red) were not analyzed[10]. A total of 1,334 boutons were identified as SSBs, MSBs, or NSBs in the unbiased volume. We calculated the density of each bouton type by dividing the number of boutons by the volume of the brick. At 30 min and 2 hours, the frequency of MSBs and NSBs during LTP was not significantly different from control conditions. However, at 2 hours but not 30 minutes, we uncovered a significant reduction of SSBs during LTP (**Fig. 2.5**). When TBS was delivered in the presence of APV, which blocks induction of LTP, the reduction of SSBs was prevented (APV-control: SSB = 2.04 ± 0.11; MSB = 0.54 ± 0.08; NSB = 0.58 ± 0.02; APV-TBS: SSB = 1.72 ± 0.13; MSB = 0.2 ± 0.11; NSB = 0.73 ± 0.13). These results suggest that the SSBs reduced 2 hours during LTP were the original partners of the small thin dendritic spines that were also eliminated during LTP. (See discussion below for alternate interpretation of these data.)

Vesicular Composition of Boutons

Vesicles in boutons exist in a variety of states (Alabi and Tsien, 2012; Rizzoli and Betz, 2005), which influence their release competency (Dobrunz, 2002; Murthy et al., 1997) and several studies have shown evidence that induction of plasticity is mediated in part by modulation of vesicular dynamics

---

[10] We refer to this analysis as "unbiased", because care is taken to prevent over-counting structures of interest (Fiala and Harris, 2001b). Here, by using a sample frame, we are estimating the frequency of boutons in the tissue from a population of sampled boutons. One can imagine that, if it were possible on these EM images to place two sample frames immediately adjacent to one another, a problem arises: Which sampling frame does a bouton belong to if it touches them both? To prevent "double counting", each sample frame includes two exclusion lines, which would overlap two inclusion lines of theoretical adjacent sample frames.
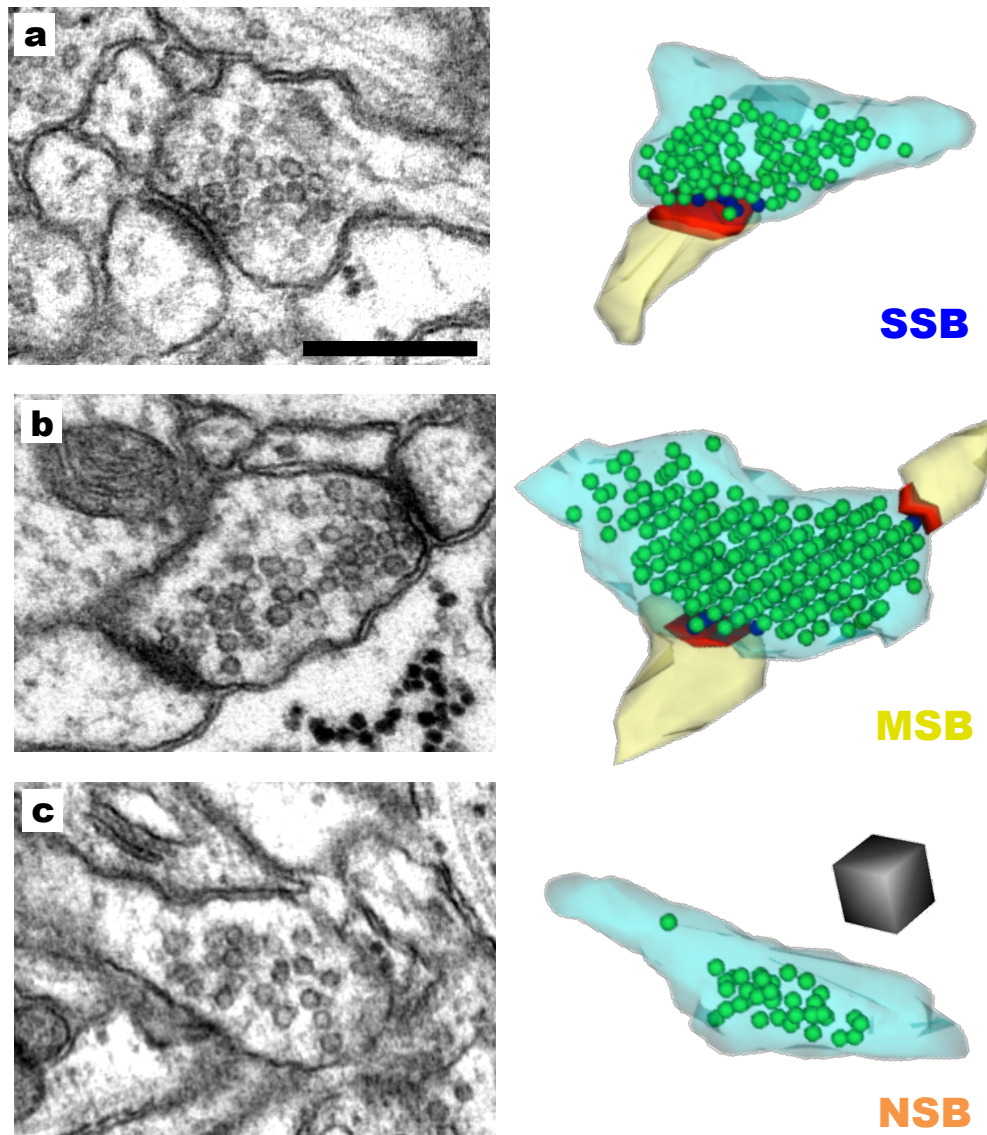
Figure 2.3 Boutons in area CA1 classified by number of postsynaptic partners. Boutons are shown in teal, non-docked synaptic vesicles in green, vesicles docked along the presynaptic active zone in dark blue, dendritic spine heads in yellow, and PSDs in red. (a) Single synaptic boutons (SSBs) form synapses with single postsynaptic partners. (b) Multisynaptic boutons (MSBs) form partners with multiple dendritic spines. (c) Non-synaptic boutons (NSBs) are varicosities along an axon containing more than 10 vesicles and do not have postsynaptic partners. Scale bar = 0.5 µm. Scale cube = 0.125 µm^3. Note: text color for type of bouton will carry through the rest of the figures in this chapter (i.e., blue for SSBs, yellow for MSBs, and orange for NSBs).

49
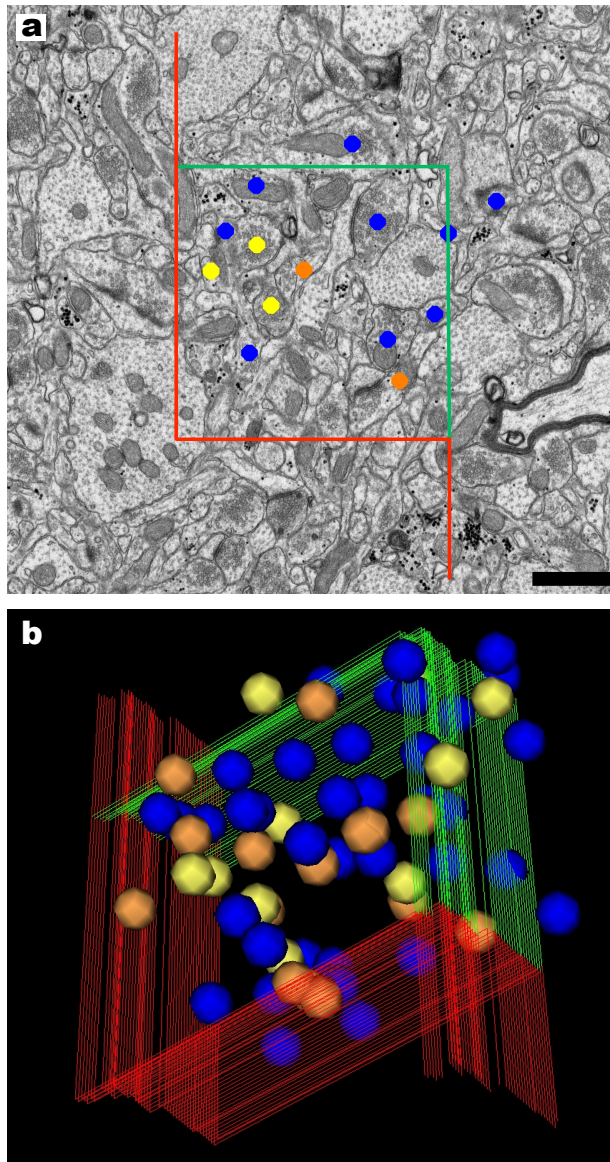
Figure 2.4: The unbiased "brick" allows sampling of bouton types in the neuropil.
(a) Example of a sampling frame overlaid on an electron micrograph. Each side of the sampling fame = 3.5 µm. Exclusion lines (red) and inclusion lines (green) are shown. See text for explanation of sampling methods. (b) Reconstructing multiple sampling frames over 50 sections reveals the construction of a virtual volume, which can be used to sample boutons in the neuropil. Each sphere represents the anatomical center of a bouton falling within or touching an inclusion line of the volume. SSBs are shown in blue, MSBs in yellow, and NSBs in orange. Scale bar = 1 µm.
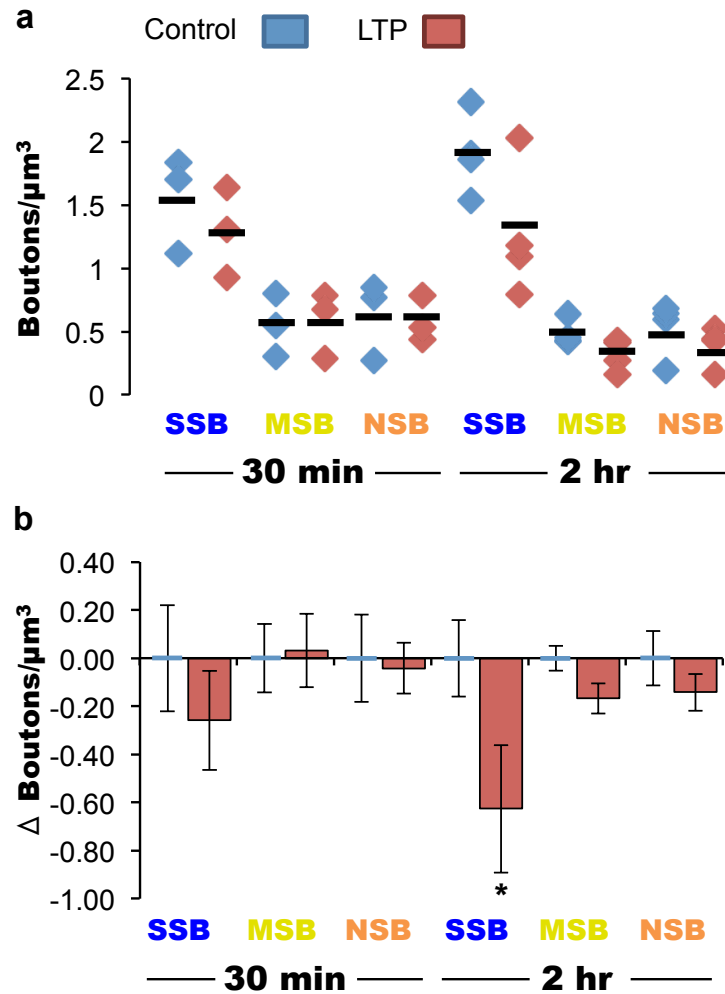
Figure 2.5: Single synaptic boutons are reduced by 2 hours during LTP. (a) The average frequency of each bouton type by time point and condition. The distribution of the data is indicated with diamonds. Superimposed black lines represent the mean of each group. 30 minute data: n = 3 bricks each for control and LTP. 2 hour data: n = 4 bricks each for control and LTP. (b) By 30 minutes during LTP, the frequencies of bouton types were not significantly different from control conditions. By 2 hours during LTP, however, single synaptic boutons were selectively reduced ($p < 0.05$, mean $\Delta \pm$ SEM).

51

(Enoki et al., 2009; Ratnayaka et al., 2012). Thus we were interested to investigate the vesicular composition of boutons during LTP. Vesicles that are docked to the presynaptic membrane are thought to be part of the readily releasable pool, vesicles available for release upon stimulation, while non-docked vesicles form the reserve vesicle pool (Branco et al., 2010; Harris and Sultan, 1995; Schikorski and Stevens, 2001). We classified vesicles as either docked if the vesicle was completely round and flush with the presynaptic active zone or non-docked (**Fig. 2.6**). By 30 min during LTP, the number of vesicles per synapse was reduced ($p < 0.01$). By 2 hours, however, the number of vesicles per synapse returned to control values (**Fig. 2.7a**). By 30 min during LTP, the size of vesicle pools was not different from control values. Interestingly, by 2 h during LTP, vesicle pools were significantly smaller than control values ($p < 0.001$, **Fig. 2.7b**). We did not observe changes in the number of docked vesicles per synapse or vesicle pool size when TBS was given in the presence of APV (APV-control: docked = 3.71 ± 0.3, non-docked = 311.39 ± 33.97; APV-TBS: docked = 3.68 ± 0.4, non-docked = 363.51 ± 41.7).

Endocytosis and Presynaptic Activity

To sustain release at synapses, vesicles must be recycled via endocytosis (Haucke et al., 2011; Lou et al., 2012; Murthy and De Camilli, 2003; Ryan, 2006). It was feasible that inducing LTP with TBS might have impaired endocytosis in our slices and this was driving the decrease in vesicle pool sizes we observed above. It was thus imperative to investigate endocytosis in our slices. Additionally, such a tight coupling of vesicular release and recycling suggests that anatomical evidence of endocytosis might serve to mark those boutons that
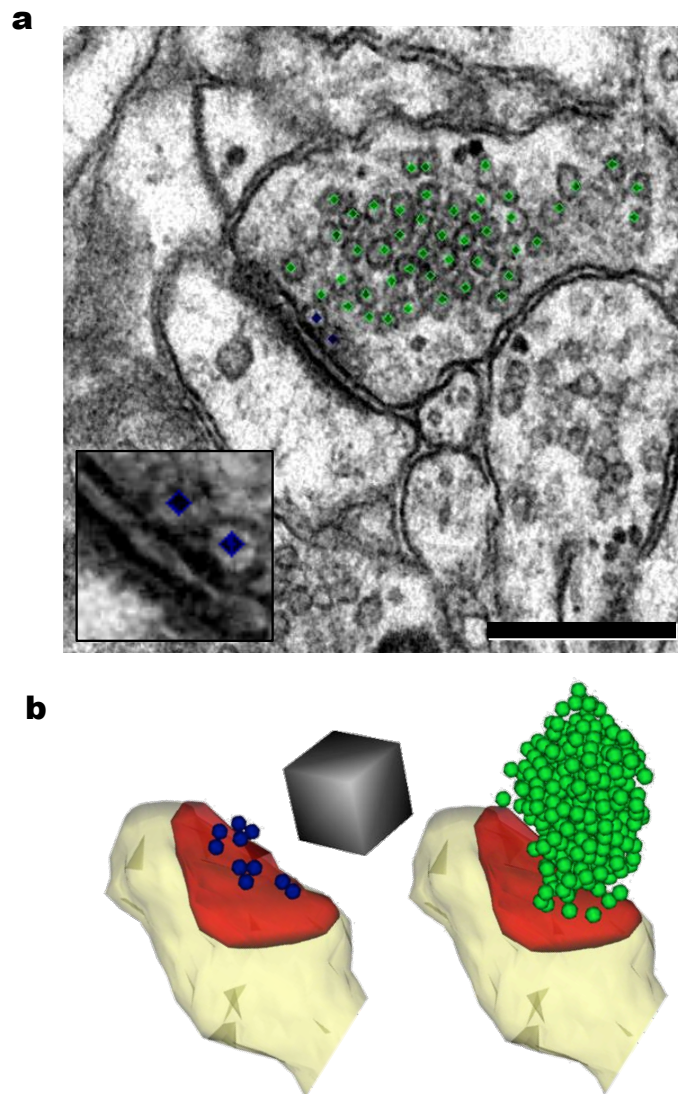
Figure 2.6: Morphology of vesicles pools at adult CA3-CA1 synapses. (a) Electron micrograph and (b) three-dimensional reconstructions of a dendritic spine (yellow), PSD (red), docked vesicles (dark blue), and non-docked vesicles (green). Vesicles were considered docked in their membrane were completely flush with that of the presynaptic active zone. Scale bar = 0.5 μm. Scale cube = 0.25 μm on each side.

53
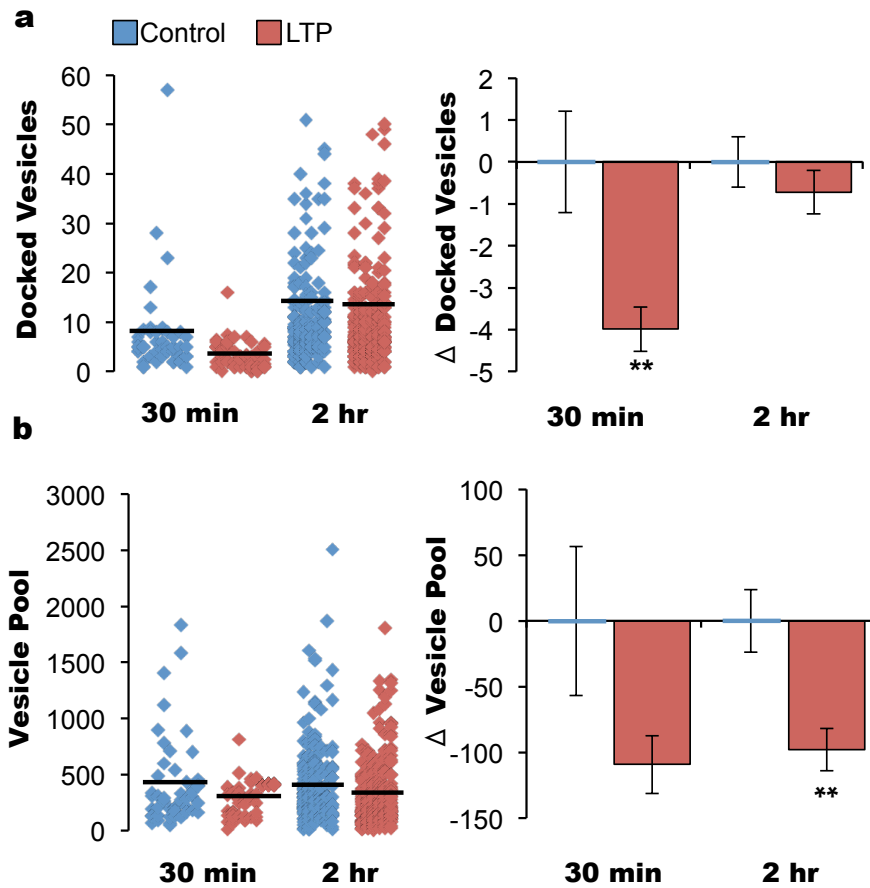
Figure 2.7: Decrease in docked vesicles followed by reduction in vesicle pool sizes during LTP. (a) Average number of docked vesicles in each condition and time point represented by superimposed black lines. Diamonds indicate the distribution of data. The number of docked vesicles per bouton decreased at 30 minutes during LTP (p < 0.01, mean Δ ± SEM). (b) Average size of vesicle pools in each condition and time point represented by superimposed black lines. Diamonds indicate the distribution of data. Vesicle pools were smaller at 2 hours during LTP (p < 0.01, mean Δ ± SEM). 30 minutes control: n = 49 boutons; 30 minutes LTP: n = 59 boutons; 2 hours control: n = 237 boutons; 2 hours LTP: n = 312 boutons.

were most active at fixation. To investigate if vesicle composition of boutons was related to endocytosis, we looked for evidence of clathrin-coated pits (CCPs), an early stage of endocytosis (**Fig. 2.8a**). In control conditions, we found CCPs in 17% of boutons (**Fig. 2.8b**). Furthermore, those boutons in control conditions with CCPs had more vesicles docked along the presynaptic active zone as well as larger vesicle pools than boutons without CCPs (**Fig. 2.8c, d**). We also observed CCPs in boutons during LTP, lending support to the notion that endocytosis was not impaired in our slices. When we categorized boutons as to whether or not they contained a CCP (**Fig. 2.9**), an interesting result emerged. At 30 min during LTP, the decrease in docked vesicles per synapse was only significant in boutons without a CCP ($p < 0.01$, **Fig. 2.10a**). The size of the vesicle pools was decreased at 30 min and 2 h during LTP in boutons with a CCP ($p < 0.05$). By 2 h, vesicles pools were also smaller in boutons without a CCP ($p < 0.01$, **Fig. 2.10b**). In the presence of APV, we did not detect a difference in docked vesicles per synapse or vesicle pool sizes regardless of the presence or absence of CCPs (APV-control: docked: +CCP = 3.57 ± 0.42, -CCP = 3.79 ± 0.4, non-docked: +CCP = 406 ± 79.17, -CCP = 266.33 ± 31.6; APV-TBS: docked, +CCP = 4.78 ± 0.91, -CCP = 3.21 ± 0.4, non-docked, +CCP = 453.87 ± 100.03, -CCP = 324.43 ± 40.7).

Vesicle Transport Packets

Vesicles are not confined to boutons but can be part of a so-called "superpool" of vesicles, that is to say vesicles that are shared between boutons along a length of axon (Darcy et al., 2006; Staras et al., 2010; Westphal et al., 2008). Vesicle "transport packets" that move between boutons might also play a
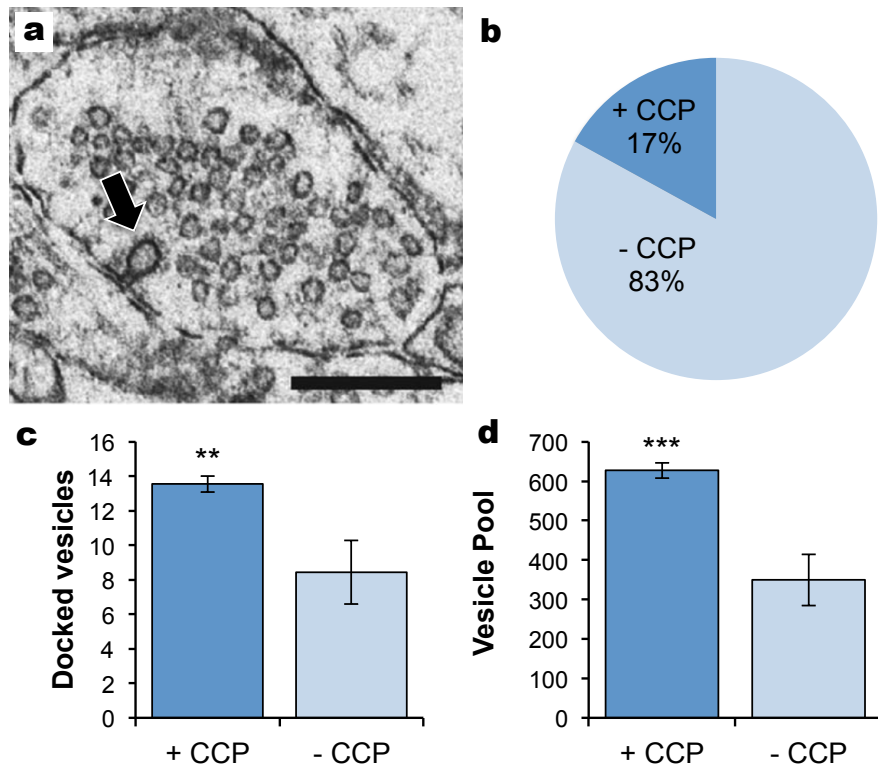
Figure 2.8: Clathrin-coated pits found in boutons with larger vesicle pools. (a) An electron micrograph from control conditions with an example of a CCP (black arrow). (b) Control data from both 30 minutes and 2 hour experiments were combined and revealed that 17% of boutons contained a CCP (n = 48 boutons with and 238 boutons without a CCP). Boutons with a CCP had significantly (c) more docked vesicles and (d) larger vesicle pools than boutons without a CCP. Scale bar = 0.5 μm.
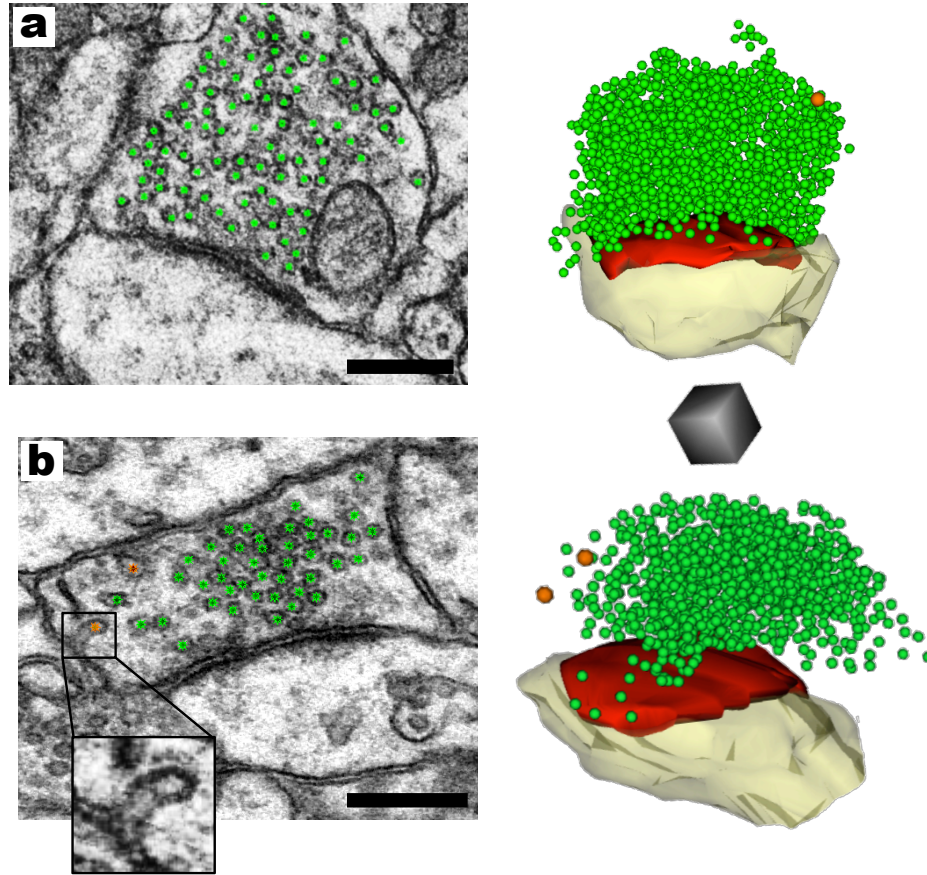
Figure 2.9: Vesicle pools and clathrin-coated pits. Example electron micrographs and reconstructions of non-docked vesicles (green), CCPs (orange), and associated dendritic spine (yellow) and PSD (red) from (a) 30 minute control data and (b) 2 hour LTP data. Inset shows magnified CCP. Scale bar = 0.25 µm. Scale cube = 0.0156 µm^3.
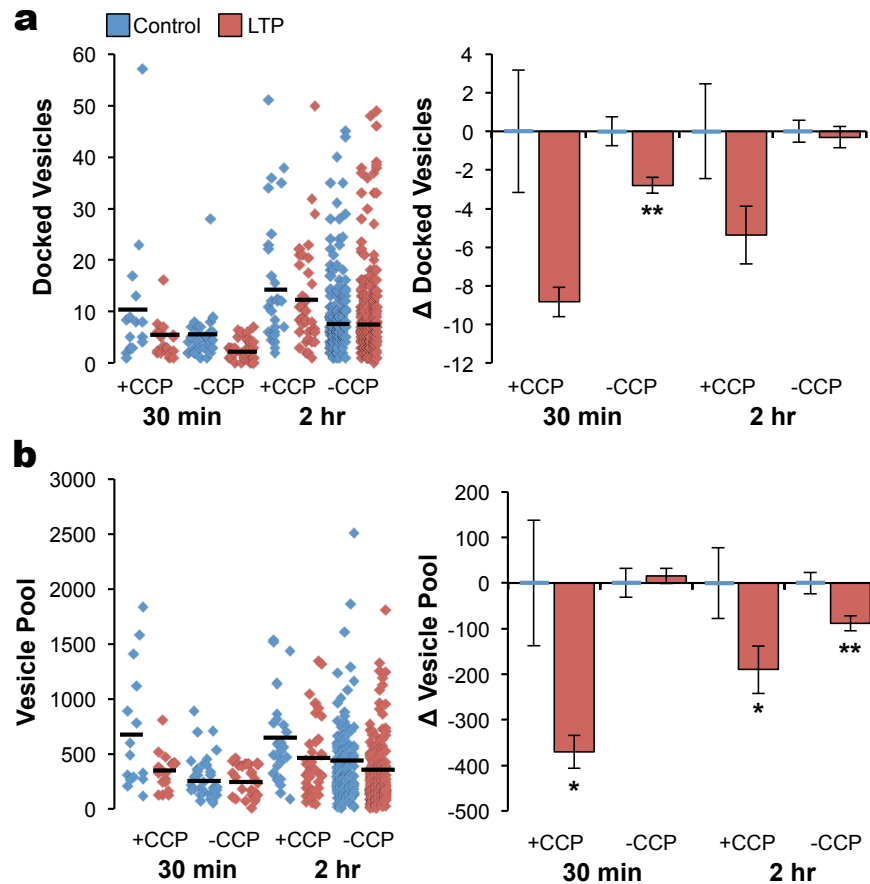
Figure 2.10: Vesicle pools are smaller in boutons with clathrin-coated pits. (a) Average number of docked vesicles shown with black lines in boutons classified by time point, condition, and presence or absence of CCPs. Individual data indicated with diamonds. At 30 minutes, the decrease in number of docked vesicles was significant in boutons without a CCP ($p < 0.01$, mean $\Delta \pm$ SEM). (b) Average size of vesicle pools shown with black lines in bouton classified by time point, condition, and presence or absence of CCPs. Individual data indicated with diamonds. Vesicles pools were smaller in boutons with CCPs at 30 minutes ($p < 0.05$) and 2 hours ($p < 0.05$). At 2 hours during LTP, boutons without CCPs were also significantly smaller during LTP ($p < 0.01$). Control: +CCP, n = 16 boutons, -CCP, n = 33 boutons; 30 minutes LTP: +CCP, n = 20 boutons, -CCP, n = 39 boutons; 2 hours Control: +CCP, n = 32 boutons; -CCP, n = 205 boutons; 2 hours LTP: +CCP, n = 43 boutons; -CCP, n = 269 boutons.

role in plasticity (Ahmari et al., 2000; Sabo et al., 2006; Ziv and Garner, 2004). To investigate if we could observe ultrastructural evidence of vesicle "sharing" between boutons, we considered the smallest NSBs, those that contained 10 vesicles or fewer, as potential vesicle transport packets (**Fig. 2.11a**). Curiously, a small fraction of transport packets in the tissue showed evidence of endocytosis (**Fig. 2.11c,d**), which suggests these vesicles were potentially release competent as they were moved along the axon. At 30 min during LTP, we found no difference in the number of transport packets. However, at 2 hours during LTP, transport packets along axons were nearly eliminated ($p < 0.01$, **Fig. 2.12**). We did not observe differences in the number of transport packets in control or LTP conditions when TBS was delivered in the presence of APV (APV-control = 21.64 ± 4.21% per axon; APV-TBS = 14.75 ± 4.01% per axon).

2.4 Discussion

This study uncovered significant presynaptic structural plasticity evident on the EM level during LTP in the adult animal. By 30 min during LTP, we found that vesicles docked at the active zone were reduced at synapses. By 2 hours during LTP, docked vesicles had returned to control levels while vesicles pools were reduced and a subset of boutons were lost. Transport packets of vesicles were nearly eliminated during LTP, which suggests that they were incorporated into boutons or released during transit. We used APV to block the induction of LTP and to control for the effects of the TBS paradigm we studied. APV prevented the loss of vesicles, boutons, and transport packets, suggesting that the results we observed were dependent on the activation of NMDA receptors.
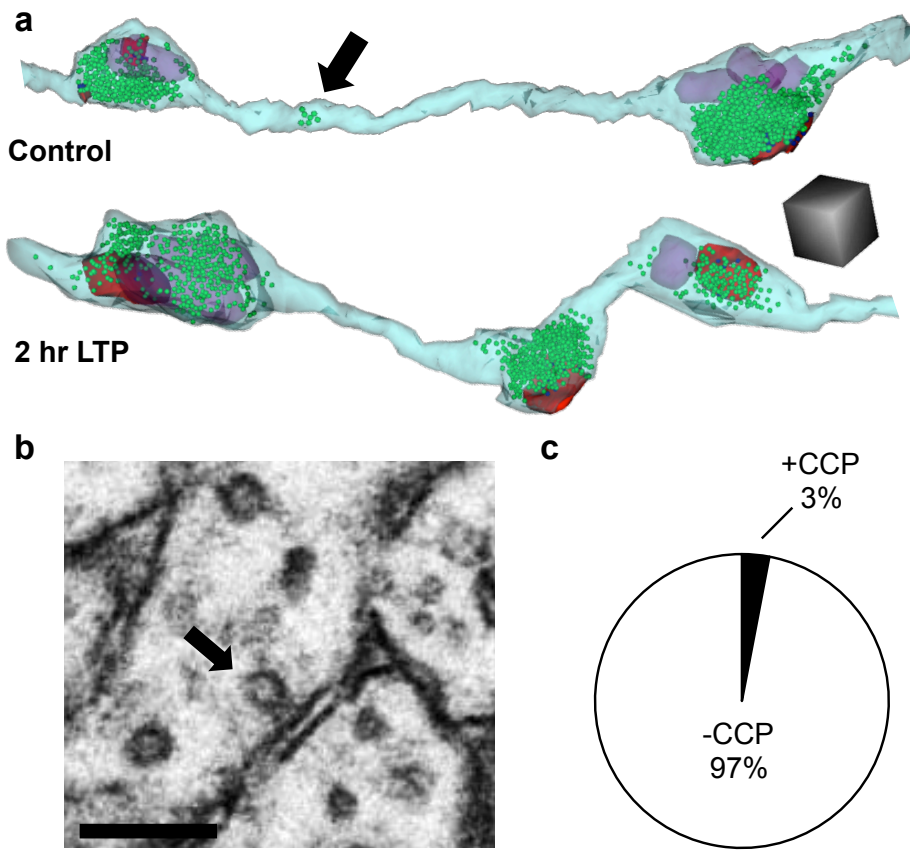
Figure 2.11: Transport packets along axons in area CA1. (a) Example reconstructions of axonal segments (teal) from each condition showing vesicle pools (green), synapses (red) and mitochondria (purple). Transport packets were non-synaptic boutons with fewer than 10 vesicles (black arrow). (b) Evidence of omega structures at transport packets (black arrow) might indicate potential for release at these sites. (c) A small fraction of transport packets contained a CCP (n = 2 transport packets with and 71 transport packets without a CCP). Scale cube = 0.125 µm^3. Scale bar = 0.25 µm.
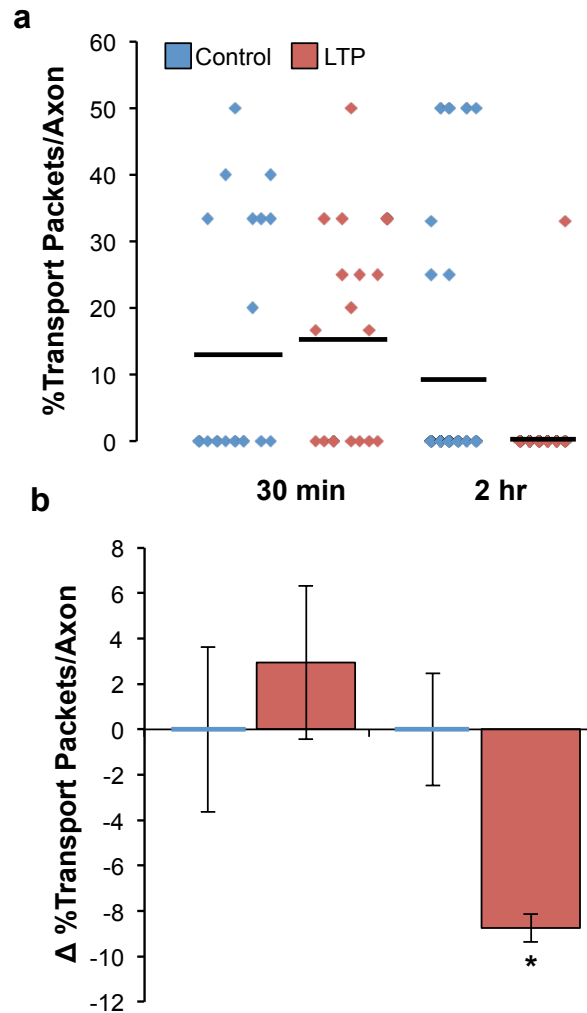
Figure 2.12: Transport packets nearly eliminated by 2 hours during LTP. (a) Average percentage of boutons along reconstructed axonal segments that were found to be transport packets in each condition shown with superimposed black lines. Diamonds indicate the distribution of data. (b) By 2 hours during LTP, the percentage of boutons along a reconstructed axonal segments that were transport packets was substantially reduced ($p < 0.05$, mean $\Delta \pm$ SEM), but not at 30 minutes. 30 minutes control: n = 21 axons, 77 boutons; 30 minutes LTP: n = 21 axons, 78 boutons; 2 hours control: n = 52 axons, 118 boutons; 2 hours LTP: n = 58 axons, 126 boutons.

Synapses as Dynamic and Cohesive Units

In a study using mice expressing a plasma membrane targeted enhanced GFP (green fluorescent protein) in a subset of neurons, De Paola et al. (2003) observed that presynaptic terminals of dentate granule cell mossy fiber axons projecting to CA3 appeared and disappeared over the course of 1-3 days in organotypic cultures. Furthermore, the group demonstrated that high frequency stimulation caused the conversion of stable presynaptic terminals into dynamic structures that lasted for 1-2 days. This conversion of stable to dynamic boutons required the activation of AMPA receptors and PKA as well at de novo protein synthesis. Several other studies have shown an increase in bouton turnover and remodeling during plasticity in cultured neurons (Antonova et al., 2001; Nikonenko et al., 2003) and this is consistent with the bouton reduction we report here in area CA1 of acute hippocampal slices.

The dynamic nature of boutons in both the hippocampus and cortex is not limited to younger animals but lasts into adulthood (Gogolla et al., 2007). In one of the first studies to demonstrate this (but see also De Paola et al., 2006), Stettler et al. (2006) employed the use of a nonreplicative adeno-associated virus to infect cells in the primary visual cortex of adult Macaque monkeys with enhanced GFP and were able to visualize boutons up to 500 μm below the cortical surface appearing and disappearing over the course of their recordings. Thus, not only does bouton turnover last into adulthood, but the dynamic nature of boutons and axons observed in rodent studies has also been replicated in other mammals more closely related to humans.

We observed a decrease in the frequency of SSBs without a concomitant change in the frequency of MSBs or NSBs. This suggests that complete synaptic

units were disassembled or prevented from forming, rather than boutons being converted to another type. To lend support to this notion, the 33% reduction in SSBs during LTP that we uncovered here corresponds perfectly to a 33% reduction in small thin spines previously reported in this tissue (Bourne and Harris, 2011a). It is likely these SSBs were the partners of those spines that were eliminated or prevented from forming by 2 hours during LTP. This finding argues that synapses in adult tissue are cohesive structures; that is to say, elimination of structures on either side of the synapse causes a reciprocal elimination of the other side. Without high temporal resolution we cannot determine definitely which unit is eliminated first. Further work is warranted to investigate whether retraction of dendritic spines triggers a disassembly of the associated presynaptic bouton or if the bouton is first to be eliminated. Furthermore, it is interesting to note that when terminal boutons at neuromuscular junctions are eliminated, the axon retracts (Bishop et al., 2004). Here, loss of en passant boutons seems to be specific to the particular synapse, as the hosting axon remains whole.

After the publication of this work, an alternate interpretation has emerged regarding the frequency of spines during LTP. Bell et al. (2014) compared the original postsynaptic data performed in slice (Bourne and Harris, 2011a) to perfusion fixed hippocampus. We found that, at 5 and 30 min in control tissue, spines were significantly reduced relative to perfusion fixed hippocampus. At 2 hours in the control tissue, this frequency had returned to perfusion fixed levels. Interestingly, this same pattern was found to occur for small but not large or medium spines. This suggested that the frequency of small thin spines were recovered by test-pulses delivered to control tissue by 2 hours. Furthermore, the frequency of small thin spines at 2 hours during LTP, which was reduced relative

63

to control conditions (Bourne and Harris, 2011a), was found to be similar to that at 5 and 30 minutes during control stimulation. This finding presents the intriguing possibility that LTP does not produce the elimination of small thin spines, but that it instead prevents the normal recovery of small thin spines that occurs between 30 min and 2 hours with test-pulses in control tissue. In light of this interpretation, the elimination of synaptic units during LTP we report above might actually be a failure to form new synaptic units as small spines are recovering. The work in Bell et al. (2014) does not, however, definitively discount the possibility that spines are eliminated during LTP. It would be crucial to increase the number of slices at each time point to guarantee variability between animals is not driving these results. Furthermore, an interesting next step would be to determine if spine number stabilizes by 2 hours or if test-pulses delivered to control tissue might produce an overproliferation of small spines at some point after 2 hours.

Vesicles and Release Probability

Using the styryl dye FM1-43, Schikorski and Stevens (2001) reported the morphological correlates of functionally distinct pools of vesicles in boutons. FM1-43 was loaded into cells in hippocampal cultures by stimulation of 40 action potentials at 20 Hz, a stimulation protocol previously identified by the same group to release a subset of vesicles immediately available for release known as the readily releasable pool (Rosenmund and Stevens, 1996). When FM1-43 releases photons upon photoconversion, free radicals are produced which oxidize and polymerize DAB (diaminobezidine), a substance that stains darkly during EM processing (Sandell and Masland, 1988). Schikorski and Stevens found that, after loading cells with FM1-43, the number of darkly stained vesicles (in other

words, those that had been released and endocytosed along with dye) equaled the number of vesicles docked along the presynaptic active zone. This finding strongly suggested that docked vesicles evident in EM sections are the morphological correlate of the readily releasable pool. Yet docked vesicles account for less than 5% of all vesicles in boutons synapsing with spiny dendrites in stratum radiatum of CA1, boutons that can have from tens to thousands of vesicles (Harris and Sultan, 1995). Release probabilities vary widely from bouton to bouton (Dobrunz and Stevens, 1997; Murthy et al., 1997) and it is thought that minimal stimulation results in release of just a single vesicle (Hanse and Gustafsson, 2001; Hjelmstad et al., 1997; Stevens and Wang, 1995).

These findings all raise an intriguing question: Why are there so many vesicles in these boutons?[11] In an interesting study investigating the site of LTP expression in CA1 pyramidal cells, Enoki et al. (2009) employed calcium dyes in tissue from rats (21-28 days old) and reported an increase in the probability of transmitter release but not a significant increase in EPSPs. Though one should question whether the use of calcium dyes affected the postsynaptic response in their preparations, these findings led the researchers to conclude that LTP at CA1 pyramidal cell synapses is driven primarily by an increase in presynaptic release probability as opposed to the postsynaptic recruitment and insertion of AMPA receptors. Though the debate over the exact location of LTP expression (pre- or postsynaptic) rages ever on, this group remarked on their use of animals older than those used in studies concluding that LTP is expressed primarily

---

[11] Questions that begin with "why" are often difficult to address when considering biology. Though they carry the same meaning, it is more appropriate scientifically to pose the following questions: *What evolutionary pressure(s) might have led this outcome?* or *What is the adaptive significance of this finding to the organism?*

postsynaptically. Thus, their assumption is that presynaptic plasticity might play a larger role during LTP in older animals. To lend further support to this idea, silent synapses (post-synaptic densities that are thought to host NMDA receptors only and are thus prime candidates for AMPA receptor insertion) become less frequent as animals develop (Durand et al., 1996). An array of other studies have supported this group's findings and have concluded that synaptic facilitation and LTP can induce a shift from release of single vesicles to multivesicular release or can result in enhanced exocytosis of the readily releasable pool (Bayazitov et al., 2007; Bolshakov et al., 1997; Christie and Jahr, 2006; Sokolov et al., 2002; Zakharenko et al., 2001). Thus, it is possible that the reduction in docked vesicles we report here is an anatomical reflection of an increase in release that accompanies LTP at these synapses. This interpretation of the data is entirely consistent with work done in culture that shows resting vesicles are recruited into the recycling pool and that also demonstrate an increase in the release and recycling of vesicles during LTP (Ratnayaka et al., 2012).

Reserve Pool Vesicles

In this work, we also uncovered a significant decrease in the size of vesicle pools 2 hours during LTP. To investigate the time course of clathrin-mediated endocytosis, Granseth et al. (Granseth et al., 2006) took advantage of sypHy, an optical reporter of exo- and endocytosis created by the fusion of a pH-sensitive GFP (Miesenböck et al., 1998) to the synaptic vesicle protein synaptophysin. They found that clathrin-mediated endocytosis played a dominant role in retrieval of vesicles at synapses and that it occurred over tens of seconds. The quick time course of clathrin-mediated endocytosis has been shown in a

variety of studies (Rizzoli and Jahn, 2007). Here, the observation of CCPs in boutons argues against the idea that exocytic/endocytic machinery was impaired in our tissue preparations and does not account for the decrease in vesicle pool size we report above.

Furthermore, while the kinetics of the readily releasable pool might not be influenced by LTP, the dynamics of the reserve pool might be influenced by plasticity. Spontaneous release of neurotransmitter at very low rates (< 0.1 Hz) has been known to occur since the earliest days of synaptic transmission research (del Castillo and Katz, 1954; Fatt and Katz, 1950; 1952). More recently, Fredj and Burrone (2009) showed evidence of a unique subset of vesicles in boutons that was not mobilized by neuronal activity but was instead released spontaneously, a so-called "resting" pool of vesicles. While the exact details of whether these vesicles are truly a unique category unto themselves or are part of the same vesicle pool that is engaged during stimulated release are still intensely investigated (Truckenbrodt and Rizzoli, 2014), it follows that an increase in spontaneous release during LTP might ultimately decrease the size of the reserve pool. Additionally, a variety of studies have demonstrated an increase in the frequency of mini-EPSPs during LTP (Bekkers and Stevens, 1990; Malgaroli and Tsien, 1992; Wiegert et al., 2009). This supports to idea that mechanisms of plasticity might engage vesicles that release in the absence of stimulation.

Vesicles and Active Zone Expansion

Another intriguing idea to consider is that some vesicles "lost" during LTP might actually have been contributing to the expansion of the presynaptic active zone, serving a structural rather than physiological role during plasticity. Yao et

al. (2009) described Flower, a novel transmembrane calcium channel in synaptic vesicles at the neuromuscular junction of drosophila. Fusion of synaptic vesicles containing Flower at the periphery of the active zone resulted in the addition of calcium channels that controlled the intracellular levels of presynaptic calcium. Dense core vesicles (DCVs), which are slightly larger than synaptic vesicles and have (as their name suggests) a characteristic dark core, carry proteins required for the assembly of the presynaptic active zone (Shapira et al., 2003; Zhai et al., 2001). However, only a quarter of boutons in perfusion-fixed hippocampus contain DCVs and even less contain DCVs in slices (Sorra et al., 2006). In a recent paper from our lab, my colleagues and I demonstrated that the frequency of DCVs increases in boutons immediately following the induction of LTP with TBS (Bell et al., 2014). Even at a time during LTP when rapid synaptogenesis is occurring (Bourne and Harris, 2011a), < 10% of boutons contain DCVs. Thus it follows that some subset of vesicles within the reserve pool might also be providing the active zone a suite of structural proteins, receptors, channels, and necessary membrane that support expansion of synapses at boutons that do not contain a DCV. If these vesicles do contain calcium channels, exocytosis could theoretically cause an increase in release probability that might further chip away at the size of vesicles pools. Immunohistochemical studies on a variety of active zone proteins might aid in uncovering if active zone proteins localize to synaptic vesicles as well as DCVs. Another more direct way to investigate this question in our tissue would be to investigate if we can detect an increase in surface area of boutons 2 hours during LTP. An increase in surface area in boutons during LTP would support the idea that vesicles have been inserted into the membrane and that the vesicle pools are not being dismantled and subsequently degraded.

68

The Vesicular Superpool during Plasticity

Synapses do not operate in isolation of their neighboring partners. In fact, neighboring synapses can have similar release probabilities (Murthy et al., 1997) and plasticity induced at one synapse can spread to nearby synapses (Bonhoeffer et al., 1989). Similarly, synaptic vesicles are not restricted to a particular bouton but have been shown in culture to move between adjacent release sites along axons (Chen et al., 2008a; Darcy et al., 2006; Westphal et al., 2008). This pool of vesicles has been referred to as the vesicular "superpool" as addressed in the introduction to this chapter. Staras et al. (2010) showed the first evidence that vesicles arising in one pool are capable of rapid exocytosis upon arrival at adjacent active zones along axons in acute hippocampal slices. Using a fixable form of FM1-43, the group demonstrated vesicles moving into neighboring boutons and fusing with membrane during ongoing stimulation. This work provided strong evidence that "non-native" vesicles in boutons are able to participate in the presynaptic function of release sites along axons, especially under conditions of ongoing stimulation. Furthermore, it was subsequently shown in culture that vesicles transported between synapses along axons are also able to fuse and release neurotransmitter at interbouton, extrasynaptic sites (Ratnayaka et al., 2011). Here, we demonstrate the first evidence of release and recycling of vesicles in transport packets along axons in hippocampal tissue from adult animals. Furthermore, we observed that transport packets of vesicles were all but eliminated 2 hours during LTP. This finding coupled with the observation that vesicle pools are smaller at 2 hours during LTP suggests that transport packets are moved into existing synaptic sites during plasticity to supplement vesicle pools.

Concluding Remarks

Collectively, these results provide evidence to support the idea that structural plasticity is coordinated at pre- and postsynaptic sides of the synapse. We show that the percentage of boutons reduced during LTP correlated perfectly with the percentages of small thin spines reduced during LTP. This finding suggests boutons were either concomitantly eliminated with small thin spines or they were prevented from forming during LTP. Furthermore, as PSDs enlarge (Bourne and Harris, 2011a), several presynaptic structural modifications occurred 2 hours during LTP, including the decrease in vesicle pool sizes and the elimination of transport packets of vesicles. Vesicle pools during LTP might shrink as release probability at synapses increases, spontaneous vesicular release increases, or vesicles needed to support active zone expansion are exocytosed. None of these possibilities are mutually exclusive. More work is necessary to uncover vesicle pool variation and whether vesicles pools are replenished back to control levels at later stages during LTP.

While this work has demonstrated that presynaptic remodeling occurs concomitantly with postsynaptic structural plasticity, the subcellular elements that might determine which synapses expand during LTP are still not clear. Smooth endoplasmic reticulum (SER) is an organelle found throughout the neuron and its position and functions suggest it might be involved. In the next chapter of this dissertation, I discuss an investigation into the plasticity of dendritic SER and how it might function to coordinate structural plasticity during LTP.

Chapter 3: Plasticity of Dendritic SER

3.1 Introduction

The endoplasmic reticulum (ER) is an elaborately interwoven, membranous network of tubules and cisterns present in nearly all eukaryotic cells[12] (**Fig. 3.1**). ER was first described by the Belgian scientist Albert Claude, who, in a 1945 EM study with Keith Porter and Ernest Fullum at the then Rockefeller Institute, described a "lace-like" reticulum in the endoplasm (granular inner core) of chick embryo cells (Porter et al., 1945)[13]. (Claude would go on to win the Nobel Prize in 1974 with Christian de Duve and George Palade "for their discoveries concerning the structural and functional organization of the cell.") The structure described by Claude is by far the largest subcellular organelle, traversing vast distances throughout the cell. Even in neurons, whose dendritic and axonal arbors put on display some of the extremes in cellular geometry, ER extends as an uninterrupted network through their many fine processes (Blaustein and Golovina, 2001; Broadwell and Cataldo, 1984; Droz et al., 1975; Martone et al., 1993; Terasaki et al., 1994). The ER has a variety of functions, including acting as a store of calcium, releasing arachidonic acid, interacting with mitochondrial apoptotic machinery, producing steroid hormones, and, in conjunction with ribosomes, contributing to the post-translational modification of proteins (Berridge, 2002). In the soma and proximal processes of hippocampal neurons, ER ornamented with ribosomes, so-called "rough" endoplasmic

---

12 Notable exceptions include red blood cells and spermatozoa.

13 The term endoplasmic reticulum (*reticulum*, Latin for "net") was first cautiously applied to this organelle in 1948 in a figure caption (Porter and Thompson, 1948). It more boldly applied by Keith Porter in a subsequent publication in the early 50s (Porter and Kallman, 1952).
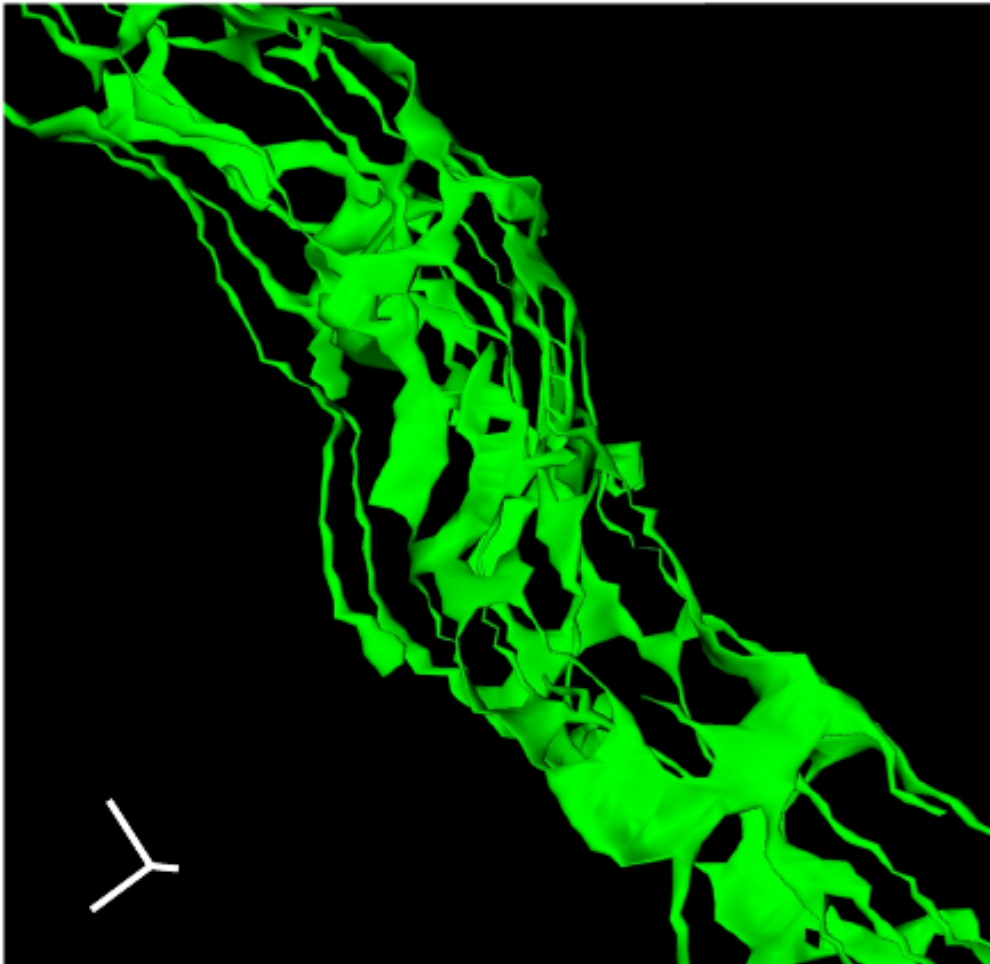
Figure 3.1: Interconnected membranous SER network in CA1 dendrites. Example reconstruction of SER (green) in a CA1 pyramidal cell dendrite from an adult rat. The SER forms a highly interconnected network of membranous tubules and cisterns that extends through the distal dendritic arbor. Each three-dimensional scale line represents 0.25 μm.
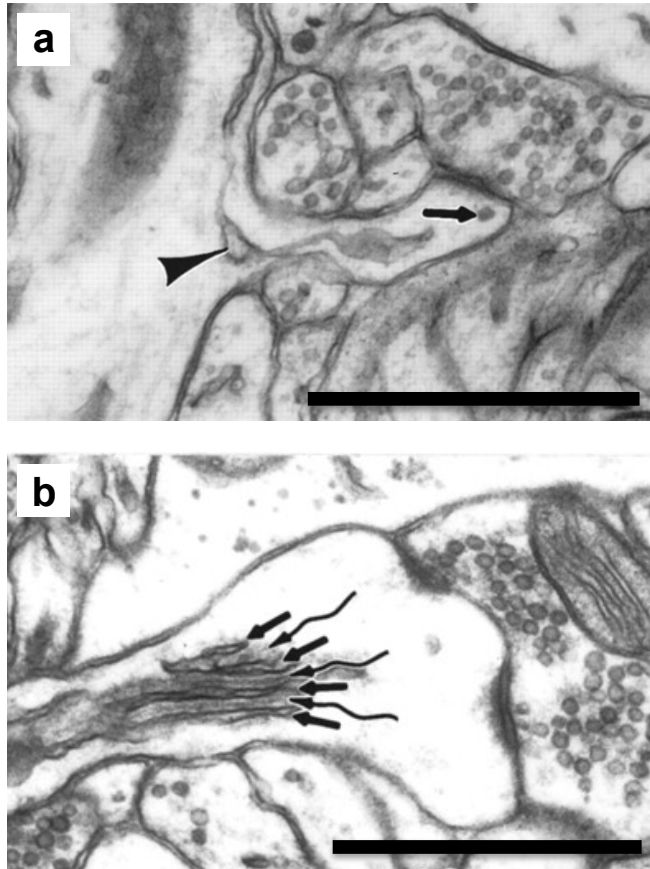
Figure 3.2: SER structures in dendrites and spines on electron micrographs. Two outstanding EM examples of SER structures in stratum radiatum of hippocampal area CA1 from an adult rat. (a) SER appears as a membranous network with a clear lumen on electron micrographs (arrowhead). Note that SER in dendritic spines in continuous with SER extending through the dendritic shaft. (b) Occasionally SER is found in dendritic spines as an elaborate spine apparatus, folds of SER (bold arrows) stacked between densely staining material (wavy arrows) that is known to be enriched in the actin-associating protein synaptopodin. Scale bars = 1 µm. Adapted from Spacek and Harris, 1997.

reticulum (RER), predominates. Smooth endoplasmic reticulum (SER), ER lacking ribosomes, is more prominent in distal neuronal processes.

In CA1 pyramidal cell dendrites, SER is non-uniformly distributed along the dendritic shaft and anatomical investigations have demonstrated that spines tend to congregate along the dendrite where more SER is found (Spacek and Harris, 1997). SER enters a subset of CA1 dendritic spines (< 20%, **Fig. 3.2**) as a simple tubule or as an elaborate SER structure known as a spine apparatus (Gray, 1959; Harris and Stevens, 1989; Mignery et al., 1989; Spacek and Harris, 1997). In other neurons, such as cerebellar Purkinje cells, SER enters almost every spine (Harris and Stevens, 1988). As further explored below, the many functions of ER, as well as its presence near synapses, mean ER is positioned to hold tremendous influence over the malleability of synaptic weight.

In this chapter of my dissertation, I discuss using three-dimensional reconstructions from serial section EM to investigate the structure of SER during LTP. Specifically, I investigate whether there is anatomical evidence that SER remodeling supports synapse enlargement during LTP in the mature hippocampus. (For clarity, ER is only referred to as SER if it was demonstrated unambiguously to lack ribosomes on EM sections. Otherwise the term ER is used.)

Calcium Stores and Synaptic Plasticity

It is well established that calcium plays a vital role in the modulation of synaptic weight thought to underlie learning and memory (Baker et al., 2013; Barad, 2006; Berridge, 1998; Franks and Sejnowski, 2002; Malenka and Bear, 2004). It follows that organelles capable of regulating calcium signaling could

serve to modulate plasticity at nearby synapses. Although the role played by the sarcoplasmic reticulum (specialized ER in skeletal muscle) in calcium homeostasis had been recognized since the late 1950s and early 1960s (Ebashi and Endo, 1968; Weber et al., 1966), the first inkling that ER was involved in neuronal calcium signaling was not demonstrated until the late 70s with calcium flux studies by Blaustein et al. (Blaustein et al., 1978a; 1978b; 1978c). Soon thereafter, anatomical studies demonstrated the presence of densely staining calcium oxalate precipitates on electron micrographs in SER stores after incubation of synaptoneurosomes in a solution containing calcium, oxalate, and saponin (McGraw et al., 1980). These findings provided nice structural evidence to support the idea that ER in neurons is acting a store of calcium, a near universal role for ER in eukaryotic cells (Pozzan et al., 1994).

Though ER had been shown to be a large store of intracellular calcium, the signaling cascades involved in calcium release from those stores were unknown. A major step forward came from investigations into the release of calcium from non-mitochondrial stores in isolated exocrine cells from the pancreas of rats (Streb et al., 1983). In this groundbreaking study, the group demonstrated that a small, water-soluble sugar phosphate, inositol 1,4,5-trisphosphate (IP_3), a product of neurotransmitter and hormone-triggered phosphoinositide hydrolysis, diffuses rapidly through the cytosol and is able to trigger calcium release from ER stores. (Over the past 30 years, these lipid-derived secondary messengers are now taught to nearly all undergraduate biology students as canonical signaling events capable of influencing a vast array of cellular processes.) Release of calcium from ER stores upon activation of IP_3 receptors parallels the release of calcium from sarcoplasmic reticulum in muscle

cells through the activation of ryanodine receptors by calcium (i.e., calcium-induced calcium release) or caffeine (Blaustein and Golovina, 2001; Kuo and Ehrlich, 2015). In fact, a large assortment of studies since the 90s have shown that IP$_3$ receptors and ryanodine receptors coexpress in both neurons and glia (Fujino et al., 1995; Galeotti et al., 2008; Kushnir et al., 2010; Seymour-Laurent and Barish, 1995; Sharp et al., 1993; Sheppard et al., 1997; Simpson et al., 1998; Walton et al., 1991). Release of calcium from these stores influences synaptic plasticity. Early studies showed that depleting calcium stores with thapsigargin, a SERCA (sarco/endoplasmic reticulum calcium ATPase) pump inhibitor, prevents the induction of LTP with a single train of tetanic stimulation (Harvey and Collingridge, 1992) but not LTP induced with stronger patterns of stimulation (Behnisch and Reymann, 1995; Raymond and Redman, 2002; 2006). In dendritic SER there appears to be an interesting differential localization of the types of receptors involved in calcium release from intracellular stores. Using immunohistochemistry, Sharp et al. (1993) found that, in hippocampal area CA1, IP$_3$ receptors are predominately expressed along the dendritic shaft and in pyramidal cell bodies, whereas ryanodine receptors are more likely to be found in dendritic spines. This contrasts with other areas of the brain. IP$_3$ receptors are highly concentrated in dendritic spines of cerebellar Purkinje cells where they contribute to a slow increase in intracellular calcium (Rose and Konnerth, 2001).

The localization of ryanodine receptors in CA1 dendritic spines and the role calcium plays in plasticity (see *Section 1.2: Early LTP/LTD Studies*) suggest these receptors are closely linked with synaptic signaling and malleability. Ryanodine receptors are activated by calcium entering through ionotropic glutamate receptors and voltage-gated calcium channels and are able to amplify

76

a weak synaptic stimulus through calcium-mediated release (Berridge, 1998; Rose and Konnerth, 2001; Segal and Korkotian, 2014; Verkhratsky and Shmigol, 1996). Caffeine and low concentrations of ryanodine (nM to ~10 µM) are ryanodine receptor agonists while high concentrations of ryanodine (> 100 µM), cyclopiazonic acid (CPA), dantrolene, and ruthenian red are ryanodine receptor antagonists (Baker et al., 2013; Segal and Korkotian, 2014). Wang et al. (1996) showed in the dentate gyrus that a low frequency stimulation pattern (5 Hz, 900 pulses) normally inducing LTD can be converted to an LTP inducing stimulus by applying low concentrations of ryanodine. The group also showed that this was blocked in the presence of ruthenian red, suggesting that the added calcium released from stores in dendritic spines is able to induce potentiation. Furthermore, in area CA1, application of low concentrations of ryanodine converts short-term LTP into a longer-lasting potentiation (Sajikumar et al., 2009). Interestingly, this effect is blocked by CPA and only occurs in the ventral hippocampus (Grigoryan et al., 2012). In CA1 of the dorsal hippocampus, where the concentration of ryanodine receptors was found to be lower, ryanodine receptor agonism does not convert short-term LTP into a longer-lasting potentiation. Intrigued in investigating the spatial dynamics of calcium release from ryanodine receptors, Raymond and Redmann (2002; 2006) showed ryanodine receptor antagonism blocks LTP induced with weak stimulation (a single train of TBS: 10 bursts at 5 Hz of 4 pulses at 100 Hz) but not with stronger stimulation (4 or 8 trains of TBS). The researchers also showed that the ryanodine-dependent release of calcium was localized to dendritic spines, supporting Sharp et al. (1993), and suggesting that stronger stimulation patterns

are able to access calcium from other intracellular stores – possibly those in the dendritic shaft as discussed below.

IP$_3$ receptors localizing to the shaft of CA1 dendrites suggests that they might be coordinating the activity of neighboring synapses. IP$_3$ receptors are blocked by heparin (Baker et al., 2013) and Wang and Kelly (1997) showed that combined blockade of IP$_3$ receptors with heparin and ryanodine receptors with dantrolene blocks the induction of LTP with tetanic stimulation. While this was not conclusive evidence to support the role of IP$_3$ receptors in the modulation of LTP, further support for the notion came when Kwon and Castillo (2008) demonstrated that IP$_3$ receptor antagonism blocks an NMDA receptor-dependent form of LTP at mossy fiber-CA3 synapses. Furthermore, IP$_3$ receptors, via the hydrolysis of phoshoinositides, act as a go-between in the modulation of AMPA and NMDA receptor function by acetylcholine (ACh) and other neuromodulators (Raymond and Redman, 2006). A set of interesting studies showed that activation of cholinergic afferents synapsing on CA1 pyramidal cells causes an enhancement of synaptic transmission through AMPA receptor insertion (Fernández de Sevilla and Buño, 2010; Fernández de Sevilla et al., 2008). The activation of muscarinic ACh receptor activation and release from IP$_3$-sensitive stores were required for this unique form of plasticity. Furthermore, this enhancement could be recreated through the uncaging of IP$_3$ alone. Thus, since the activation of both ryanodine and IP$_3$ receptors influence synaptic function and since the receptors are thought to be localized to different portions of the dendrite, an anatomical investigation into the remodeling of ER during LTP might shed light on their function during plasticity.

The Spine Apparatus

The structure of the spine apparatus is one of the more striking dendritic features one encounters on electron micrographs of neural tissue. Spine apparatuses are an elaborate structure of multiple SER folds stacked in between densely staining material (**Fig. 3.2b**), which occasionally comes in close contact with the PSD (Gray, 1959; Spacek, 1985; Spacek and Harris, 1997). Eva Fifková at the University of Colorado in Boulder proposed that the spine apparatus could serve as a large, local source of calcium immediately available to synapses after she observed calcium oxalate precipitates in the spine apparatus on electron micrographs (Fifková et al., 1983). Furthermore, she correctly posited that this would mean the spine apparatus could modulate the plasticity of those nearby synapses. Addressing this hypothesis, however, would come after a key discovery concerning the densely staining material found in spine apparatuses. Originally described in renal podocytes, synaptopodin[14], an actin-associating protein, was found to be enriched in the dense material found in spine apparatuses (Asanuma et al., 2005; Deller et al., 2000; Mundel et al., 1997). Since these first descriptions of synaptopodin, many groups have sought to uncover its association with synaptic plasticity. Synaptopodin expression has been shown to increase following tetanic stimulation and is presumed to be one mechanism underlying the transition from short- to long-term potentiation

---

[14] Even though our field rarely considers synaptopodin beyond the spine apparatus, *-podin* pays homage to the fact that this protein is highly expressed in renal podocytes. To my knowledge, the unique structure of the spine apparatus does not exist in podocytes. In fact, whereas synaptopodin knock-out mice lack spine apparatuses normally present in telencephalic dendrites, they show normal renal podocyte ultrastructure (Asanuma et al., 2005). Podocytes in these knockout mice do, however, show enhanced susceptibility to glomerular injury induced with chemical or bacterial toxins.

(Fukazawa et al., 2003; Yamazaki et al., 2001), though this has not been definitively demonstrated. Interestingly, a subset of rats exposed to a forced swim test also express increased levels of synaptopodin in stratum radiatum of area CA1 in dorsal hippocampus (Vlachos et al., 2008). Synaptopodin knockout mice completely lack spine apparatuses and a structurally related organelle knows as the cisternal organelle (Bas-Orth et al., 2007; Deller et al., 2003). Deller et al. (2003) showed that synaptopodin knockout mice have spines that appear structurally normal but they show extreme reductions in LTP induced with both tetanic stimulation and TBS. A variety of other studies have also supported the notion that synaptopodin-deficient mice have deficits in synaptic plasticity, including demonstrating impaired LTP induced in vivo (Jedlicka et al., 2009), development (Zhang et al., 2013), and abnormal network activity (Korkotian et al., 2014).

What is more interesting is that the spine apparatus appears to be able to regulate distinct forms of plasticity. Vlachos et al. (2009) transfected hippocampal cultures with GFP-tagged synaptopodin and monitored the differences in plasticity expressed at synaptopodin+ and synaptopodin- cells. Cells were patch clamped and responses to flash photolysis of caged glutamate at individual synapses were recorded. Currents generated in spines with synaptopodin were twice as large as those without synaptopodin. As this was found to be true in similarly sized spines, their findings suggested that spine apparatuses are able to amplify signals generated within the spine. Building upon Sharp et al. (1993), the group showed that synaptopodin fluorescence overlapped with ryanodine receptors and that ryanodine receptor antagonism with high concentrations of ryanodine or CPA treatment reduced AMPA receptor subunit expression in

dendritic spines by ~40%. Furthermore, treatment with CPA reduced synapse enlargement after chemical induction of LTP. Holbro et al. (2009) investigated the role ER plays in another form of plasticity, long-term depression (LTD), and showed that ER associated with synaptopodin influences the magnitude of plasticity at individual synapses. The group visualized ER by transfecting organotypic slice cultures with an enhanced GFP with ER targeting and retention sequences. Interestingly, CA1 spines with ER (most likely spine apparatuses) were able to express LTD induced by metabotropic glutamate receptor (mGluR) activation while those without were not. Spines with ER had a large, slow-onset calcium signal that was blocked with mGluR antagonism, heparin, and thapsigargin and mimicked with application of IP_3. (The group did not, however, test ryanodine.) mGluR antagonism or heparin blocked mGluR-LTD induced at individual spines. The findings of this work suggested that the spine apparatus is capable of influencing the magnitude of physiological depression in spines and this requires hydrolysis of phosphoinositides. Finally, there is evidence that suggests the spine apparatus plays a role in homeostatic synaptic plasticity as well. Using entorhinal denervation of organotypic hippocampal slice cultures, Vlachos et al. 2013 (2013) demonstrated that a normal increase in excitatory synaptic strength exhibited by dentate granule cells after denervation was not present in synaptopodin knockout mice. Strikingly, the group was able to rescue this homeostatic synaptic scaling by crossing synaptopodin knockout mice with mice expressing a mutant synaptopodin gene under the control of the Thy1.2 promoter. Thus, the spine apparatus seems to influence bidirectional as well as homeostatic synaptic plasticity.

SER Contributions to Protein Synthesis

The maintenance of LTP requires de novo protein synthesis (Aakalu et al., 2001; Frey and Morris, 1997; Frey et al., 1988; Huber et al., 2000; Kang and Schuman, 1996; Nguyen et al., 1994; Otani et al., 1989) and investigations into polyribosomes, the cell's protein synthetic machinery, have generated some interesting findings. Work in the Harris lab demonstrated that polyribosomes redistribute from the shaft of the dendrite into spines at 2 hours during LTP induced with tetanic stimulation in young (Ostroff et al., 2002) and mature rats (Bourne et al., 2007). Synapses on spines that contained polyribosomes were larger and it was posited that local protein synthesis was serving to support growth of potentiated synapses. At 2 hours during LTP induced with TBS in adult animals, although there is a reduction in the frequency of polyribosomes, synapses on spines that had polyribosomes were still larger during LTP (Bourne and Harris, 2011a). These findings suggest that polyribosomes are either "used up" in the processes of supporting synapse expansion during LTP or they are preferentially redistributed to other synapses.

Dendritic mRNAs are trafficked from the soma along dendrites toward synapses (Hazelrigg, 1998; Kindler and Kreienkamp, 2012; Tiedge et al., 1999) where they are translated on demand by polyribosomes (Steward and Levy, 1982; Steward and Schuman, 2001). The mRNAs that are trafficked to synapses encode a variety of products, including cytosolic, secretory, and integral membrane proteins (Gao, 1998; Huang, 1999; Kindler and Kreienkamp, 2012; Kuhl and Skehel, 1998). Proteins that are inserted into the plasma membrane (such as receptors) and proteins that are secreted from the neuron require entry into the secretory pathway where posttranslational modifications, such as

82

glycosylation and disulfide bond formation, can occur (Hanus and Ehlers, 2008; Palade, 1975). AMPA receptor subunits are an example of locally translated integral membrane proteins that presumably must interact with the secretory pathway (Ju et al., 2004; Kacharmina et al., 2000). As noted above, however, RER is not readily found distally in the dendritic arbor. Polyribosomes located distally at synapses might, however, be able to interact with SER. Pierce et al. (2000) provided evidence to support this hypothesis by immunogold labeling Sec61, the main protein complex constituent of channels that allow translocation of the nascent polypeptide chain from the cytosol into the ER (Görlich and Rapoport, 1993; Matlack et al., 1998). The group found gold particles labeling the Sec61α subunit associated with SER in both distal and proximal dendrites and spines in hippocampal area CA1. Thus, SER located near synapses is presumably able to provide a platform for the posttranslational modification of integral membrane proteins. Interestingly, the group also showed that Sec61α was associated with the spine apparatus suggesting that it might represent a large protein modification hub in addition to its known role in calcium storage.

Cui-Wang et al. (2012) and the Current Study

Secretory organelles are required for the local production and processing of integral membrane proteins, such as AMPA receptors and other membrane cargo (Hanus and Ehlers, 2008). It was not known, however, how the geometry of dendritic ER might influence the diffusion of receptors along dendrites, even though several studies had pointed to the powerful influence ER could have on spatially restricting receptors for plasma membrane delivery (Greger et al., 2002; Herpers and Rabouille, 2004; Penn et al., 2008). A collaborative investigation

between the Harris laboratory and the laboratory of Dr. Michael Ehlers at Duke University Medical Center shed considerable light on the influence SER morphology has on cargo movement along dendritic SER (Cui-Wang et al., 2012) and directly led to the main hypothesis tested in this chapter of my dissertation. A brief description of those findings is warranted and follows below.

The Ehlers group monitored the movement of fluorescently tagged integral membrane proteins through the ER of cultured hippocampal neurons by measuring fluorescence recovery time after photobleaching. To compare the motion of nascent AMPA receptors, two ER-retained versions of AMPA receptors subunits, GluA1 and GluA2, were investigated as well as an ER-retained version of the vesicular stomatitis viral glycoprotein. Using super-resolution light microscopy, the group observed clusters of fluorescence along dendrites. These clusters became more prominent with time in vitro. Photobleaching experiments demonstrated that fluorescence recovery time also increased with time in vitro. The Ehlers group hypothesized that local areas of ER complexity might impede the diffusion of membrane cargo and that ER complexity must have increased during neuronal development. As the fine structure of the SER lies well below the resolution of light microscopy (Spacek and Harris, 1997), Jennifer Bourne and Deborah Watson of the Harris lab sought to generate structural support for their hypothesis by reconstructing SER along CA1 stratum radiatum dendrites of young (15 day old) and adult (~60 day old) rats. They were able to confirm that SER complexity does increase with age (**Fig. 3.3**). It was also shown that SER tended to be most complex at the base of spines in either age, confirming previous work suggesting the same (Spacek and Harris, 1997). These findings
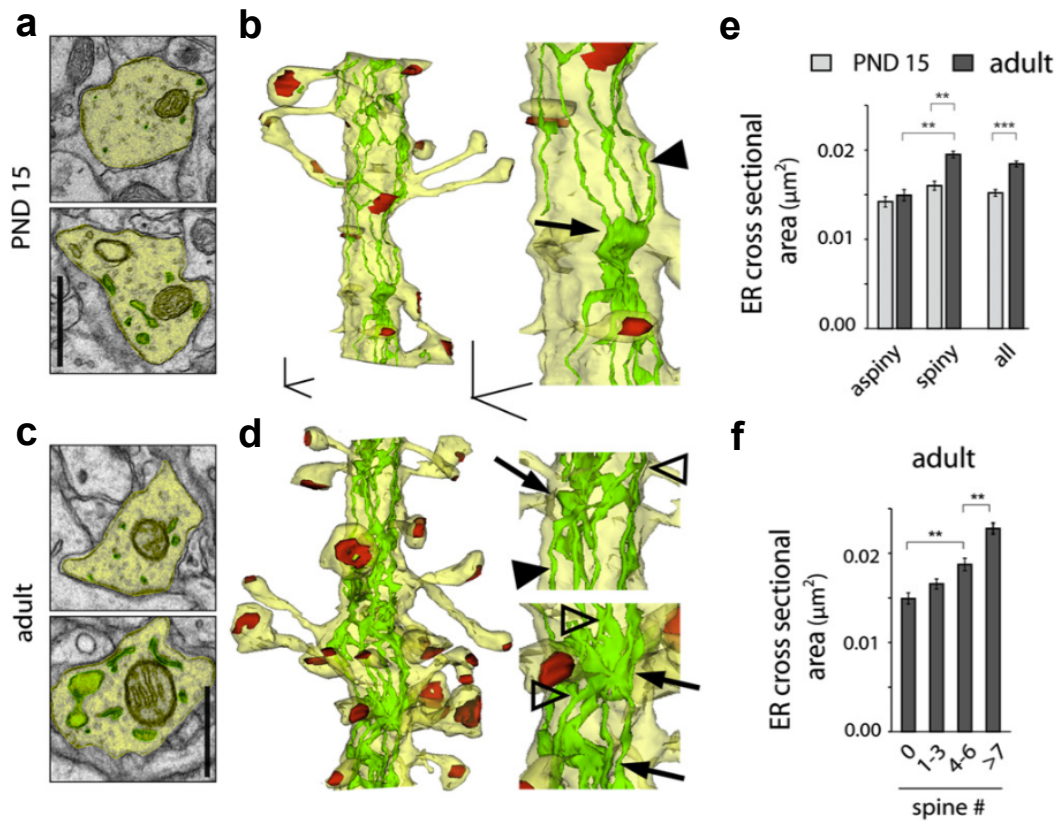
Figure 3.3: SER complexity during development. Electron micrographs (a and c) and three-dimensional reconstructions (b and d) of CA1 dendritic segments (yellow), synapses (red), and SER (green) from young and adult rats. ER tubules (arrowheads), ER branching (open arrowheads), and local complexity of SER at the base of spines (arrows) are shown. Scale bars = 1 μm (a and c) and 0.5 μm (b and d). (e and f) Average SER cross sectional area in spiny, aspiny, and all segments. Mean ± SEM, n = 528-539 sections in young aspiny and spiny segments, and n = 433-544 sections in adult aspiny and spiny segments, n = 10-17 dendrites from 2-4 animals. ANOVA: **p < 0.01, ***p < 0.001. (Adapted from Cui-Wang et al., 2012.)

provided a structural basis for the reduced membrane cargo mobility during development observed in the Ehlers lab.

Further EM investigation revealed that SER was extremely complex at dendritic branch points, where, curiously, ER-bound polyribosomes were found to be concentrated. This finding suggests that dendritic branch points might constitute a cellular hub for locally translated proteins entering the secretory pathway. In fact, the Ehlers lab provided some support for this idea by showing that dendritic branch points are also sites of secretory exocytosis. This finding further demonstrated that diffusional confinement of membrane cargo in highly complex ER facilitates the off-loading and delivery of that cargo to the nearby plasma membrane. This result left the Ehlers lab keen to investigate whether ER complexity might influence the number of AMPA receptors expressed at the surface of the neuron. By monitoring miniature excitatory postsynaptic currents in neurons expressing a mutant SER-microtubule binding protein that promotes an increase in the geometric complexity of ER, the group demonstrated an increase in surface and synaptic levels of AMPA receptors in neurons with more complex ER. Cui-Wang et al. (2012) thus provided substantial support for the idea that SER complexity holds tremendous influence not only over the mobility of membrane cargo but also over the export of that cargo to the plasma membrane.

Since we previously demonstrated that SER complexity influences the movement and off-loading of membrane cargo (Cui-Wang et al., 2012) and since SER calcium stores influence plasticity (Segal and Korkotian, 2014), we were curious to investigate if structural remodeling of SER along dendrites during LTP might support synapse enlargement or elimination in tissue that was previously analyzed for dendritic spines and synapses (Bourne and Harris, 2011a) as well

as for presynaptic axons, boutons, and vesicles (Chapter 2 of this dissertation and Bourne et al., 2013).

Specifically, we hypothesized that redistribution of SER along dendrites and into dendritic spines would determine which synapses would be enlarged during LTP. To test this hypothesis, we analyzed three-dimensional reconstructions from serial section electron microscopy of SER in mature hippocampal CA1 dendrites that had undergone LTP induced with TBS for 2 hours. Four novel and functionally important changes in the structure of SER were discovered. First, SER in dendritic spines was more likely to form a spine apparatus and occupied a greater volume during LTP. Second, SER in dendritic shafts was less complex in regions of the dendrite lacking spines, suggesting a more rapid movement of membrane cargo along regions lacking spines and synapses. Third, the synapses on spines that contained SER were larger in both control and LTP conditions and underwent the most growth during LTP. Finally, during LTP the complexity of SER in the dendritic shaft was conserved beneath most spines and became significantly more complex at the base of spines that contained both polyribosomes and SER. These findings suggest that SER was preferentially redistributed along the dendritic shaft to target membrane trafficking into dendritic spines where synapse growth was greatest and to support local protein synthesis 2 hours during LTP. The work presented in this chapter is, at the time of the completion of this dissertation, currently under review for publication. The manuscript has also been uploaded to bioRxiv (www.biorxiv.org, doi: 10.1101/015974), an online archive and distribution service for unpublished manuscripts maintained by Cold Spring Harbor Laboratory (Chirillo et al., 2015).

3.2 Methods

Physiology, Electron Microscopy, and Reconstructions

The work presented in this study was performed on tissue analyzed for postsynaptic content in Bourne and Harris (2011a) and presynaptic content in Chapter 2 of this dissertation. All methods relating to physiology, electron microscopy, and three-dimensional reconstructions can be found in Section 2.2 of this dissertation. We reconstructed SER in tissue that had undergone LTP for 2 hours. We have not yet investigated SER remodeling at 5 minutes or 30 minutes during LTP.

Identification of SER Branches

To identify points where SER branched, we wrote a simple script in Python, which treated individual SER traces created in RECONSTRUCT™ as vertices. Edges between vertices were identified when the traces overlapped one another on adjacent serial sections. We defined the number of SER branching events existing on a particular EM section, *b(v)*, as follows:

$$b(v) = \max(\deg(v) - 2, 0)$$

The degree of a vertex *v*, *deg(v)*, was the number of edges to which the vertex belonged. Tubular, non-branching SER traces existed when the vertex had no neighboring traces (0 edges, *deg(v)* = 0), had one neighboring trace (1 edge, *deg(v)* = 1), or had two neighboring traces (2 edges, *deg(v)* = 2). Branching SER existed when the vertex had > 2 neighbors (*deg(v)* > 2). This metric proceeded linearly.

Statistical Analyses

In this study, 9 control dendrites (4 from animal 1, 5 from animal 2) and 9 LTP dendrites (5 from animal 1, 4 from animal 2) were analyzed. Statistical analyses were performed in R (r-project.org) and STATISTICA (StatSoft, Tulsa, OK). Hierarchical nested ANOVAs (hnANOVAs) were used (with dendrite nested in condition and experiment and experiment nested in condition) to ensure results were not driven by a particular dendrite or experiment. The sample sizes of spines with SER and polyribosomes versus those without varied widely. Therefore, for LTP-related comparisons of data categorized by spine content (SER and/or polyribosomes), we performed separate hnANOVAs on each group. The sample sizes of dendritic segments categorized as spiny or aspiny were comparable, thus a hnANOVA was performed across these groups followed by Tukey's HSD post-hoc test to determine significant differences among the groups. Simple regression was used to investigate the effect of a continuous predictor on a dependent variable (e.g., PSD area v. SER volume) and chi-square tests were used to investigate changes in proportions of spines categorized by content during LTP. Statistical tests are reported in results and figure legends where appropriate. Significance was set to $p < 0.05$ and asterisks in figures denote $p < 0.05$ (*), $p < 0.01$ (**), and $p < 0.001$ (***).

3.3 Results

SER Identification on Electron Micrographs

Slices were prepared from the middle of adult rat hippocampus, and two stimulating electrodes were placed on either side of a recording electrode in the middle of *stratum radiatum* of area CA1 (Bourne and Harris, 2011a). LTP was

induced with theta-burst stimulation (TBS) at one stimulating electrode while the other received control pulses. At 2 hours post-TBS, the slices were rapidly fixed, processed, and prepared for 3DEM (see Chapter 2 Methods). SER was identified as before (Cui-Wang et al., 2012; Spacek and Harris, 1997) on the basis of its appearance as irregularly shaped, membranous cisternae with a clear lumen (**Fig. 3.4**).

Correlation between SER and Synaptic Input

In control conditions, we found that the volume of SER per unit length of dendrite was strongly and positively correlated with the amount of synaptic input supported by the dendritic segment (**Fig. 3.5**). Interestingly, even though the total amount of SER per length of dendrite did not change significantly during LTP, the correlation between SER volume and synaptic input broke down by 2 hours during LTP, suggesting that SER was being remodeled. This finding prompted us to investigate the underlying structural alterations in SER that might be occurring during plasticity.

SER in Dendritic Spines

SER enters less than 20% of hippocampal dendritic spines (Cooney et al., 2002; Spacek and Harris, 1997). In those spines that contain SER, SER exists as either a simple tubule (**Fig. 3.6a**) or as a larger and more complex spine apparatus, with folds of SER stacked between densely stained material (**Fig. 3.6b**). It is not known whether the occupancy, complexity, or volume of SER in dendritic spines changes with LTP. To explore this, SER was reconstructed in dendritic spines and identified as a simple SER tubule or as a spine apparatus. Overall, the volume of SER in spines was significantly greater during LTP, but we
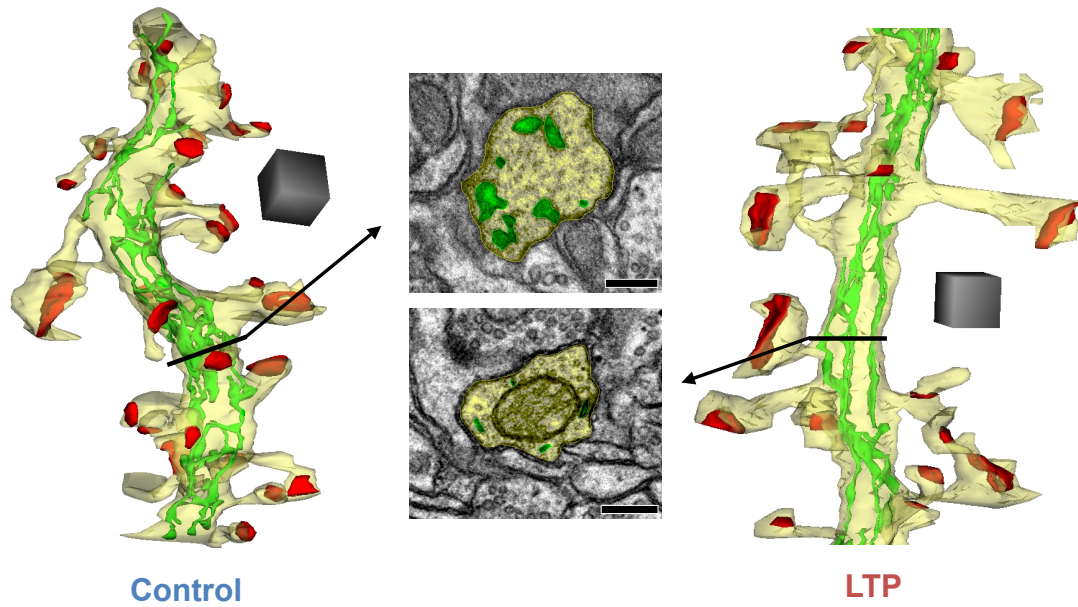
Figure 3.4: Identification of SER on electron micrographs. Example reconstructions of dendrites (yellow) with associated PSDs (red) and SER (green) in the dendritic shaft from both conditions. Scale cubes = 0.5 µm on each side. Two micrographs illustrate a section of the dendritic shaft (yellow) from the dendrites with SER (green). SER was identified on EM sections as membranous cisternae with a clear lumen. Scale bar = 250 µm.

a

Control
Σ(PSD)/μm = 0.372
SER vol/μm = 0.023

LTP
Σ(PSD)/μm = 0.400
SER vol/μm = 0.012

b
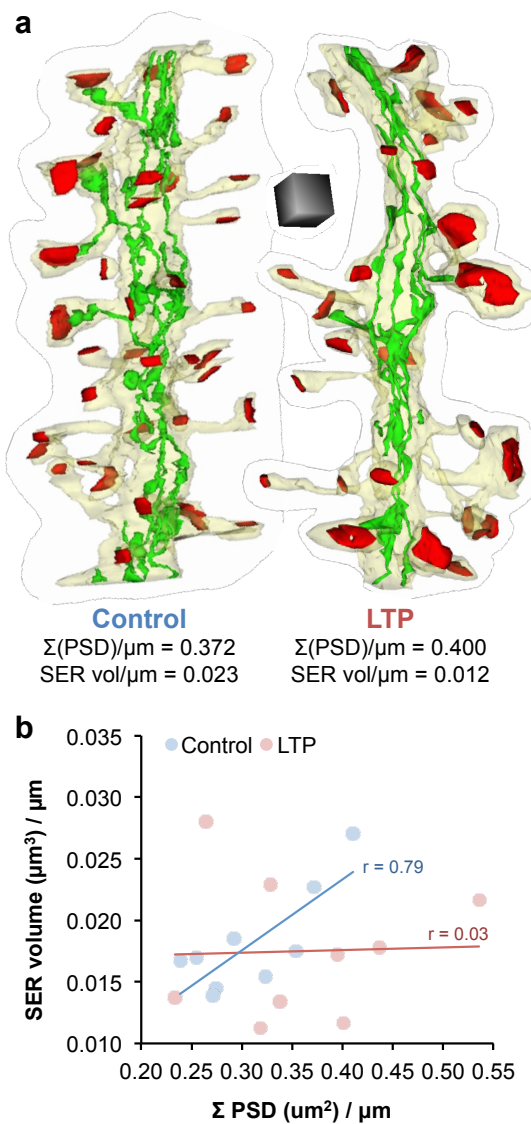
Figure 3.5: Total synaptic input and SER volume correlation breaks down during LTP. (a) Examples of reconstructed dendritic segments (yellow) with synapses (red) and SER (green). Scale cube = 0.5 μm on each side. (b) SER volume versus summed PSD area per unit length of dendrite in both conditions. Total SER volume per unit length of dendrite did not change with LTP (control: 0.018 ± 0.001 μm^3/μm, LTP: 0.018 ± 0.002 μm^3/μm, hnANOVA: $F_{(1, 14)}$ = 0.18 , p = 0.67). Total synaptic input along dendritic segments was tightly correlated with total SER volume in control conditions (simple regression: r = 0.63, $F_{(1, 7)}$ = 12.01, $p < 0.05$) but not with LTP (simple regression: r = 0.03, $F_{(1, 7)}$ = 0.01, p = 0.93).
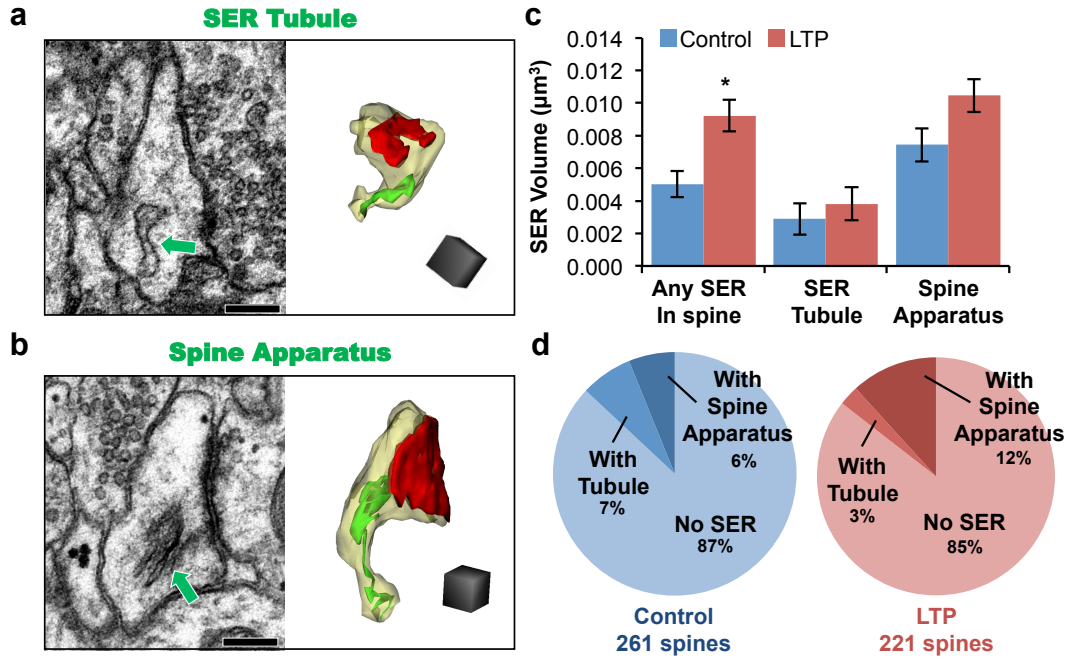
Figure 3.6: SER is more likely to form a spine apparatus during LTP. (a) Example electron micrograph and reconstruction of a dendritic spine (yellow) and PSD (red) with a single tubule of SER (green arrow in micrograph, green surface in the reconstruction). (b) Example electron micrograph and reconstruction of a dendritic spine with a spine apparatus using same color scheme as in A. Scale bars and cubes = 250 μm on each side in A and B. (c) Volume of SER in spines increased with LTP (hnANOVA: $F_{(1, 47)}$ = 6.23, $p < 0.05$); however, there was no difference in the volume of SER tubules in spines ($F_{(1, 12)}$ = 1.37, $p = 0.26$) or in the volume of spine apparatuses during LTP ($F_{(1, 24)}$ = 0.63, $p = 0.44$). (d) Percentages of spines with SER tubules, with spine apparatuses, and without SER. During LTP, there was a shift to more spines containing a spine apparatus (chi-squared test: $\chi^2_{(1, N = 6)}$ = 8.59, $p < 0.05$).

93

did not detect a significant change in volume of either SER tubules or spine apparatuses (**Fig. 3.6c**). Under both conditions, we found similar percentages of spines containing SER (13-15%); however, there was a significant shift during LTP from tubules of SER to spines apparatuses (**Fig. 3.6d**). Thus, the increase in SER volume in spines during LTP was accounted for by the observed shift from SER tubules to larger and more complex spine apparatuses.

Complexity of SER along the Dendritic Shaft

Integral membrane proteins such as AMPARs move through the dendritic shaft more rapidly along simple, tubular SER and more slowly where SER is more complex (Cui-Wang et al., 2012). SER tends to be more complex at the base of spines (Cooney et al., 2002; Spacek and Harris, 1997), which facilitates cargo delivery and ultimately receptor insertion at nearby synapses (Cui-Wang et al., 2012). To test whether structural remodeling of dendritic SER could influence its complexity during LTP, we analyzed regions of aspiny versus spiny dendritic segments. An aspiny dendritic segment was defined as a length of dendrite at least 100 nm long without a spine origin (**Fig. 3.7a**). In the prior paper, SER complexity was estimated by a simple index of SER area summed across spiny vs. aspiny segments (Cui-Wang et al., 2012). Here we refined this index to account for the combined effects of SER volume and branching and to normalize for dendritic segment length and caliber as defined by the equation below (**Fig. 3.7b**, see Methods above):

$$SER\ Complexity = \frac{\left(\frac{SER\ Volume}{Length}\right) \times Branching\ Factor}{Microtubule\ Count}$$

SER volume was computed for each segment by summing the SER profile areas across EM sections and multiplying by section thickness. The branching factor was computed by summing the number of branch points in each dendritic segment and then adding 1 to ensure a non-zero value for segments with unbranched tubules of SER (**Fig. 3.7b**). Microtubule count scales with dendrite caliber (Fiala et al., 2003), hence the SER complexity index was normalized by the number of microtubules to control for larger dendrites having a greater capacity for SER. Overall, SER complexity was greater in spiny versus aspiny segments of the dendrite (hnANOVA: $F_{(1,\ 195)}$ = 12.09, p < 0.001). Furthermore, during LTP, SER complexity was sustained in spiny segments of the dendrite but substantially reduced in the aspiny segments (**Fig. 3.7c**). Thus, as spines acquired spine apparatuses during LTP (see **Fig. 3.6d**), SER was shuttled from aspiny segments to spiny segments of the dendrite. Furthermore, the lower complexity of SER in the aspiny segments would speed trafficking across regions of the dendrite lacking synapses.

Synapses on Spines with SER and Polyribosomes

Next, we considered whether the increase in SER in dendritic spines influenced synapse growth during LTP. Dendritic spines with polyribosomes have been shown to have larger PSDs than spines without polyribosomes at 2 hours during LTP (Bourne and Harris, 2011a; Ostroff et al., 2002). SER is also involved in protein synthesis and posttranslational modification of proteins (Pierce et al., 2001). Hence, we analyzed whether co-localization of polyribosomes and SER in spines enhanced synapse enlargement during LTP. Under both control and LTP conditions, most spines had neither polyribosomes nor SER (**Fig. 3.8a-b, e**).

95
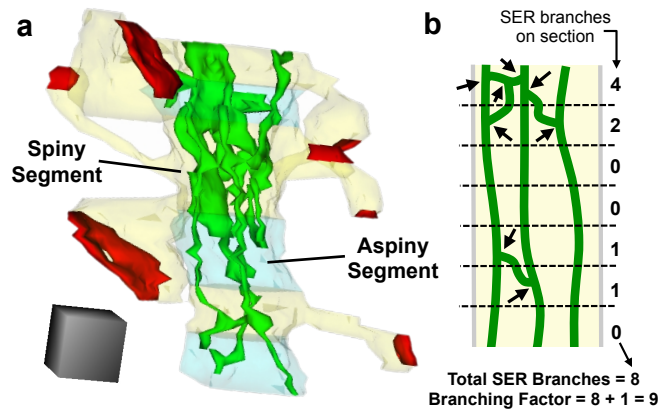
Figure 3.7: SER is simplified in aspiny dendritic segments during LTP. (a) Example reconstruction of dendrite showing spiny (yellow) and aspiny (teal) segments, PSDs (red), and SER (green) extending through the dendritic shaft. An aspiny dendritic segment was defined as having a length of at least 100 nm without a spine origin. Scale cube = 250 µm on each side. (b) Diagram showing identification of SER (green) branches in a model dendritic segment (yellow). SER branch points (black arrows) were quantified on each EM section (separated by dotted lines) across the dendritic segment. For example, an aspiny dendritic segment 100 nm long, containing 0.0246 µm^3 of SER with 0 branches, and 12 microtubules, would have a SER complexity value = (0.0246/.1 × (0+1))/12 = 0.0205. In contrast, a similar dendritic segment that differed only by having 1 SER branch point would have a SER complexity value = (0.0246/.1 × (1+1))/12 = 0.0410, etc. (c) During LTP, SER complexity in aspiny segments was substantially reduced relative to spiny segments in both LTP (hnANOVA: $F_{(3, 195)}$ = 4.88, p < 0.01, Tukey post-hoc, p < 0.01) and control conditions (Tukey post-hoc, p < 0.01). In the control condition alone, the difference in SER complexity between spiny and aspiny dendritic segments did not reach statistical significance (Tukey post-hoc, p = 0.13). The SER complexity was comparable for spiny dendritic segments from both control and LTP conditions (Tukey post-hoc, p = 0.99). Sample sizes for each group are shown on the corresponding bar of the graph.

96
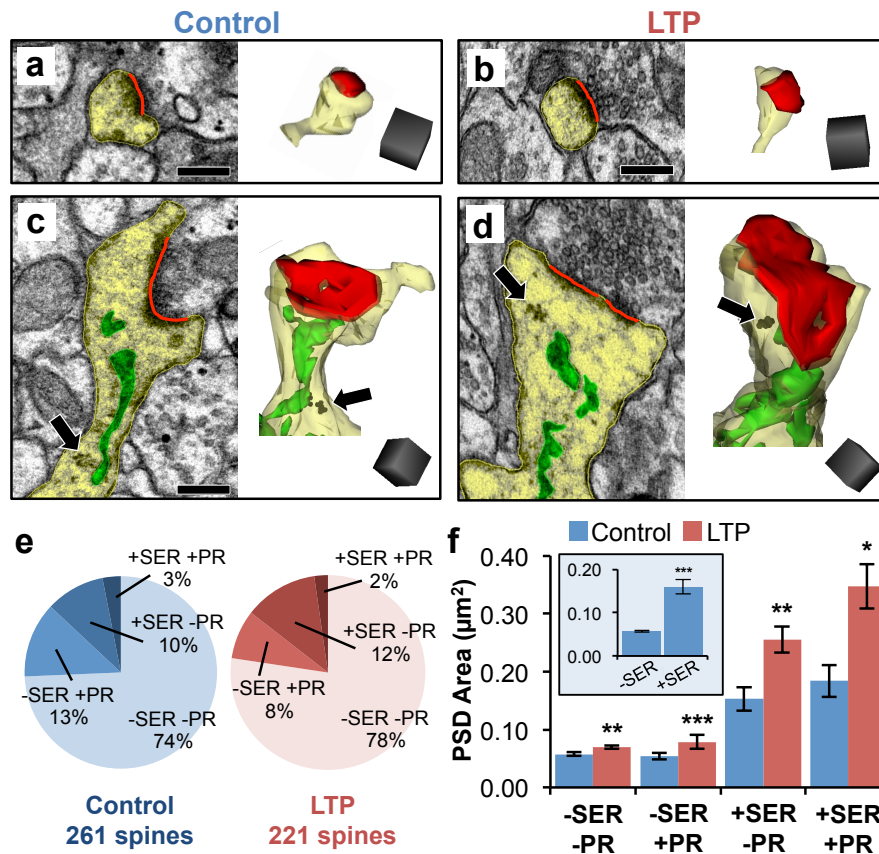
Figure 3.8: Spines with larger synapses are more likely to contain SER. (a-b) Example electron micrographs and reconstructions of dendritic spines (yellow) with no SER or polyribosomes from both conditions. (c-d) Example electron micrographs and reconstructions of dendritic spines with SER (green), PSDs (red) and polyribosomes (PR, black arrows). Scale bars = 250 µm. Scale cube = 250 µm on each side. (e) Frequency of spines with just polyribosomes (SER- PR+), just SER (SER+ PR-), neither (SER- PR-), or both (SER+ PR+) in control and LTP conditions. SER+ PR+ spines were rare and were found in control conditions of one experiment and LTP conditions in another experiment. There were no differences in the proportions of spines containing SER, PR, neither, or both between control and LTP conditions (chi-square: p = 0.35). (f) Comparison of average PSD size in control and LTP conditions on spines with or without SER or polyribosomes. Mean PSD area on spines without SER or polyribosomes was modestly larger with LTP (hnANOVA: $F_{(1, 347)}$ = 8.39, p < 0.01). PSDs on spines with just polyribosomes were even larger with LTP ($F_{(1, 35)}$ = 20.43, p < 0.001). PSDs on spines with just SER were larger still with LTP ($F_{(1, 35)}$ = 9.38, p < 0.01). The largest increase in PSD area with LTP was on spines with both SER and polyribosomes ($F_{(1, 6)}$ = 9.8167, p < 0.05). PSD were larger on control spines that had SER (inset, hnANOVA: $F_{(1, 243)}$ = 126.68, p < 0.001).

Some spines had either polyribosomes or SER, and a small percentage had both (Fig. 5c-d, e). Under control conditions, synapses on spines without SER were smaller than those on spines with SER, regardless of whether the spine contained a polyribosome or not (**Fig. 3.8f inset**). Synapses on spines without SER showed a small but statistically significant increase in size 2 hours during LTP whether or not they contained polyribosomes (**Fig. 3.8f**). In contrast, synapses on spines with SER had a more dramatic increase in size (**Fig. 3.8f**). Interestingly, the largest synapses were on spines that contained both SER and polyribosomes during LTP. These results suggest that spines with SER were primed to undergo greater synaptic enlargement during LTP than those without SER. Such a dramatic increase in synapse size on spines containing both SER and polyribosomes suggests that these spines were able to mobilize these resources, which worked synergistically to support synapse growth during LTP.

SER Complexity at the Base of Enlarging Synapses

Finally, since synapses on spines containing both SER and polyribosomes were the largest during LTP, we were interested to learn whether the complexity of SER at the base of those spines was altered. We reasoned that these spines might benefit from highly complex SER at their bases, which would serve as a local source of proteins the spine could access during synapse growth (Cui-Wang et al., 2012). We analyzed SER complexity 0.5 µm around the base of each spine (**Fig. 3.9a**). We removed spines from this analysis if 0.5 µm around their base fell outside the length of the analyzed dendritic segment. In agreement with our findings above (see Fig. 3.4d), when we analyzed all spines together we found that SER complexity was retained at their bases during LTP (control:
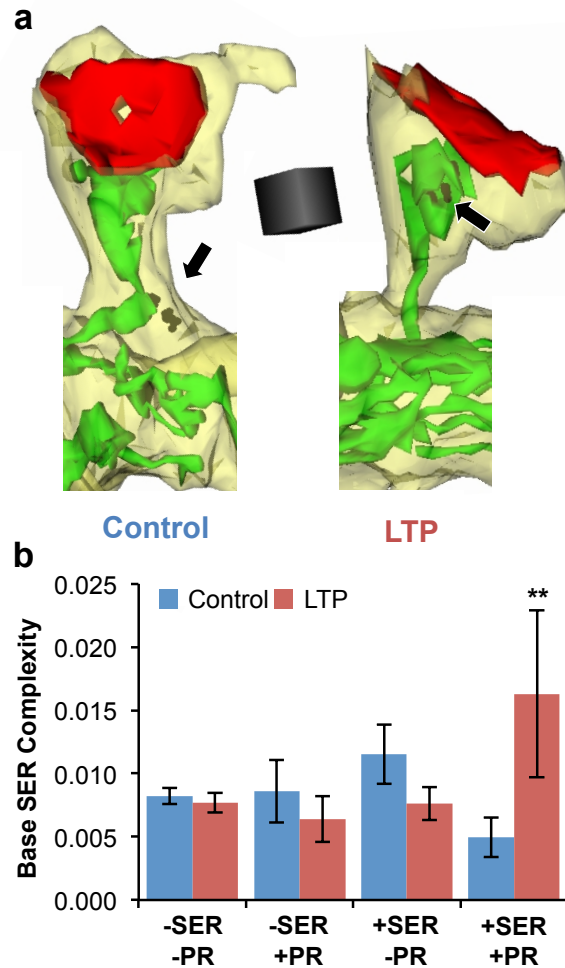
Figure 3.9: SER complexity is greatest at the base of spines that contain polyribosomes and SER during LTP. (a) Example reconstructions of dendritic spines (yellow) with PSDs (red) and SER (green) in spines containing both SER and polyribosomes from each condition. SER 0.5 µm around the base of each of the spines has also been reconstructed. (b) SER complexity 0.5 µm around the base of spines with or without SER or polyribosomes under control conditions and during LTP. During LTP, SER complexity was conserved at the base of spines without SER or polyribosomes (-SER -PR, hnANOVA: $F_{(1, 316)}$ = 0.06, p = 0.81), at the base of spines with polyribosomes only (-SER +PR, $F_{(1, 30)}$ = 0.13, p = 0.72), and at the base of spines with SER only (+SER -PR, $F_{(1, 33)}$ = 2.17, p = 0.15). SER complexity was, however, increased at the base of the few spines that contained both polyribosomes and SER during LTP (+SER +PR, $F_{(1, 5)}$ = 23.15, p < 0.01).

0.0082 ± 0.0006, LTP: 0.0077 ± 0.0008, hnANOVA: $F_{(1, 424)}$ = 0.04, p = 0.84). Interestingly, only SER complexity at the base of spines that contained both SER and polyribosomes was significantly greater during LTP (**Fig. 3.9b**). Thus, not only is SER complexity conserved at the base of spines during LTP, SER complexity was even greater at the base of the few "privileged" spines that contained both SER and polyribosomes, spines that expanded their synapses the most during LTP. This finding suggests that LTP induces structural changes in SER that facilitate the movement of cargo to and from the largest synapses, providing a local mechanism to enhance their growth.

3.4 Discussion

Here we have demonstrated for the first time that the structure of dendritic SER is dynamic in ways that support enlargement of specific synapses during LTP in the adult hippocampus. Trafficking of membrane and proteins along SER is critical for the expression of synaptic plasticity, and movement throughout the dendrite is slowed in regions where SER structure is most complex, thereby enhancing local delivery of the cargo (Cui-Wang et al., 2012). Under baseline conditions in vivo, SER is more complex in portions of the dendritic shaft with more or larger dendritic spines (Cui-Wang et al., 2012; Spacek and Harris, 1997). We now show that under control conditions in adult hippocampal slices, the complexity of dendritic shaft SER was greater where total synaptic input was higher, consistent with the prior in vivo findings. By 2 hours during LTP, the total SER volume per dendritic segment length was unchanged, yet the structure of SER underwent substantial reorganization. Both the volume and complexity of SER increased in dendritic spines, and synapse enlargement was greatest on

those spines containing SER and a polyribosome. During LTP, SER became more complex at the base of spines that contained both SER and a polyribosome, and became less complex along portions of the dendrite that lacked spines. These findings suggest that spines containing SER and polyribosomes were primed to undergo greater synapse enlargement during LTP than those lacking them. Furthermore, SER was redistributed from portions of the dendritic shaft with no spines to portions where synapses underwent the greatest enlargement during LTP.

SER Remodeling along the Dendritic Shaft

SER also contributes to the regulation of calcium dynamics (Berridge, 1998; Emptage et al., 1999; Raymond and Redman, 2002; Sala et al., 2005; Simpson et al., 1995). Elevations in calcium can be localized within spines or spread through the dendritic shaft (Berridge, 1998; Segal and Korkotian, 2014), ultimately propagating to the nucleus where calcium transients influence gene transcription (Bading, 2013). In the hippocampus, RyRs localize to SER in dendritic spines (Sharp et al., 1993) and respond to calcium entering through ionotropic glutamate receptors and voltage gated calcium channels (Berridge, 1998). RyR activation results in calcium-mediated calcium release that amplifies an otherwise weak signal (Blaustein and Golovina, 2001; Raymond and Redman, 2002; 2006; Rose and Konnerth, 2001; Verkhratsky and Shmigol, 1996). IP_3Rs, on the other hand, are localized to SER in the dendritic shaft (Sharp et al., 1993; Simpson et al., 1995) and are activated by calcium and IP_3 (Berridge, 1998). Hotspots of IP_3Rs occur along SER in CA1 dendrites where SER is more elaborate (Fitzpatrick et al., 2009). Furthermore, calcium released from SER via

IP$_3$R activation during LTP is involved in coordinating plasticity among synaptic sites along dendrites (Nagase et al., 2003; Nishiyama et al., 2000). Thus, the SER elaboration during LTP in spines and at their bases could enhance local calcium signaling and serve as a potentiating signal to sustain and enlarge those synapses (Mellentin et al., 2007; Sajikumar et al., 2009). In contrast, where dendritic SER became simplified, less calcium would be released and phosphatases would be more likely to be activated (Lisman, 1989; Mulkey et al., 1993), possibly leading to spine loss along these portions of the dendrite.

SER Remodeling in Dendritic Spines

During LTP, the SER in dendritic spines was more likely to form a complex spine apparatus, while under control conditions spine SER usually formed just a simple tubule. Immuno-reactive markers for the Golgi apparatus, which is required for the translation and insertion of integral membrane proteins, have been identified in dendritic shafts and the spine apparatus, suggesting the spine apparatus could act as a mobile Golgi outpost (Gardiol et al., 1999; Grigston et al., 2005; Horton et al., 2005; Pierce et al., 2001). Synaptopodin is an essential component of the spine apparatus (Deller et al., 2003) and live-imaging experiments in cultured neurons show that dendritic spines containing synaptopodin have larger AMPAR-mediated excitatory postsynaptic potentials due to ryanodine-triggered calcium release (Vlachos et al., 2009). Two-photon microscopy reveals that synaptic depression is also regulated by calcium influx into large spines associated with synaptopodin (Holbro et al., 2009). Thus, spine apparatus elaboration and polyribosome recruitment to a subset of spines could serve to regulate intra-spine calcium and local protein synthesis and support

enhanced bidirectional synaptic plasticity, namely enlargement or shrinkage during LTP and LTD respectively, at those spines.

Linking LTP Induction with SER Remodeling

Several molecular mechanisms could be triggered that would link the induction of LTP to the local elaboration and redistribution of dendritic SER. One likely mechanism involves CLIMP63, an integral membrane protein in SER, and protein kinase C (PKC), which phosphorylates CLIMP63 (Cui-Wang et al., 2012) and is activated during LTP (Malinow et al., 1989). PKC-mediated phosphorylation of CLIMP63 causes SER to dissociate from microtubules and become more elaborate (Cui-Wang et al., 2012; Klopfenstein et al., 1998; Vedrenne et al., 2005). Other signaling molecules are also activated in dendritic spines and the neighboring dendritic shaft during LTP, such as CaMKII (Lee et al., 2009) and the small GTPase Ras (Harvey et al., 2008), which stimulates extracellular signal-regulated kinase (ERK). Together with PCK, CAMKII or ERK may also phosphorylate CLIMP63 during LTP, resulting in the elaboration of SER that would facilitate offloading of cargo and support growth of activated synapses. Further along the dendrite, away from activated spines, the dephosphorylation of CLIMP63 would cause SER to associate with microtubules and become straighter and more tubular (Cui-Wang et al., 2012). This simplification of SER during LTP would enhance movement of proteins and other cargo away from less active synapses, possibly preventing the formation of new spines or resulting in the elimination of weak spines in those dendritic regions (Bourne and Harris, 2011a).

Concluding Remarks

The study presented in this chapter demonstrates a dramatic remodeling of SER structure during LTP and supports an important role for SER in coordinating synaptic plasticity along adult hippocampal dendrites. So far we have only investigated the plasticity of SER occurring at 2 hours during LTP. The next step in this investigation would be to reconstruct SER along dendrites at 30 minutes during LTP, before synapses have expanded. This would reveal if SER complexity increased at the base of spines before or after their synapses enlarged. If before, this would argue that complex SER is a necessary component for synapse growth. If after, this would argue that enlarged synapses were able to "capture" SER necessary to support their stability. 30 minute LTP data is available (Bourne and Harris, 2011a) and is at the time of completion of this dissertation being investigated for SER content.

In Chapter 2, I showed that structural plasticity is evident on both sides of the synapse during LTP and in this chapter I provided evidence to support the idea that dendritic SER might coordinate plasticity along hippocampal dendrites. As both of these investigations were done in the normal rodent hippocampus, it would be interesting to describe how these mechanisms might go awry under conditions of synaptic pathology. The Fmr1 knock out (KO) mouse has been used as model of the human neurodevelopmental disorder Fragile X. The well-described synaptic signaling abnormalities in this KO animal (Zoghbi and Bear, 2012) indicate normal mechanisms of structural plasticity might also be disorganized. In the next chapter of this dissertation, I discuss preliminary studies meant to determine whether obvious signs of anatomical pathology are present

at synapses in the adult Fmr1 KO hippocampus as a first step in addressing this question.

Chapter 4: Synaptic Structure in Fragile X

4.1 Introduction

The studies presented in Chapters 2 and 3 investigated structural plasticity that occurs concurrently on both sides of the synapse in the normal adult hippocampus. An interesting next step would be to explore how normal structural remodeling might break down under conditions of synaptic pathology. Fragile X (FX), the most common inheritable cause of autism and intellectual impairment in humans (Hagerman et al., 2010), has become the archetypal model researchers use to study these disorders (Portera-Cailliau, 2012). Investigations into the *Fmr1* knockout (KO) mouse, a mouse model of FX, indicate that synaptic pathology is the most likely basis for impaired cognition in FX (Sidorov et al., 2013; Zoghbi and Bear, 2012). Thus, structural plasticity in the *Fmr1* KO mice is likely categorically distinct from that in the normal rodent brain. A first step in understanding how hippocampal structural plasticity might go awry in FX would be to characterize and compare the ultrastructure of synapses in the *Fmr1* KO mouse with their wild-type (WT) counterparts. This chapter presents preliminary probe studies characterizing the synaptic ultrastructure in the adult *Fmr1* KO mouse on the EM level.

Autism, Fragile X, and Synaptic Pathology

Autism spectrum disorders (ASDs) are neurodevelopmental disorders characterized by social interaction deficits, difficulty with verbal and non-verbal communication, and stereotyped repetitive behaviors. An estimated 43,000,000 people worldwide are affected by an ASD (Elsabbagh et al., 2012). These patients suffer poor behavioral, emotional, and medical outcomes as adults (Gray

et al., 2012). They are ~50% more likely to have an intellectual disability (Chakrabarti and Fombonne, 2001) and nearly a third of these individuals will suffer epilepsy (Tuchman et al., 2010). The majority of autistic patients present with comorbid psychiatric disorders such as social anxiety disorder, attention-deficit/hyperactivity disorder, and oppositional defiant disorder (Simonoff et al., 2008). Furthermore, autistic patients live shorter lives than non-autistics (Shavelle and Strauss, 1998). These diseases have negative consequences for society as well. As autism prevalence rises alongside increasing healthcare costs, ASD-related healthcare expenditures represent the highest rate of increase among all intellectual disabilities in the past decade (Angelis et al., 2014; Wang and Leslie, 2010). This increase results in greater financial difficulty for those raising children with autism.

Martin and Bell (1943) first described a family with a history of intellectual disability that seemed to be sex-linked[15] and this disorder would come to be known as "fragile X" when researchers characterized a "fragile" site at band q27.3 on the long arm of the X-chromosome of FX patients (Lubs, 1969; Lubs et al., 2012; Sutherland, 1977). FX occurs in roughly 1 in 4,000 men and 1 in 6,000-8,000 women (Saul and Tarleton, 2012). It has nearly 100% penetrance and a highly variable clinical presentation (Hersh et al., 2011). Prepubertal males grow normally but show delays in developmental motor milestones (e.g., sitting and walking) and speech. Physical features that typify FX usually develop after the onset of puberty and postpubertal FX patients usually present with a suite of

---

[15] Fragile X is also known as Martin-Bell Syndrome in reference to J. Purdon Martin and Julia Bell who first characterized the disorder in the 1940s. In Latin American countries, it is also known as Escalante Syndrome in reference to Julio Anibal Escalante and his work on sex-linked intellectual disabilities.

characteristic facial features (a long face, prominent forehead and jaw, and protruding ears) and macro-orchidism. FX patients typically have an abnormal, hyperactive temperament and occasionally display a distinctive flapping motion of their hands. While FX is the single most common inheritable form of autism, only about 25% of FX patients display autistic behaviors according to criteria established by the Childhood Autism Rating Scale (Hatton et al., 2006), but it appears that autistic traits become more prominent with age.

Research into the pathophysiology of FX, the most common genetic cause of autism (Hagerman et al., 2010), has greatly increased our knowledge of synaptic function and promises to lead to effective treatment for the disease and other ASDs (Krueger and Bear, 2011). FX is caused by the transcriptional silencing of the *FMR1* (*fragile X mental retardation protein 1*) gene on the X chromosome (Pieretti et al., 1991; Verkerk et al., 1991), which codes for FMRP (fragile X mental retardation protein), an RNA-binding protein and repressor of protein synthesis at the synapse (Bhakar et al., 2012). Stimulation of group 1 metabotropic glutamate receptors (mGluRs) leads to an increase in synthesis of FMRP, which acts in a feedback manner to inhibit further protein synthesis. An unchecked increase in protein synthesis at the synapse in the absence of FMRP is thought to be pathognomonic of FX (Kelleher and Bear, 2008). Protein synthesis in the *Fmr1* knockout (KO) mouse is increased both in vitro and in vivo (Dölen et al., 2007; Hagerman et al., 2010; Muddashetty et al., 2007; Osterweil et al., 2010; Qin et al., 2005). mGluR-dependent long-term depression (mGluR-LTD), a protein synthesis-dependent form of synaptic plasticity, was found to be exaggerated in *Fmr1* KO mouse (Huber et al., 2000; 2002; Krueger and Bear, 2011). This discovery has led to the mGluR theory of FX, whereby a constellation

of FX symptoms is thought to be due to excessive mGluR signaling (Bear et al., 2004; Pieretti et al., 1991; Verkerk et al., 1991). Manipulation of group 1 mGluRs by pharmacological or genetic downregulation corrects several aspects of the FX phenotype in the *Fmr1* KO mouse such as exaggerated mGluR-LTD (Bhakar et al., 2012; Choi et al., 2011; Dölen et al., 2007), increased AMPA receptor internalization (Darnell et al., 1975; Kelleher and Bear, 2008; Nakamoto et al., 2007), increased audiogenic seizures (Dölen et al., 2007; Min et al., 2009; Thomas et al., 2012; Yan et al., 2005), and abnormal social interactions (Thomas et al., 2011).

Synaptic Structure in the Fmr1 KO

Golgi staining suggested that cortical spines in postmortem human brain appeared developmentally immature, namely long, thin, and tortuous (Hinton et al., 1991; Rudelli et al., 1985; Wisniewski et al., 1991). Further work in human autopsy material noted that, in addition to the presence of malformed spines, spine density along cortical neuron dendrites was increased (Irwin et al., 2001). These findings have led to the suggestion that a lack of spine pruning during development is a key feature of FX pathology (Bagni and Greenough, 2005; Irwin et al., 2002). Golgi studies in the *Fmr1* KO mouse generally corroborate the increase in spine density in cortical neurons (Comery et al., 1997; Dölen et al., 2007; Hayashi et al., 2007; McKinney et al., 2005). Other studies have, however, suggested the problem might lie not in defective spine pruning but in defective spine stabilization and maturation. Viral transduction of enhanced GFP in occipital cortex of *Fmr1* KO mice demonstrated that by 4 weeks, spine lengths and densities in KO animals were similar to WT controls (Nimchinsky et al.,

109

2001). GFP electroporation in somatosensory cortex of *Fmr1* KO animals revealed no difference in spine length or density from WT animals but did demonstrate FX spines were more dynamic and less able to stabilize than WT spines (Cruz-Martín et al., 2010). Super-resolution light microscopy such as STED (stimulated emission depletion) microscopy also corroborates the idea that spine maturation seems delayed in KO animals (Wijetunge et al., 2014). Research in the hippocampus has pointed to spine density that is decreased (Braun and Segal, 2000; Segal et al., 2003) and also to spine density that does not differ from WT mice (de Vrij et al., 2008; Grossman et al., 2006). Thus, light level studies have not yet definitively characterized a spine deficit in the KO mouse.

Less is known about the ultrastructure of spines in the *Fmr1* KO mouse. EM has been employed only sparingly in FX structural work and much of it has been done on single EM sections. Quantification of PSD length on single human EM sections hinted at the possibility that synaptic input might be reduced (Rudelli et al., 1985), but the same technique applied in the *Fmr1* KO mouse has produced conflicting reports (Klemmer et al., 2011; Till et al., 2012). Investigating ultrastructure in this manner might be confounding results, since structural features only evident in three dimensions are lost (Bourne and Harris, 2011b). Three-dimensional reconstructions from serial EM from perfusion-fixed brain are thus necessary to investigate unambiguously the synaptic ultrastructure. It is of interest to determine if protrusions in the *Fmr1* KO mouse make synaptic contacts or if there is a build-up of nonsynaptic filopodia (Fiala et al., 1998). The necessity of using three-dimensional EM is further warranted, as mature hippocampal dendrites are very spiny and, as predicted by light level studies,

might be even more so in the *Fmr1* KO animal. Moreover, work from our lab has shown that polyribosomes in dendrites are dynamic during plasticity. During long-term potentiation (LTP) in developing animals, polyribosomes moved from the dendritic shaft into spines and these spines were more likely to have larger PSDs (Ostroff et al., 2002). In the adult, LTP also induced an increase in spines and, again, spines with polyribosomes had PSDs that were larger than spines without polyribosomes (Bourne et al., 2007). Unchecked protein synthesis is thought to cause FX (Bhakar et al., 2012). Thus, it is of interest to quantify the number and location of polyribosomes in the *Fmr1* KO mouse to determine whether protein synthesis machinery in the KO differs from that of the WT.

The Current Study

As the majority of studies investigating synaptic malformation in FX has been restricted to light level microscopy, any underlying subcellular pathology has been left largely unexplored. Structural abnormalities that lie below the resolution of light microscopy might negatively influence normal synaptic plasticity that was uncovered in Chapters 2 and 3. As a first step in understanding how structural plasticity might go awry in FX, it is necessary to characterize and compare in vivo synaptic ultrastructure of the *Fmr1* KO with that of the WT mouse. Thus, the purpose of this study was to preliminarily characterize hippocampal area CA1 synaptic ultrastructure in the *Fmr1* KO by reconstructing dendritic spines and synapses on serial EM sections. We began our analysis by investigating the synaptic anatomy of the adult *Fmr1* KO mouse to determine if structural malformation that might begin during development persists in adulthood. In contrast to light level studies in cortex, we demonstrate

111

that synapses in area CA1 of the *Fmr1* KO hippocampus differ little from their WT counterparts in number and subcellular composition. These findings suggest synaptic malformation in FX might be restricted to the developing animal or to other areas of the brain.

4.2 Methods

Animals and Perfusion-Fixation

C5BL/6 mice were bred and raised in our university animal care facility (Norman Hackerman Building Vivarium, UT Austin). WT ($Fmr1^{y/+}$) male mice were crossed with hemizygous ($Fmr1^{-/+}$) female mice to produce litters with both WT and KO males. Animals were genotyped by polymerase chain reaction in house after each perfusion from tail clippings collected after administration of anesthetic. To investigate the structure of synapses in vivo, one male WT and one male *Fmr1* KO animal from the same litter were transcardially perfused with fixatives for this study. Both animals were 69 days old at the time of the perfusions, well into adulthood (McCutcheon and Marinelli, 2009). The animals were anesthetized with continual isoflurane administration throughout the perfusion. The chest cavity was opened and retracted to expose the heart. The right atrium was clipped and a needle was inserted into the left ventricle to rapidly flush the cerebral vasculature of blood with oxygenated Krebs-Ringer-Carbicarb buffer for 3-5 seconds. Immediately thereafter, the flush was followed by 37 ℃ fixative (2% formaldehyde/2.5% gluataraldehyde) in a 0.1 M cacodylate buffer with 2 nM $CaCl_2$ and 4 mM $MgCl_2$ at pH 7.4 for 30 minutes. The tissue was allowed to rest for an hour, after which the brain was removed from the skull and stored in fixative overnight.

Electron Microscopy and Ultrastructure Analysis

As many of the methods used in this study for processing and imaging the tissue for serial section EM are similar to those used in Chapters 2 and 3, they are briefly mentioned here (for more detail see *Section 2.2 Methods*). Brains were examined under a dissecting microscope to guarantee they were well cleared of blood. The brains were bisected along the midsagittal plane and glued, medial-side down, onto a vibratome stage. In phosphate buffer, the brains were sliced into 70-µm thick parasagittal sections. Brain slices containing the middle of the hippocampus were selected. Area CA1 was dissected out of the slice and embedded in 7% agarose. The tissue in agarose was then processed for electron microscopy as outlined in Chapter 2. Longitudinal sections through CA1 were collected and mounted on pioloform-coated slot grids (Synaptek, Ted Pella Inc.). The sections were stained with saturated aqueous uranyl acetate followed by lead citrate for 5 minutes each. For these sections, large field-of-view images were automatically acquired on a transmission-mode scanning electron microscope (Zeiss Supra40) at 28 kV detection at 2 nm pixel size (Kuwajima et al., 2013).

EM images were aligned and cropped using TrakEM2 in Fiji (fiji.sc/TrakEM2) and analyzed using RECONSTRUCT™. Measurements were calibrated using a diffraction grating replica (Ernest Fullam Inc., Lantham, NY) and section thickness was determined using the cylindrical diameters method. Other methods for ultrastructural analyses are described in detail in Chapter 2.

Statistical Analyses

As a preliminary probe study investigating the ultrastructure in the *Fmr1* KO mouse, two littermate animals (1 WT and 1 *Fmr1* KO) were used. Statistical

analyses were performed in R (r-project.org) and STATISTICA (StatSoft, Tulsa, OK). To investigate differences in spine volume and synapse size between WT and KO mice, parametric one-way ANOVAs and non-parametric Kolmogorov-Smirnov (KS) tests were performed. A chi-square test was performed to investigate proportions of synapses associated with SER. A two-way ANOVA was used to investigate the effect of SER and genotype on synapse size. Statistical tests are reported in results and figure legends where appropriate. Significance was set to $p < 0.05$ and asterisks in figures denote $p < 0.05$ (*), $p < 0.01$ (**), and $p < 0.001$ (***).

4.3 Results

General Ultrastructure in WT and Fmr1 KO Mice

Low magnification views of hippocampal area CA1 stratum radiatum of adult WT (**Fig. 4.1**) and KO mice (**Fig. 4.2**) reveal no obvious structural differences in any synaptic compartment or organelle. There are very few degradative structures on EM sections in either genotype. Mitochondria are not swollen and cristae appear crisp and unbroken. SER also appears to be intact and not swollen. Glial processes can be seen on EM sections and contain darkly staining glycogen granules. Boutons are present along axons and contain similarly sized, round vesicles in pools and in close apposition with the plasma membrane. PSDs in postsynaptic spines are also clearly evident at low magnification and do not appear loose or dislodged from the plasma membrane. Thus, the general ultrastructure in the *Fmr1* KO mouse appears similar to that of the WT mouse.

Wild-type (WT)
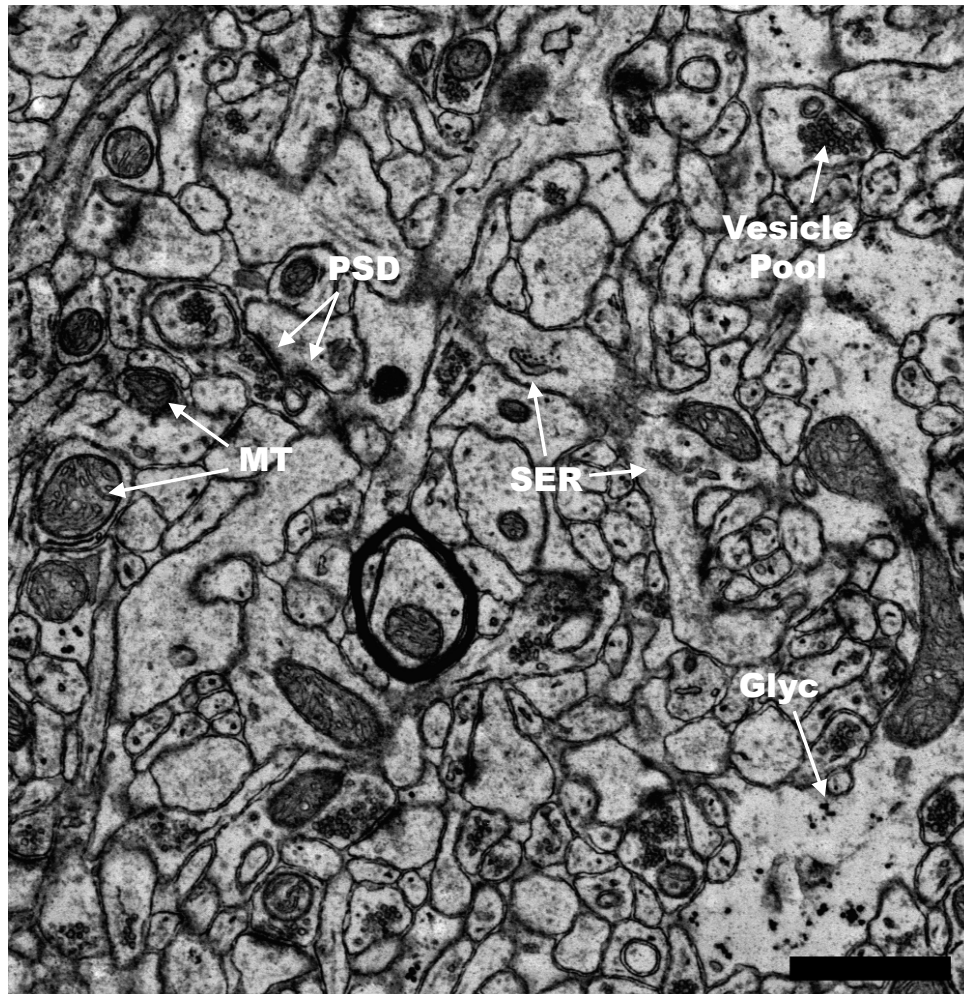
Figure 4.1: Low magnification view of area CA1 of an adult WT mouse. A low magnification view of hippocampal area CA1 stratum radiatum of an adult WT mouse reveals structures evident in area CA1 of the adult rat. PSDs are visible. Mitochondria (MT) are not swollen and have cristae that are crisp. Glia processes are present and contain darkly staining glycogen granules (Glyc). SER is not swollen. PSDs are clearly visible and do not appear loose or dislodged from the plasma membrane. Boutons as well as pools of synaptic vesicles are visible along axons. Scale bar = 1 µm.

Fmr1 Knockout (KO)
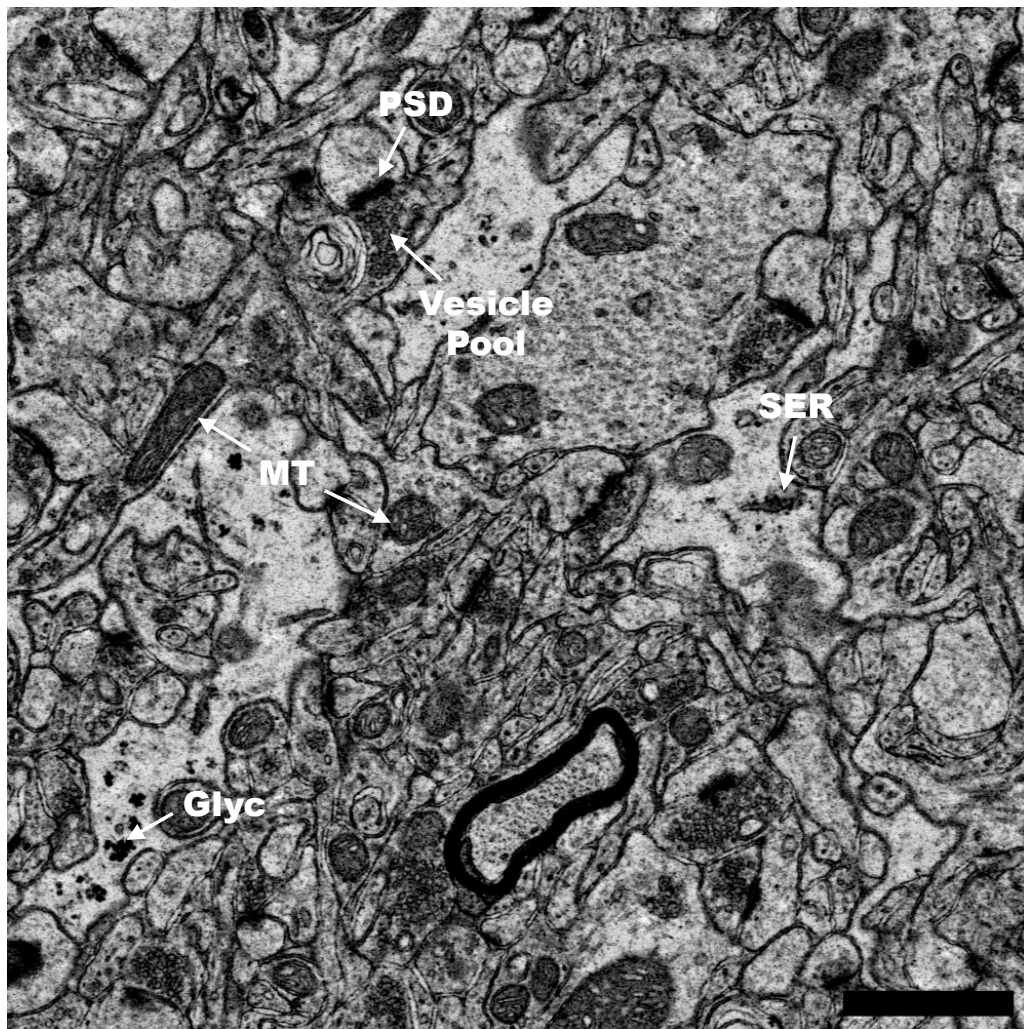
Figure 4.2: Low magnification view of area CA1 of an adult *Fmr1* KO mouse. A low magnification view of hippocampal area CA1 stratum radiatum in the *Fmr1* KO mouse reveals that the general ultrastructure in the KO appears similar to that of its WT counterpart. PSDs and presynaptic vesicle pools are evident. Mitochondria (MT) are not swollen and have crisp cristae. SER is not swollen. Glial processes are present and filled with darkly staining glycogen granules (Glyc). Scale bar = 1 μm.

Dendritic Spines and Synapses

As several light level studies indicate an overabundance of small thin protrusions along cortical dendrites of the *Fmr1* KO mouse (Comery et al., 1997; Hayashi et al., 2007; McKinney et al., 2005), we were curious to investigate if hippocampal dendritic protrusions also appeared thin and developmentally immature. To address this question, we performed an unbiased three-dimensional volume analysis by placing a 3.5 µm × 3.5 µm sampling frame on 50 consecutive sections of each series. All dendritic spines and associated PSDs falling within the sampling frame or touching two inclusion lines were included in the analysis. Spines and PSDs falling outside the sampling frame or touching two exclusion lines were not analyzed. (We performed a similar analysis for presynaptic content of adult rats in Chapter 2.) In the WT mouse, we identified 86 total spines with 93 PSDs in a 37.19 µm^3 volume (**Fig. 4.3 and 4.4**) and in the KO mouse, we identified 94 total spines with 98 PSDs in a 35.06 µm^3 volume (**Fig. 4.5 and 4.6**). Curiously, in the analyzed volumes from both WT and KO mice we were unable to identify any dendritic protrusions that were non-synaptic. Furthermore, although light level studies suggest cortical spine density is increased in the *Fmr1* KO mouse, EM reconstructions performed here revealed that the density of CA1 spines (2.68 spines/µm^3) and synapses (2.80 synapses/µm^3) in hippocampal area CA1 of the KO mouse differed only slightly from that in the WT mouse (WT spine density: 2.31 spines/µm^3, WT synapse density: 2.50 synapses/µm^3).

To investigate if CA1 spines in the *Fmr1* KO mouse were smaller than their WT counterparts, we calculated and compared the volume of dendritic spines that we had identified in each volume analysis (**Fig. 4.7**). A one-way

Wild-type
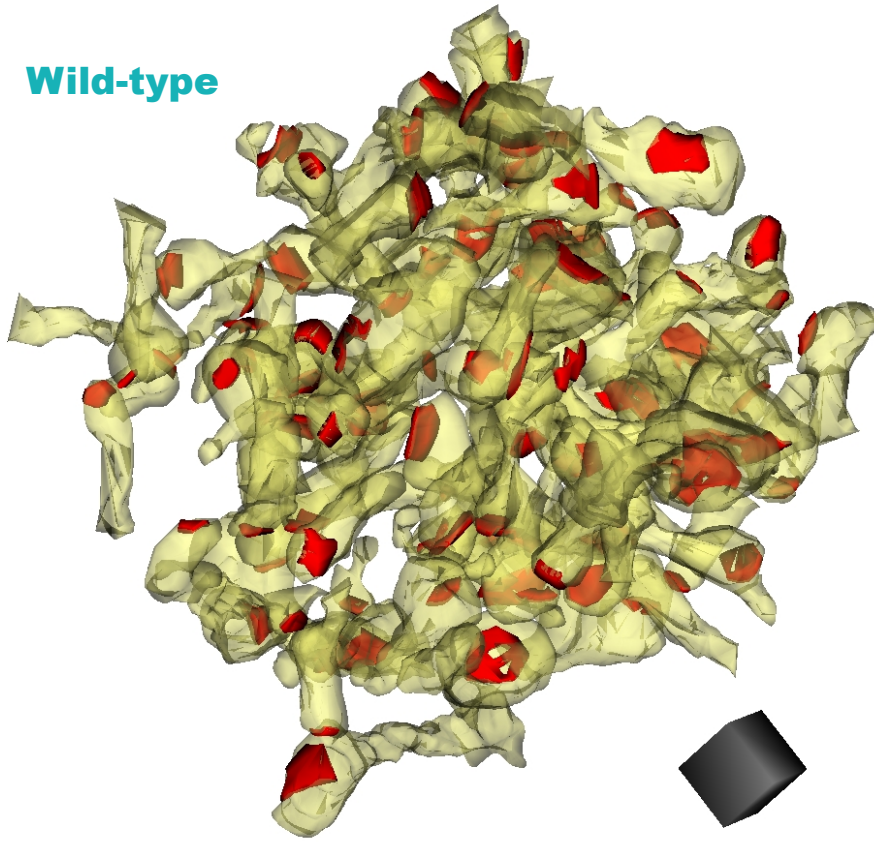
86 total spines/37.19 μm^3
= 2.31 spines/μm^3

Figure 4.3: CA1 dendritic spines of the adult WT mouse. Three-dimensional reconstructions of analyzed dendritic spines (n = 86, yellow) with synapses (red) falling within a 37.19-μm^3 unbiased volume in the middle of area CA1 stratum radiatum of an adult WT mouse. Scale cube = 0.5 μm on each side.

Wild-type

93 total synapse/37.19 µm^3
= 2.50 synapses/µm^3
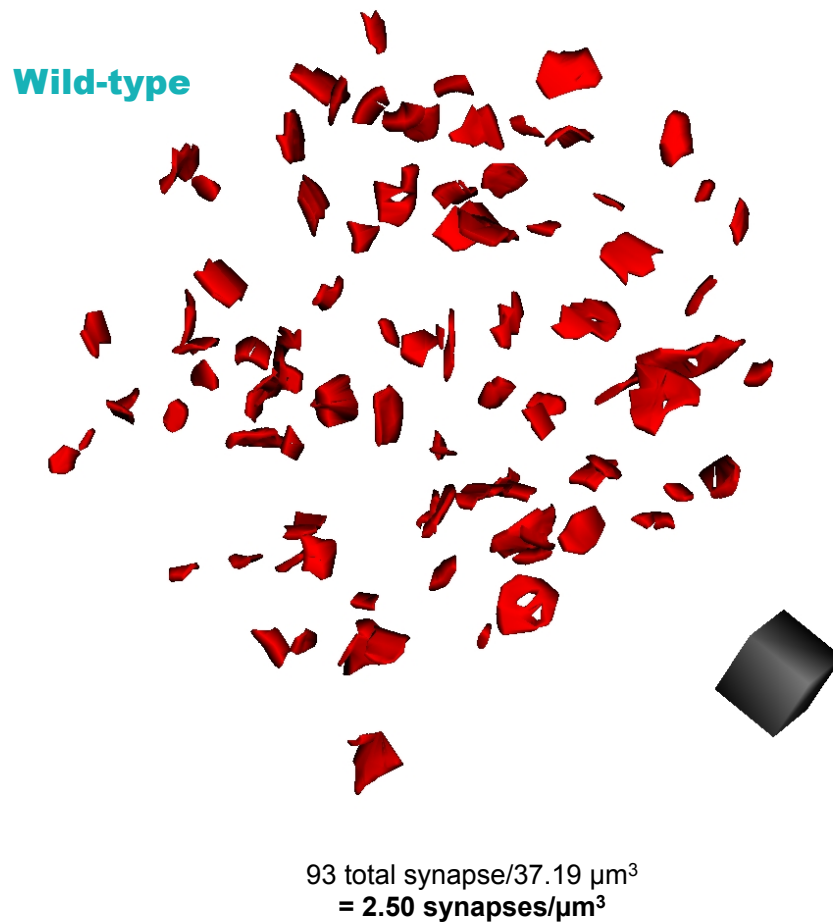
Figure 4.4: CA1 synapses of the adult WT mouse. Three-dimensional reconstructions of analyzed synapses (n = 93, red) falling within a 37.19-µm^3 unbiased volume in the middle of area CA1 stratum radiatum of an adult WT mouse. Scale cube = 0.5 µm on each side.

Fmr1 KO

94 total spines/35.06 µm^3
= 2.68 spines/µm^3
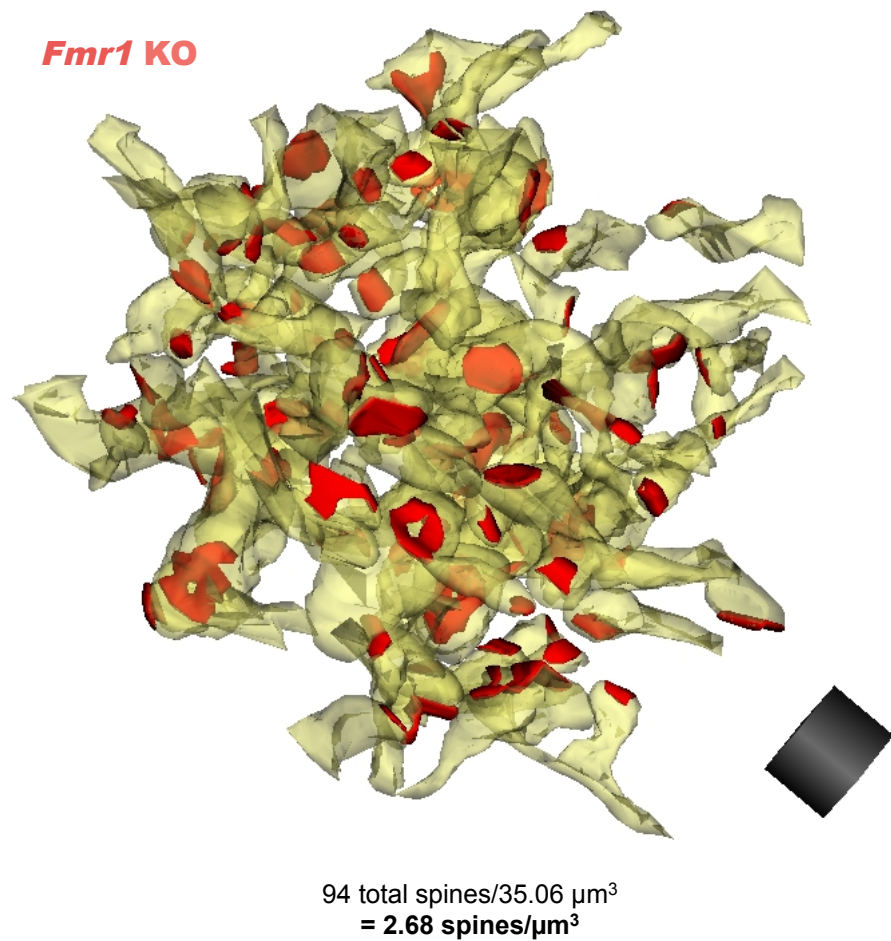
Figure 4.5: CA1 dendritic spines of the adult *Fmr1* KO mouse. Three-dimensional reconstructions of analyzed dendritic spines (*n* = 94, yellow) with synapses (red) falling within a 35.06-µm^3 unbiased volume in the middle of area CA1 stratum radiatum of an adult *Fmr1* KO mouse. Scale cube = 0.5 µm on each side.

98 total synapses/35.06 μm^3
= 2.80 synapses/μm^3

Figure 4.6: CA1 synapses of the adult _Fmr1_ KO mouse. Three-dimensional reconstructions of analyzed synapses (_n_ = 98, red) falling within a 35.06-μm^3 unbiased volume in the middle of area CA1 stratum radiatum of an adult _Fmr1_ KO mouse. Scale cube = 0.5 μm on each side.

a

0.011 µm^3 0.048 µm^3 0.080 µm^3 0.352 µm^3

Wild-type

b

0.008 µm^3 0.037 µm^3 0.060 µm^3 0.263 µm^3

Fmr1 **KO**

Figure 4.7: Example spine reconstructions from WT and *Fmr1* KO mice. Example reconstructions of spines (yellow) and PSDs (red) in hippocampal area CA1 stratum radiatum of WT (a) and *Fmr1* KO (b) mice. Spines represent the 0th, 33rd, 67th, and 100th percentile in volume from each condition. Scale cube = 500 nm on each side.

122

ANOVA revealed that, on average, spines in the KO were slightly smaller than spines in the WT mouse (**Fig. 4.8b**). Several of the largest spines were found in the WT mouse. To uncover if these large outliers were influencing the ANOVA result, we isolated spines with volumes larger than 4 standard deviations from the overall population mean (WT and KO spines combined: μ = 0.077 μm^3, σ = 0.064 μm^3). When these spines were removed from the analysis (2 WT spines), the ANOVA did not reveal a significant difference in spine volume between genotypes ($F_{(1,174)}$ = 2.03, p = 0.16). Because the distribution of spine volumes is not normal and because a few, large outlier spines drove our ANOVA result, we performed a KS test on spine volumes in each genotype. The KS test revealed that spines in the KO mouse were slightly, but significantly smaller than WT spines (p < 0.01, **Fig. 4.8c**). Thus, spines in the *Fmr1* KO are modestly smaller than their WT counterparts, but do not appear to be filopodia or developmentally immature.

Fmr1 KO mice express exaggerated mGluR-LTD (Huber et al., 2002; Krueger and Bear, 2011) and LTD drives the removal of AMPA receptors from the PSD (Collingridge et al., 2010; Lüscher and Malenka, 2012). To investigate if we could detect a difference in synapse size in the *Fmr1* KO mouse, we compared the size of PSDs in each genotype (**Fig. 4.9**). Curiously, both a one-way ANOVA (**Fig. 4.10b**) and a KS test (**Fig. 4.10c**) failed to reveal any difference in synapse size between the WT and *Fmr1* KO mouse. Thus, it appears as if the size of CA1 synapses in the *Fmr1* KO mouse is comparable with that in the WT mouse.
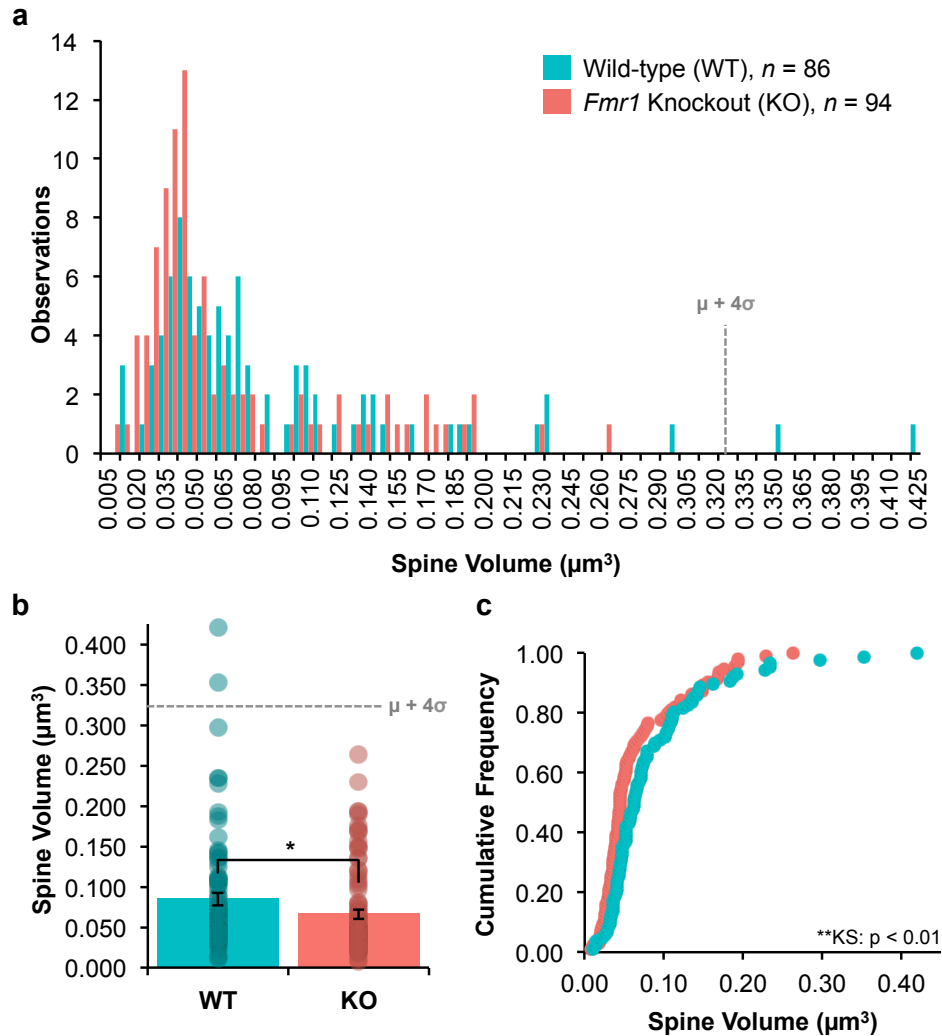
Figure 4.8: Comparison of spine volume in WT and *Fmr1* KO mice. (a) A histogram reveals that the distributions of WT spine volumes (n = 86, teal) and *Fmr1* KO spine volumes (n = 94, pink) appear to be similar. (b) Bars represent average spine volume in each genotype. Error bars represent standard error of the mean. Transparent circles represent spread of the data. A one-way ANOVA revealed that the average spine volume in the *Fmr1* KO mouse was slightly, but significantly smaller than the average spine volume in the WT mouse ($F_{(1, 178)}$ = 3.9735, $p < 0.05$), but when spine volumes greater than 4 standard deviations from the overall mean ($\mu + 4\sigma$, gray dotted line) were removed from the analysis (2 WT spines), the effect became non-significant ($F_{(1, 176)}$ = 2.03, p=.16). (c) A follow-up, non-parametric KS test did, however, reveal that spine volumes were slightly smaller in the *Fmr1* KO mouse (D = 0.25, p < 0.01).

a

0.009 µm² 　　0.034 µm² 　　0.061 µm² 　　0.151 µm²

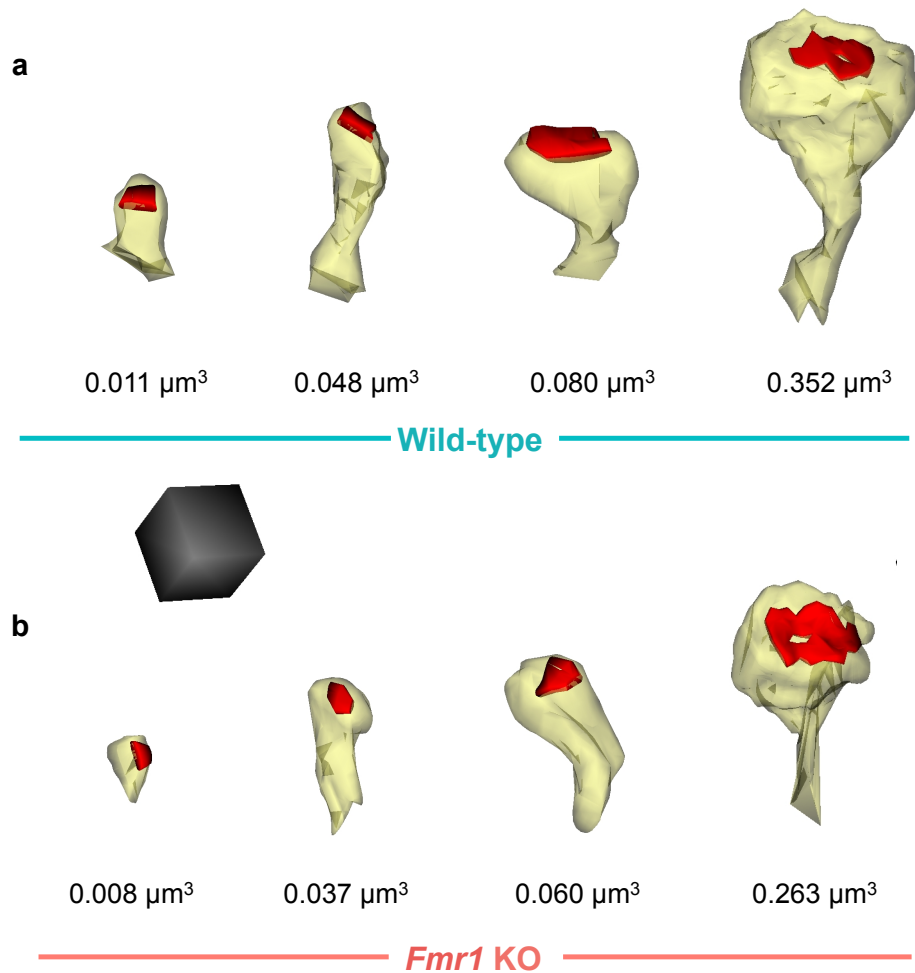**Wild-type**

b

0.006 µm² 　　0.035 µm² 　　0.059 µm² 　　0.207 µm²
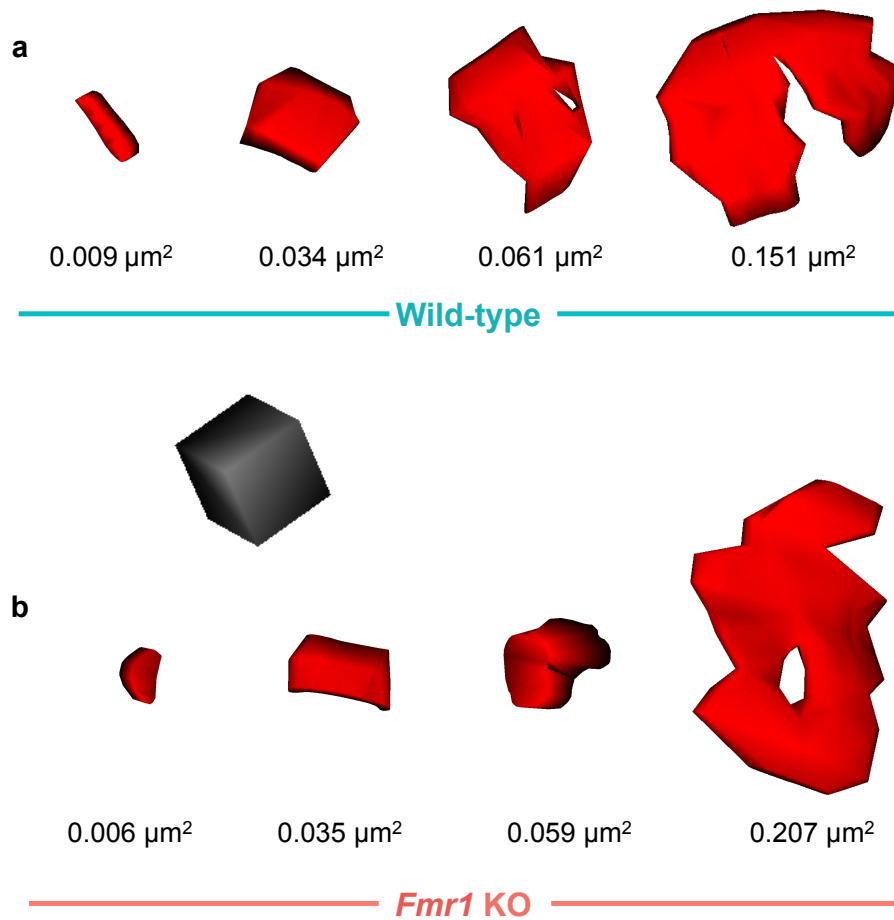
***Fmr1* KO**

Figure 4.9: Example PSD reconstructions from WT and *Fmr1* KO mice. Example reconstructions of PSDs in hippocampal area CA1 stratum radiatum of WT (a) and *Fmr1* KO (b) mice. PSDs represent the 0th, 33rd, 67th, and 100th percentile in size from each condition. Scale cube = 200 nm on each side.
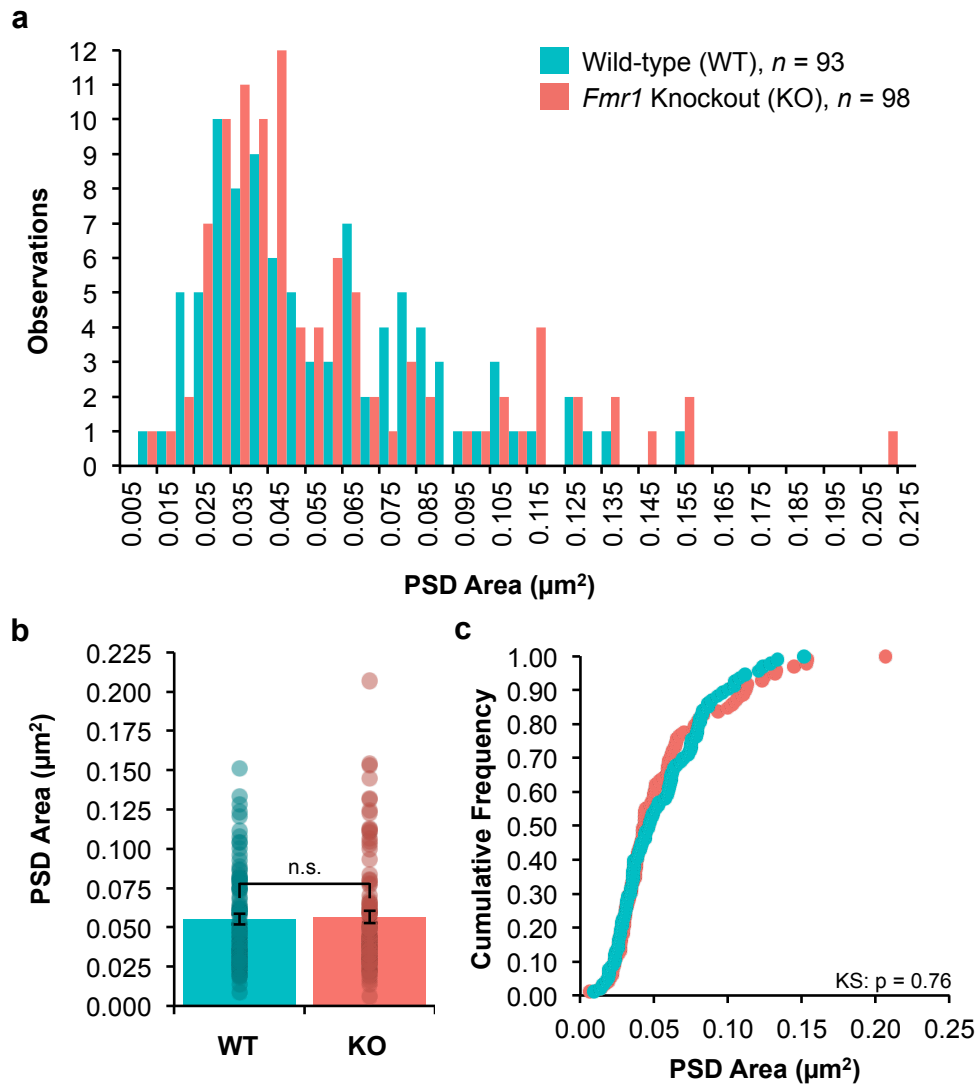
Figure 4.10: Comparison of PSD area in WT and *Fmr1* KO mice. (a) A histogram reveals that the distributions of WT PSD areas (n = 93, teal) and *Fmr1* KO PSD areas (n = 98, pink) appear to be similar. (b) Bars represent average PSD area in each genotype. Error bars represent standard error of the mean. Transparent circles represent spread of the data. A one-way ANOVA revealed that the average PSD area in the *Fmr1* KO mouse did not differ significantly from the average PSD area in the WT mouse ($F_{(1,189)}$ = 0.054, p = 0.82). (c) A follow-up, non-parametric KS test confirmed that the distributions of PSD areas in WT and *Fmr1* KO mice did not differ significantly (D = 0.092, p = 0.76).

126

SER and Spine Apparatuses

Because we had revealed that plasticity induces dramatic dendritic SER remodeling in the adult rat (Chapter 3), we reasoned that pathologically elevated mGluR signaling and protein synthesis in the *Fmr1* KO mouse (Bhakar et al., 2012) might be associated with changes in SER structure. We preliminarily addressed this hypothesis by evaluating SER tubules and spine apparatuses associated with synapses in each volume analysis (**Fig. 4.11a**). Of the 93 WT synapses, 13 were closely associated with an SER tubule and 4 with a spine apparatus. Of the 98 KO synapses, 11 were associated with an SER tubule and 9 with a spine apparatus (**Fig 4.11b**). A chi-square test revealed that the proportions of synapses associated with SER and spine apparatuses in the *Fmr1* KO mouse did not differ with that in the WT mouse (p = 0.37). In Chapter 3, it was demonstrated that SER in spines was associated with larger PSDs and we wanted to determine if this was true in WT and KO mice. A two-way ANOVA revealed a main effect of SER on synapse size (p < 0.001) but did not reveal a main effect of genotype (p = 0.59) or an interaction (p = 0.49, **Fig. 4.11c**). Thus, as in the adult rat (see Chapter 3), WT and KO mouse synapses associated with SER are larger than those without and the absence of FMRP does not alter this relationship.

Polyribosomes

Finally, an unchecked increase in protein synthesis is thought to be pathognomonic of FX. Thus, we were interested to learn whether the number of polyribosomes is altered in synapses from hippocampal area CA1 of the mature *Fmr1* KO mouse. Polyribosomes were identified as clusters of 3 or more ribosomes, which appear as opaque, roughly 10-25 nm in diameter puncta that

have a blurry, gray halo (**Fig. 4.12a**). Because individual ribosomes are difficult to identify unambiguously from other protein complexes in the cytosol on EM sections, we selected 15 consecutive EM sections from each genotype that had the least staining artifact. (Staining artifact such as lead citrate precipitate might obscure these small organelles.) We placed a 7.5 μm × 7.5 μm sampling frame on each section and identified every polyribosome that fell completely within the volume or touched an inclusion line. Any polyribosomes touching an exclusion line were excluded from the analysis. We identified 17 polyribosomes in a 51.47-$μm^3$ volume in the WT mouse (0.33 polyribosomes/$μm^3$) and 9 polyribosomes in a 48.09-$μm^3$ volume in the KO mouse (0.19 polyribosomes/$μm^3$). As the number of ribosomes were somewhat comparable between genotypes, we were curious to investigate if each polyribosome had more or fewer ribosomes in the *Fmr1* KO mouse. To investigate this, we summed ribosomes in each polyribosome cluster. A one-way ANOVA revealed that the number of ribosomes per polyribosome in the *Fmr1* KO mouse did not differ significantly with its WT counterpart (**Fig. 4.12b**). Each genotype had polyribosomes containing on average ~5 ribosomes.

4.4 Discussion

In stark contrast to light level studies that suggest FX is associated with an overabundance of small dendritic protrusions (Comery et al., 1997; Dölen et al., 2007; Hayashi et al., 2007; McKinney et al., 2005), CA1 synapses in this *Fmr1* mouse were similar to those in its WT counterpart. Synapse size, proportion of synapses with SER, and polyribosome numbers in the KO mouse were comparable to that of the WT mouse. While spine volume was modestly smaller in the KO mouse, small, thin dendritic protrusions were not overly abundant in
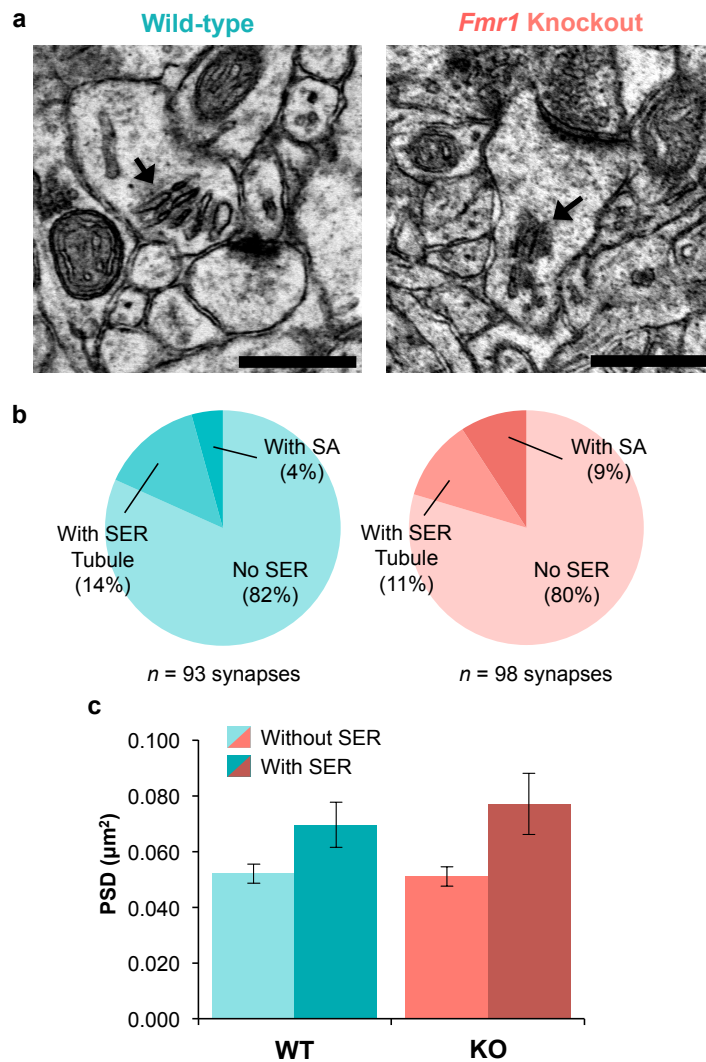
Figure 4.11: SER Tubules and Spine Apparatuses in WT and *Fmr1* KO mice. (a) Example electron micrographs of a spine apparatus in a large dendritic spine from each condition. Note that SER folds in the spine apparatus appear normal and not swollen in either genotype. Scale bars = 0.5 µm. (b) Percentages of synapses in each genotype in close association with an SER tubule, a spine apparatus (SA), or neither. A chi-square test revealed that the these proportions did not differ significantly between genotypes ($\chi^2_{(1, N = 6)}$ = 1.99, p = 0.37). (c) Bars represent average PSD area of synapses in both genotypes associated with or without SER. Error bars represent standard error of the mean. A two-way ANOVA revealed that, as in adult rats (see Chapter 3), WT and *Fmr1* KO synapses in close association with SER were larger ($F_{(1, 187)}$ = 12.865, p < 0.001). The ANOVA did not, however, reveal a main effect of genotype ($F_{(1, 187)}$ = 0.29, p = 0.59) or an interaction ($F_{(1, 187)}$ = 0.49, p = 0.49).

a **Wild-Type** (*n* = 17)   *Fmr1* **Knockout** (*n* = 9)

0.33 polyribosomes/μm^3 0.19 polyribosomes/μm^3

b
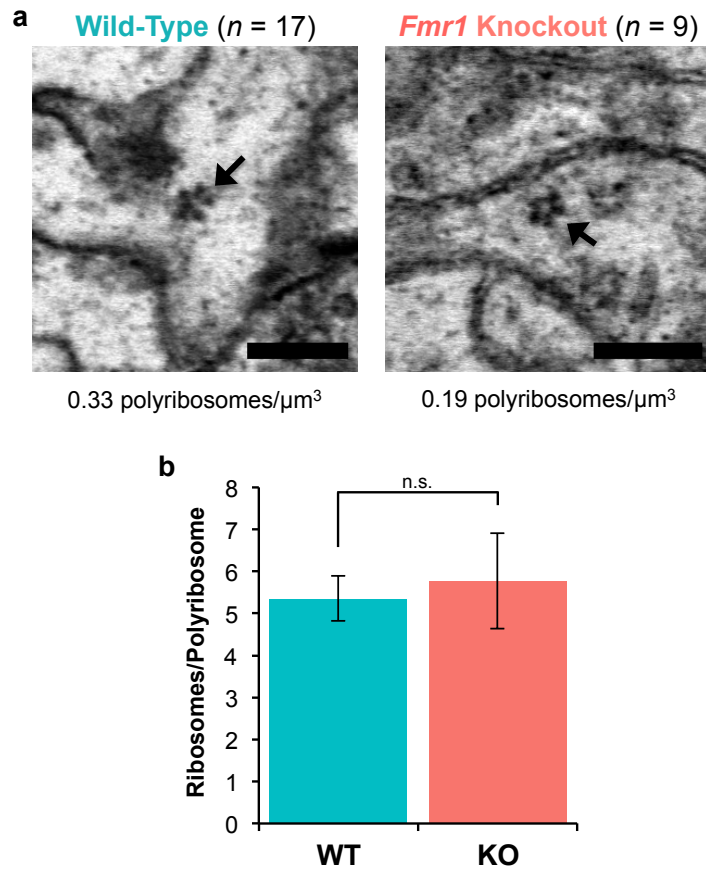
Figure 4.12: Polyribosomes in adult WT and *Fmr1* KO mice. (a) Example electron micrographs of polyribosomes at the base of a spine from each genotype (arrows). Polyribosomes were identified on the basis of their appearance as clusters of ≥ 3, roughly 10-25-nm darkly staining puncta with gray halos. Scale bars = 200 nm. (b) Bars represent average number of ribosomes in each polyribosome in each condition. Error bars represent standard error of the mean. A one-way ANOVA revealed that the number of ribosomes in each polyribosome cluster did not differ significantly between genotypes ($F_{(1, 24)}$ = 0.15, p = 0.70).

the KO adult. Although the investigation presented in this chapter is a probe study employing only two animals, these preliminary findings tentatively indicate that gross synaptic malformation might not be readily apparent in this region of the adult *Fmr1* KO mouse brain. Thus, synaptic malformation might be restricted to the developing mouse, might be restricted to other brain regions, or might more nuanced than can be detected with the methods employed here. These findings do, however, support live imaging studies in occipital and somatosensory cortex that demonstrated synaptic malformation was only apparent in animals less than a month old (Cruz-Martín et al., 2010; Nimchinsky et al., 2001). Thus, any step forward with this project would most likely involve characterizing the structure of synapses in area CA1 of younger animals.

Aberrant Signaling in FX and SER

FX symptomology is thought to be due to excessive mGluR signaling at the synapse (Bear et al., 2004; Krueger and Bear, 2011). In fact, several studies have shown that reduction of mGluR signaling reduces the severity of the FX phenotype. Dölen et al. (2007) showed that, in FX mice, genetic reduction (but not elimination) of the *Grm5* gene, which encodes mGluR5, corrected a variety of phenotypes associated with these mice including audiogenic seizures (AGSs), pathologically increased protein synthesis, and excessive LTD. Other studies have shown that pharmacological antagonism of mGluR signaling also corrects phenotypes associated with the disorder including protein synthesis (Osterweil et al., 2010; 2013), CA3 epileptiform-like activity (Chuang et al., 2005), and spine malformation in cultured neurons (de Vrij et al., 2008). mGluR signaling is linked to the SER via phosphoinositol hydrolysis pathways described in Chapter 3. In

this study, the proportion of synapses in close association with SER were similar in WT and KO mice. But the exaggerated mGluR signaling in the KO mouse might influence the volume or shape of SER tubules and spine apparatuses without altering their numbers. Thus, a next step would be to reconstruct the 37 SER tubules and spine apparatuses near synapses that were identified and compare their volumes. This analysis might demonstrate an influence of aberrant FX signaling on SER dimensions.

Possible Presynaptic Phenotype

As investigated in Chapter 2, the presynaptic compartment and its vesicles are dynamic during normal plasticity. Recently, it was shown that *Fmr1* KO mice express an abnormal form of presynaptic LTP in the anterior cingulate cortex (Koga et al., 2015) and that FMRP is involved in the regulation of vesicular release probability at CA3-CA1 synapses (Wang et al., 2014). However, very little is known about the structure and composition of the presynaptic compartment in the *Fmr1* KO mouse. What is known, however, is conflicting. In primary somatosensory cortex of P14 and P35 animals, vesicle pool size and number of docked vesicles have been reported to be normal in the *Fmr1* KO animal (Till et al., 2012). Moreover, in hippocampal area CA1, vesicle pools have been reported to be larger (Deng et al., 2011) and smaller (Klemmer et al., 2011) in the KO mouse. Thus, conflicting reports suggest there might be underlying presynaptic malformation that has yet to be pinned down. A simple next step in the current investigation would be to characterize the presynaptic compartment in the *Fmr1* KO animal in perfusion fixed hippocampus. If neurotransmitter release

is affected by signaling deficits, differences in the number of vesicles docked along the presynaptic active zone might be apparent in three dimensions.

Therapeutic Intervention and Synaptic Structure

Recently, it has been demonstrated that excessive protein synthesis in the *Fmr1* KO mouse can be corrected by treating animals with lovastatin (Osterweil et al., 2013), a commonly prescribed statin drug used to treat high cholesterol. Statin drugs are relatively cheap, widely available, well-tolerated, and FDA-approved for use in both adults and children, making them attractive therapeutic agents. By mildly reducing Ras activation (Li et al., 2005a; Liao, 2002; Vaughan, 2003), lovastatin reduces ERK1/2 signaling, which links mGluR activation and excessive protein synthesis in FX (Osterweil et al., 2010). In hippocampal slices from *Fmr1* KO mice, application of the GABA-A receptor antagonist bicuculline induces epileptiform activity in area CA3 (Chuang et al., 2005). Preincubating the slice in lovastatin blocks the induction of this activity. Furthermore, preincubating *Fmr1* KO visual cortical slices with lovastatin reduces their hyperexcitability. *Fmr1* KO mice are susceptible to audiogenic seizures (Osterweil et al., 2010; Yan et al., 2004), which is thought to be reflective of the increased seizure prevalence in humans with FX. Amazingly, lovastatin delivery via food pellets for just 2 days, which mimics human administration of the drug, reduces the incidence of audiogenic seizures in *Fmr1* KO mice by 53%. Thus, it would be very interesting to investigate if lovastatin administration is exerting its therapeutic effect through structural remodeling of the synapse. While striking structural malformations did not appear in this adult animal, treating younger animals, which have been proposed to exhibit the most obvious structural deficits

in FX (Cruz-Martín et al., 2010; Nimchinsky et al., 2001), with lovastatin might reveal a therapeutic structural effect exerted by the drug.

Concluding Remarks

Though there are several more detailed analyses than can be undertaken in this tissue, this preliminary study revealed no strikingly obvious structural malformation in CA1 synapses of the adult *Fmr1* KO mouse. Thus, it might be more fruitful to investigate structural malformation and abnormal structural plasticity in younger KO animals. We currently have CA1 perfusion tissue from 2 WT and 2 *Fmr1* KO animals that are ~22 days old in blocks. Cutting single EM sections would be a quick way to assess if spine malformation is obvious in area CA1 of developing KO animals.

Chapter 5: Concluding Remarks and Future Directions

The studies presented in this dissertation demonstrate that coordinated structural remodeling of the synapse is evident on EM sections and occurs on both sides of the synapses during late-phase LTP in the adult animal. The reduction in dendritic spines described earlier (Bourne and Harris, 2011a) was coupled with a reduction in presynaptic boutons, which argues entire synaptic units act as dynamic and cohesive structures. We also uncovered EM evidence of the dynamic nature of presynaptic vesicle pools. The findings suggest that reserve pool vesicles move toward the plasma membrane, possibly to support increased vesicular release or to support active zone expansion that occurs during LTP. Vesicles trafficked through interbouton regions of the axon were eliminated during LTP suggesting they were either moved into boutons to support smaller vesicle pools or they were released during trafficking. Postsynaptically, dendritic SER was extensively remodeled during LTP in the adult animal. SER was redistributed into dendritic spines where SER formed larger spine apparatuses. To conserve SER at the base of spines, SER was redistributed from areas of the dendrite that lacked spines. SER at the base of spines with synapses that expanded the most during LTP was found to be the most complex. As previous investigations have shown that SER complexity slows the diffusion of SER cargo through the dendrite and facilitates its offloading (Cui-Wang et al., 2012), an increase in SER complexity at the base of spines hosting expanding synapses could provide those synapses with integral membrane receptors and a platform for posttranslational protein modification. As a preliminary investigation into how normal mechanisms of structural plasticity might go awry during

135

abnormal synaptic signaling, the structure of CA1 synapses in the adult *Fmr1* KO mouse was shown to be similar to that of its WT counterpart. Synapse size, proportion of SER structures, and polyribosomes are comparable in adult WT and KO animals. A next step would be to characterize abnormal synaptic structure in developing *Fmr1* KO animals to uncover if synaptic malformations disappear with age. Of the vastly different directions these results could lead, several of the more interesting questions that emerge from the combined findings are discussed below.

As explored in Chapters 2 and 3, neurotransmission and calcium signaling alone might be coordinating plasticity across the synapse; however, it would be interesting to know if other molecular signals might also support structural coordination across the synapse. As LTP is induced postsynaptically via activation of NMDA receptors at CA3-CA1 synapses, there is much interest in investigating how retrograde signals produced and released postsynaptically might alter presynaptic dynamics (Padamsey and Emptage, 2014; Regehr et al., 2009). One such diffusible molecule is nitric oxide (NO), which was first identified as a possible retrograde signal involved in LTP in the early 1990s (Böhme et al., 1991; O'Dell et al., 1991; Schuman and Madison, 1991). CA1 pyramidal cells express both neuronal and endothelial forms of NO synthase (NOS, Dinerman et al., 1994), which is activated by NMDA receptors (Boehning and Snyder, 2003; Garthwaite, 2008) and converts L-arginine to NO. Guanylate cyclase appears to be a major NO target and subsequent cyclic GMP production further modulates a variety of downstream molecules (Garthwaite, 2008). Both genetic deletion and pharmacological inhibition of NOS attenuates LTP at CA3-CA1 synapses (Padamsey and Emptage, 2014). Application of NO scavengers (e.g.,

hemoglobin) to hippocampal slices and cultures also severely attenuates LTP (Arancio et al., 1996; Schuman and Madison, 1991). Arancio et al. (1996) demonstrated that LTP induced by tetanus could be blocked with postsynaptic, but not presynaptic, application of N^G-monomethyl-L-arginine, a NOS inhibitor. Furthermore, when paired with presynaptic stimulation, release of NO by activation of an NO donor molecule with UV light can cause LTP. This effect is blocked by presynaptic, but not postsynaptic, application of hemoglobin. Thus, these findings indicate NO is produced postsynaptically and diffuses into the presynaptic compartment where it induces changes that support LTP.

Curiously, other groups have demonstrated that NO is somehow required to produce normal presynaptic plasticity following LTP induction. Nikonenko et al. (2003) showed that, in organotypic slice cultures, LTP is accompanied by an increase in the rate of bouton remodeling and turnover. The group was able to produce similar remodeling in a subset of boutons by incubating slices with NO donor molecules. Application of the NOS inhibitor *N*-omega-nitro-L-arginine-methylester blocked the effect. Stanton et al. (2005) used FM1-43 to monitor changes in vesicular release associated with LTP. The group found that the increase in probability of release at CA3-CA1 synapses following the induction of LTP was initially reduced with application of L-nitroarginine, a NOS inhibitor. Application of NO donors increased release probability when paired with stimuli that normally do not alter release. Thus, there is some evidence supporting the role of NO in coordinating postsynaptic LTP induction with presynaptic structural plasticity. An interesting next step would be to bath-apply low levels of NOS inhibitors or NO scavengers to hippocampal slices and induce LTP. Three-dimensional reconstructions of CA3-CA1 synaptic ultrastructure might reveal

137

whether normal postsynaptic remodeling occurs while presynaptic remodeling requires unperturbed NO signaling. If presynaptic structural remodeling is impaired and this impairment were to correlate directly with attenuated LTP, this follow-up experiment would lend further support to the role presynaptic remodeling plays during LTP and provide a molecular mechanism for structural coordination across the synapse.

Molecules physically linking both sides of the synapse might also be playing a role in coordinating structural plasticity across the synapse. A variety of cell adhesion molecules (CAMs) bridge the synaptic cleft. CAMs act not only in a structural role but are also involved in trans-synaptic signaling (Benson and Huntley, 2012; Dalva et al., 2007; Missler et al., 2012). CAMs include a variety of proteins characterized by their extracellular domains, which include immunoglobulin- (Ig-) domains, cadherin domains, laminin A, neurexin, and sex hormone-binding protein domains, and leucine-rich repeats. There are several lines of evidence that demonstrate CAMs are involved in calcium signaling. In particular, three members of the Ig-superfamily of CAMs, neural cell adhesion molecules (NCAMs), neuroplastins (NPs), and limbic system-associated membrane protein (LAMP), might be functionally linked to the SER at synapses. Application of purified NCAM (Bohlen Und Halbach et al., 1992), artificial ligands (Kiryushko et al., 2006; Rønn et al., 2002), or antibodies against NCAM (Frei et al., 1992; Schuch et al., 1989) all increase intracellular calcium fluorescence. Similar results are shown with recombinant NP and LAMP in hippocampal neurons (Owczarek et al., 2010; 2011; Zhukareva et al., 1997). While inhibition of L- and T-type calcium channels reduces intracellular calcium fluorescence in response to NCAM activation, in cultured hippocampal neurons depletion of

calcium stores with thapsigargin also attenuates the calcium signal peak with NCAM activation (Kiryushko et al., 2006; Shima et al., 2007). Another set of canonical CAMs at the synapse are the cadherins and application of recombinant forms of atypical cadherins, Celsr2 and Celsr3, both highly expressed in hippocampal and forebrain neurons (Shima et al., 2002), also increases intracellular calcium in cells, which can be blocked by thapsigargin administration (Shima et al., 2007). The link between CAMs and intracellular stores is still murky but might involve phosphoinositide hydrolysis pathways described in Chapter 3. In fact, inhibitors of diacylglycerol lipase reduce the increase in intracellular calcium following NCAM and NP activation (Archer et al., 1999; Owczarek et al., 2010). Thus, activation of several CAMs present at the synapse appears to engage intracellular stores of calcium. Couple these findings with the fact that SER is occasionally seen in close physical apposition with the PSD (Harris and Weinberg, 2012; Spacek and Harris, 1997) and there might be physical protein linkages between cellular adhesion molecules and the SER that have yet to be described. Thus, it would be interesting to pharmacologically manipulate NCAMs and NPs in particular in hippocampal slices (much in the same vein as the proposed NO experiments above) and investigate the resultant ultrastructure of dendritic SER.

SER is not confined to the soma and the postsynaptic compartment of the neuron. It can also be found streaming through presynaptic axons and boutons in stratum radiatum in area CA1 (for beautiful images see Sorra and Harris, 1993; Sorra et al., 2006). As synaptic vesicle exocytosis is under the control of presynaptic calcium influx (Sudhof, 2012), intracellular calcium stores might serve to modulate presynaptic release. In fact, there is ample evidence that

ryanodine receptors are expressed presynaptically in hippocampal neurons of the rodent as well as in a variety of species (Llano et al., 2000; Ouyang et al., 1997; Padua et al., 1996; Sharp et al., 1993). Presynaptically localized ryanodine receptors also seem important in modulating both LTP and LTD. BDNF, which is released at CA3-CA1 synapses during TBS (Zakharenko et al., 2003) and which alone can induce a slow-onset, long-lasting form of LTP (Kang and Schuman, 1996), is released presynaptically upon ryanodine receptor activation with caffeine and ryanodine receptor blockade with dantrolene inhibits its release (Balkowiec and Katz, 2002).

Likewise, CA3-CA1 synaptic depression induced by low frequency stimulation can be blocked by inhibiting ryanodine receptors (Unni et al., 2004). Plasticity regulation by ryanodine receptors might be occurring through modulation of neurotransmitter release (Bouchard et al., 2003; Collin et al., 2005). By monitoring calcium transients in axons and boutons with fluorescent dyes, Emptage et al. (2001) demonstrated that blockade of calcium-induced calcium release from internal bouton stores attenuated the frequency of spontaneous transmitter release. A variety of studies have also demonstrated that the frequency of spontaneous synaptic events increases with LTP (Bekkers and Stevens, 1990; Malgaroli and Tsien, 1992; Wiegert et al., 2009). Thus, it is possible that changes in the morphology of presynaptic SER are, to some degree, regulating the changes in neurotransmitter release that follow the induction of LTP. It would be interesting to determine if, with LTP, there are concomitant changes in presynaptic SER volume. SER in the presynaptic compartment is more difficult to follow in serial sections as the cloud of vesicles frequently obscures SER's fine, membranous tubules. Changes in SER

morphology following the induction of LTP might however increase its discernibility as vesicle pools become smaller (Chapter 2 and Bourne et al., 2013). An increase in presynaptic SER volume might serve boutons as a large source of calcium that could function in the tuning of neurotransmitter release.

As noted in Chapter 3, SER also serves as a site of posttranslational modification of proteins. Once thought to occur exclusively in the soma, local translation of proteins in the postsynaptic compartment has been investigated since polyribosomes were first shown to exist near and in dendritic spines (Bourne et al., 2007; Harris and Weinberg, 2012; Ostroff et al., 2002; Steward and Levy, 1982). Presynaptic protein synthesis is well known to occur in axonal growth cones and during nerve degeneration (Holt and Schuman, 2013; Jung et al., 2012), but its role under normal, non-developmental synaptic function is just now coming online (Akins et al., 2009; 2012; Christie et al., 2009). This is curious, however, as axonal protein synthesis in invertebrates and vertebrates was first demonstrated nearly 50 years ago (Giuditta et al., 1968; Koenig, 1967; Zelená, 1970) and a variety of translational regulators have been shown to exist in axons, including FMPR (Antar et al., 2006; Hanson and Madison, 2007; Li et al., 2009), survival of motor neuron (SMN, Fallini et al., 2011; Zhang et al., 2006), and Hu-antigen D (HuD, Aronov et al., 2002; Smith et al., 2004). This might be in part, because axonal ribosomes do not readily form polyribosomes (Bunge, 1973; Tennyson, 1970; Yamada et al., 1971) and ultrastructural evidence of presynaptic polyribosomes are exceedingly rare on electron micrographs (from personal observations in area CA1). Finding monosomes (single ribosomes) would be challenging on EM sections, as they might be indistinguishable from other similarly sized molecular complexes in the cytoplasm. However, as SER

acts as a platform for some forms of protein synthesis, it would be interesting to know if presynaptic SER takes on a more "beaded" appearance as monosomes attach to SER if protein synthesis does increase in axonal compartments following LTP induction. This might prove very interesting as active zone expansion is thought to occur through arrival of discrete packets known as DCVs that carry active zone proteins (Bell et al., 2014; Shapira et al., 2003; Zhai et al., 2001). An increase in ribosomes at presynaptic SER might suggest that local translation of proteins is also necessary to support active zone expansion during LTP, allowing for the rarity of DCVs in hippocampal tissue (Sorra et al., 2006).

The FX study presented in Chapter 4 was a preliminary probe study investigating whether structural pathology was evident in the adult *Fmr1* KO mouse. In addition to possible studies outlined in the discussion of Chapter 4, it would be interesting to describe what structural mechanisms might be supporting LTP in a system with continual aberrant synaptic signaling such as in this KO mouse. Preliminary data from the Harris lab suggests that induction of robust LTP in hippocampal area CA1 of the *Fmr1* KO mouse begins at the same time as the WT mouse (~P35, Guan Cao, unpublished data) and pinning down a definitive LTP deficit in the *Fmr1* KO mouse has been difficult (Sidorov et al., 2013). Cohen and Abraham (1996) found that LTP can be "primed" by weakly stimulating mGluRs with ACPD (1-amino-cyclopentane-1S,3R-dicarboxylic acid). This mGluR-associated LTP priming requires protein synthesis (Raymond et al., 2000). Interestingly, in the *Fmr1* KO mouse, Auerbach and Bear (2010) showed that the protein synthesis requirement for LTP priming does not apply. This finding fits nicely with the exaggerated protein synthesis occurring under basal conditions in the KO mouse (Kelleher and Bear, 2008). Thus, it does appear that

LTP modulation is influenced in part by the absence of FMRP and might suggest altered structural remodeling to support LTP in its absence. Our lab is currently exploring this hypothesis by performing LTP experiments in WT and KO hippocampal slices, which will ultimately be imaged in the electron microscope. Reconstructions of CA1 neuropil might uncover that, although physiological expression of LTP appears normal in the KO mouse, the structural mechanisms underlying synaptic enhancement are wildly different from those of the WT mouse.

Finally, LTD results in the active removal of AMPA receptors from the PSD via endocytosis (Beattie et al., 2000; Brown et al., 2005; Man et al., 2000; Xiao et al., 2001) and light level studies have indicated that LTD causes actin depolymerization that results in spines shrinking or disappearing (Chen et al., 2004; He et al., 2011; Nägerl et al., 2004; Okamoto et al., 2004; Zhou et al., 2004). LTD induced by activation of mGluRs requires protein synthesis (Huber et al., 2000; 2001) and it appears that spines might require SER in order to undergo LTD (Holbro et al., 2009). It is curious that, even though there seems to be dramatic subcellular remodeling occurring with LTD (PSD structural dynamics, polyribosomes supporting protein synthesis, SER modulation) and that LTP has been shown over and over to induce dynamic structural plasticity, there are precious few studies investigating ultrastructure at the EM level following LTD induction (Bourne and Harris, 2008). As a first step into characterizing abnormal structural plasticity in the *Fmr1* KO mouse, which expresses an exaggerated form of LTD (see *Section 4.1: Autism, Fragile X, and Synaptic Pathology*), it would be crucial to use EM to characterize the synaptic remodeling associated with LTD in the WT mouse, much in the same vein of Bourne and Harris (2011).

143

The structural mechanisms supporting NMDA receptor-dependent and mGluR-dependent forms of LTD might be categorically distinct (Bliss et al., 2007; Collingridge et al., 2010). Characterizing synaptic remodeling in response to LTD induced via mGluR activation might illuminate aberrant structural plasticity in the *Fmr1* KO mouse. LTD in the *Fmr1* KO mouse might involve exaggerated but normal synaptic remodeling that is present in the WT mouse. On the other hand, LTD associated with unchecked protein synthesis and exaggerated mGluR signaling might trigger a host of other structural mechanisms that are unique to the pathology.

References

Aakalu, G.N., Smith, W.B., Nguyen, N., Jiang, C., and Schuman, E.M. (2001). Dynamic visualization of local protein synthesis in hippocampal neurons. Neuron *30*, 489–502.

Abraham, W.C. (2003). How long will long-term potentiation last? Philos Trans R Soc Lond, B, Biol Sci *358*, 735–744.

Abraham, W.C., Logan, B., Greenwood, J.M., and Dragunow, M. (2002). Induction and experience-dependent consolidation of stable long-term potentiation lasting months in the hippocampus. Journal of Neuroscience *22*, 9626–9634.

Ahmari, S.E., Buchanan, J., and Smith, S.J. (2000). Assembly of presynaptic active zones from cytoplasmic transport packets. Nat Neurosci *3*, 445–451.

Ahmari, S.E., and Smith, S.J. (2002). Knowing a nascent synapse when you see it. Neuron *34*, 333–336.

Ahmed, M.S., and Siegelbaum, S.A. (2009). Recruitment of N-Type Ca2+ Channels during LTP Enhances Low Release Efficacy of Hippocampal CA1 Perforant Path Synapses. Neuron *63*, 372–385.

Akins, M.R., Berk-Rauch, H.E., and Fallon, J.R. (2009). Presynaptic translation: stepping out of the postsynaptic shadow. Front Neural Circuits *3*, 17.

Akins, M.R., Leblanc, H.F., Stackpole, E.E., Chyung, E., and Fallon, J.R. (2012). Systematic mapping of fragile X granules in the mouse brain reveals a potential role for presynaptic FMRP in sensorimotor functions. J Comp Neurol *520*, 3687–3706.

Alabi, A.A., and Tsien, R.W. (2012). Synaptic vesicle pools and dynamics. Cold Spring Harb Perspect Biol *4*, a013680–a013680.

Amaral, D., and Lavenex, P. (2007). Hippocampal Neuroanatomy. In The Hippocampus Book, pp. 37–114.

Andersen, P., Bliss, T.V., and Skrede, K.K. (1971). Lamellar organization of hippocampal pathways. Exp Brain Res *13*, 222–238.

Angelis, A., Tordrup, D., and Kanavos, P. (2014). Socio-economic burden of rare diseases: A systematic review of cost of illness evidence. Health Policy.

Antar, L.N., Li, C., Zhang, H., Carroll, R.C., and Bassell, G.J. (2006). Local functions for FMRP in axon growth cone motility and activity-dependent regulation of filopodia and spine synapses. Mol Cell Neurosci *32*, 37–48.

Antonini, A., and Stryker, M.P. (1993). Rapid remodeling of axonal arbors in the visual cortex. Science *260*, 1819–1821.

Antonova, I., Arancio, O., Trillat, A.C., Wang, H.G., Zablow, L., Udo, H., Kandel, E.R., and Hawkins, R.D. (2001). Rapid increase in clusters of presynaptic proteins at onset of long-lasting potentiation. Science *294*, 1547–1550.

Araki, R., Sakagami, H., Yanagawa, Y., Hikima, T., Ishizuka, T., and Yawo, H. (2005). Transgenic mouse lines expressing synaptopHluorin in hippocampus and cerebellar cortex. Genesis *42*, 53–60.

Arancio, O., Kiebler, M., Lee, C.J., Lev-Ram, V., Tsien, R.Y., Kandel, E.R., and Hawkins, R.D. (1996). Nitric oxide acts directly in the presynaptic neuron to produce long-term potentiation in cultured hippocampal neurons. Cell *87*, 1025–1035.

Archer, F.R., Doherty, P., Collins, D., and Bolsover, S.R. (1999). CAMs and FGF cause a local submembrane calcium signal promoting axon outgrowth without a rise in bulk calcium concentration. Eur J Neurosci *11*, 3565–3573.

Aronov, S., Aranda, G., Behar, L., and Ginzburg, I. (2002). Visualization of translated tau protein in the axons of neuronal P19 cells and characterization of tau RNP granules. Journal of Cell Science *115*, 3817–3827.

Asanuma, K., Kim, K., Oh, J., Giardino, L., Chabanis, S., Faul, C., Reiser, J., and Mundel, P. (2005). Synaptopodin regulates the actin-bundling activity of alpha-actinin in an isoform-specific manner. J. Clin. Invest. *115*, 1188–1198.

Ascher, P., and Nowak, L. (1988). The role of divalent cations in the N-methyl-D-aspartate responses of mouse central neurones in culture. The Journal of Physiology *399*, 247–266.

Auerbach, B.D., and Bear, M.F. (2010). Loss of the fragile X mental retardation protein decouples metabotropic glutamate receptor dependent priming of long-term potentiation from protein synthesis. Journal of Neurophysiology *104*, 1047–1051.

Ault, B., Evans, R.H., Francis, A.A., Oakes, D.J., and Watkins, J.C. (1980). Selective depression of excitatory amino acid induced depolarizations by magnesium ions in isolated spinal cord preparations. The Journal of Physiology *307*, 413–428.

Bading, H. (2013). Nuclear calcium signalling in the regulation of brain function. Nat Rev Neurosci *14*, 593–608.

Bagni, C., and Greenough, W.T. (2005). From mRNP trafficking to spine dysmorphogenesis: the roots of fragile X syndrome. Nat Rev Neurosci *6*, 376–387.

Bailey, C.H., and Chen, M. (1983). Morphological basis of long-term habituation and sensitization in Aplysia. Science *220*, 91.

Bailey, C.H., and Chen, M. (1988a). Long-term memory in Aplysia modulates the total number of varicosities of single identified sensory neurons. Proc Natl Acad Sci USA *85*, 2373–2377.

Bailey, C.H., and Chen, M. (1988b). Long-term sensitization in Aplysia increases the number of presynaptic contacts onto the identified gill motor neuron L7. Proc Natl Acad Sci USA *85*, 9356–9359.

Baker, K.D., Edwards, T.M., and Rickard, N.S. (2013). The role of intracellular calcium stores in synaptic plasticity and memory consolidation. Neurosci Biobehav Rev *37*, 1211–1239.

Balkowiec, A., and Katz, D.M. (2002). Cellular mechanisms regulating activity-dependent release of native brain-derived neurotrophic factor from hippocampal neurons. Journal of Neuroscience *22*, 10399–10407.

Barad, M. (2006). Divide and conquer: an L-type voltage-gated calcium channel subtype finds a role in conditioned fear. Learning & Memory *13*, 560–561.

Barnes, C.A. (1979). Memory deficits associated with senescence: a neurophysiological and behavioral study in the rat. J Comp Physiol Psychol *93*, 74–104.

Barnes, C.A., and McNaughton, B.L. (1985). An age comparison of the rates of acquisition and forgetting of spatial information in relation to long-term enhancement of hippocampal synapses. Behavioral Neuroscience *99*, 1040–1048.

Barria, A., Muller, D., Derkach, V., Griffith, L.C., and Soderling, T.R. (1997). Regulatory phosphorylation of AMPA-type glutamate receptors by CaM-KII during long-term potentiation. Science *276*, 2042–2045.

Bas-Orth, C., Schultz, C., Müller, C.M., Frotscher, M., and Deller, T. (2007). Loss of the cisternal organelle in the axon initial segment of cortical neurons in synaptopodin-deficient mice. J Comp Neurol *504*, 441–449.

Bashir, Z.I., Bortolotto, Z.A., Davies, C.H., Berretta, N., Irving, A.J., Seal, A.J., Henley, J.M., Jane, D.E., Watkins, J.C., and Collingridge, G.L. (1993). Induction of LTP in the hippocampus needs synaptic activation of glutamate metabotropic receptors. Nature *363*, 347–350.

Bastrikova, N., Gardner, G.A., Reece, J.M., Jeromin, A., and Dudek, S.M. (2008). Synapse elimination accompanies functional plasticity in hippocampal neurons. Proc Natl Acad Sci USA *105*, 3123–3127.

Bayazitov, I.T., Richardson, R.J., Fricke, R.G., and Zakharenko, S.S. (2007). Slow presynaptic and fast postsynaptic components of compound long-term potentiation. Journal of Neuroscience *27*, 11510–11521.

Bear, M.F., Cooper, L.N., and Ebner, F.F. (1987). A physiological basis for a theory of synapse modification. Science *237*, 42–48.

Bear, M.F., Huber, K.M., and Warren, S.T. (2004). The mGluR theory of fragile X mental retardation. Trends in Neurosciences *27*, 370–377.

Beattie, E.C., Carroll, R.C., Yu, X., Morishita, W., Yasuda, H., Zastrow, von, M., and Malenka, R.C. (2000). Regulation of AMPA receptor endocytosis by a signaling mechanism shared with LTD. Nat Neurosci *3*, 1291–1300.

Behnisch, T., and Reymann, K.G. (1995). Thapsigargin blocks long-term potentiation induced by weak, but not strong tetanisation in rat hippocampal CA1 neurons. Neurosci. Lett. *192*, 185–188.

Bekkers, J.M., and Stevens, C.F. (1990). Presynaptic mechanism for long-term potentiation in the hippocampus. Nature *346*, 724–729.

Bell, M.E., Bourne, J.N., Chirillo, M.A., Mendenhall, J.M., Kuwajima, M., and Harris, K.M. (2014). Dynamics of nascent and active zone ultrastructure as synapses enlarge during long-term potentiation in mature hippocampus. J Comp Neurol *522*, 3861–3884.

Bender, V.A., Pugh, J.R., and Jahr, C.E. (2009). Presynaptically expressed long-term potentiation increases multivesicular release at parallel fiber synapses. Journal of Neuroscience *29*, 10974–10978.

Benson, D.L., and Huntley, G.W. (2012). Synapse adhesion: a dynamic equilibrium conferring stability and flexibility. Current Opinion in Neurobiology *22*, 397–404.

Berridge, M.J. (1998). Neuronal calcium signaling. Neuron *21*, 13–26.

Berridge, M.J. (2002). The endoplasmic reticulum: a multifunctional signaling organelle. Cell Calcium *32*, 235–249.

Betz, W.J., and Bewick, G.S. (1992). Optical analysis of synaptic vesicle recycling at the frog neuromuscular junction. Science *255*, 200–203.

Bhakar, A.L., Dölen, G., and Bear, M.F. (2012). The pathophysiology of fragile X (and what it teaches us about synapses). Annu. Rev. Neurosci. *35*, 417–443.

Bienenstock, E.L., Cooper, L.N., and Munro, P.W. (1982). Theory for the development of neuron selectivity: orientation specificity and binocular interaction in visual cortex. J Neurosci *2*, 32–48.

Bishop, D.L., Misgeld, T., Walsh, M.K., Gan, W.-B., and Lichtman, J.W. (2004). Axon branch removal at developing synapses by axosome shedding. Neuron *44*, 651–661.

Blaustein, M.P., and Golovina, V.A. (2001). Structural complexity and functional diversity of endoplasmic reticulum Ca(2+) stores. Trends in Neurosciences *24*, 602–608.

Blaustein, M.P., Ratzlaff, R.W., and Kendrick, N.K. (1978a). The regulation of intracellular calcium in presynaptic nerve terminals. Ann. N. Y. Acad. Sci. *307*, 195–212.

Blaustein, M.P., Ratzlaff, R.W., and Schweitzer, E.S. (1978b). Calcium buffering in presynaptic nerve terminals. II. Kinetic properties of the nonmitochondrial Ca sequestration mechanism. J. Gen. Physiol. *72*, 43–66.

Blaustein, M.P., Ratzlaff, R.W., Kendrick, N.C., and Schweitzer, E.S. (1978c). Calcium buffering in presynaptic nerve terminals. I. Evidence for involvement of a nonmitochondrial ATP-dependent sequestration mechanism. J. Gen. Physiol. *72*, 15–41.

Bliss, T.V., and Lomo, T. (1973). Long-lasting potentiation of synaptic transmission in the dentate area of the anaesthetized rabbit following stimulation of the perforant path. The Journal of Physiology *232*, 331–356.

Bliss, T.V.P., and Collingridge, G.L. (2013). Expression of NMDA receptor-dependent LTP in the hippocampus: bridging the divide. Mol Brain *6*, 5.

Bliss, T., Collingridge, G.L., and Morris, R. (2007). Synaptic Plasticity in the Hippocampus. In The Hippocampus Book, pp. 343–474.

Bloodgood, B.L., and Sabatini, B.L. (2007). Ca(2+) signaling in dendritic spines. Current Opinion in Neurobiology *17*, 345–351.

Boehning, D., and Snyder, S.H. (2003). Novel neural modulators. Annu. Rev. Neurosci. *26*, 105–131.

Bohlen Und Halbach, Von, F., Taylor, J., and Schachner, M. (1992). Cell Type-specific Effects of the Neural Adhesion Molecules L1 and N-CAM on Diverse Second Messenger Systems. Eur J Neurosci *4*, 896–909.

Bolshakov, V.Y., Golan, H., Kandel, E.R., and Siegelbaum, S.A. (1997). Recruitment of new sites of synaptic transmission during the cAMP-dependent late phase of LTP at CA3-CA1 synapses in the hippocampus. Neuron *19*, 635–651.

Bonhoeffer, T., Staiger, V., and Aertsen, A. (1989). Synaptic plasticity in rat hippocampal slice cultures: local "Hebbian" conjunction of pre- and postsynaptic stimulation leads to distributed synaptic enhancement. Proc Natl Acad Sci USA *86*, 8113–8117.

Bosch, M., and Hayashi, Y. (2012). Structural plasticity of dendritic spines. Current Opinion in Neurobiology *22*, 383–388.

Bouchard, R., Pattarini, R., and Geiger, J.D. (2003). Presence and functional significance of presynaptic ryanodine receptors. Prog Neurobiol *69*, 391–418.

Bourne, J.N., and Harris, K.M. (2007). Do thin spines learn to be mushroom spines that remember? Current Opinion in Neurobiology *17*, 381–386.

Bourne, J.N., and Harris, K.M. (2008). Balancing structure and function at hippocampal dendritic spines. Annu. Rev. Neurosci. *31*, 47–67.

Bourne, J.N., and Harris, K.M. (2011a). Coordination of size and number of excitatory and inhibitory synapses results in a balanced structural plasticity along mature hippocampal CA1 dendrites during LTP. Hippocampus *21*, 354–373.

Bourne, J.N., and Harris, K.M. (2011b). Nanoscale analysis of structural synaptic plasticity. Current Opinion in Neurobiology.

Bourne, J.N., Chirillo, M.A., and Harris, K.M. (2013). Presynaptic ultrastructural plasticity along CA3→CA1 axons during long-term potentiation in mature hippocampus. J Comp Neurol *521*, 3898–3912.

Bourne, J.N., Sorra, K.E., Hurlburt, J., and Harris, K.M. (2007). Polyribosomes are increased in spines of CA1 dendrites 2 h after the induction of LTP in mature rat hippocampal slices. Hippocampus *17*, 1–4.

Bowden, J.B., Abraham, W.C., and Harris, K.M. (2011). Differential effects of strain, circadian cycle, and stimulation pattern on LTP and concurrent LTD in the dentate gyrus of freely moving rats. Hippocampus.

Böhme, G.A., Bon, C., Stutzmann, J.M., Doble, A., and Blanchard, J.C. (1991). Possible involvement of nitric oxide in long-term potentiation. Eur. J. Pharmacol. *199*, 379–381.

Branco, T., Marra, V., and Staras, K. (2010). Examining size-strength relationships at hippocampal synapses using an ultrastructural measurement of synaptic release probability. J. Struct. Biol. *172*, 203–210.

Braun, K., and Segal, M. (2000). FMRP involvement in formation of synapses among cultured hippocampal neurons. Cereb. Cortex *10*, 1045–1052.

Broadwell, R.D., and Cataldo, A.M. (1984). The neuronal endoplasmic reticulum: its cytochemistry and contribution to the endomembrane system. II. Axons and terminals. J Comp Neurol *230*, 231–248.

Brown, T.C., Tran, I.C., Backos, D.S., and Esteban, J.A. (2005). NMDA receptor-dependent activation of the small GTPase Rab5 drives the removal of synaptic AMPA receptors during hippocampal LTD. Neuron *45*, 81–94.

Bunge, M.B. (1973). Fine structure of nerve fibers and growth cones of isolated sympathetic neurons in culture. J Cell Biol *56*, 713–735.

Busetto, G., Higley, M.J., and Sabatini, B.L. (2008). Developmental presence and disappearance of postsynaptically silent synapses on dendritic spines of rat layer 2/3 pyramidal neurons. The Journal of Physiology *586*, 1519–1527.

Buzsáki, G. (2002). Theta oscillations in the hippocampus. Neuron *33*, 325–340.

Byth, L.A. (2014). Ca(2+)- and CaMKII-mediated processes in early LTP. Ann Neurosci *21*, 151–153.

Cao, G., and Harris, K.M. (2012). Developmental regulation of the late phase of long-term potentiation (L-LTP) and metaplasticity in hippocampal area CA1 of the rat. Journal of Neurophysiology *107*, 902–912.

Carrillo, J., Cheng, S.-Y., Ko, K.W., Jones, T.A., and Nishiyama, H. (2013). The long-term structural plasticity of cerebellar parallel fiber axons and its modulation by motor learning. J Neurosci *33*, 8301–8307.

Carroll, R.C., Beattie, E.C., Zastrow, von, M., and Malenka, R.C. (2001). Role of AMPA receptor endocytosis in synaptic plasticity. Nat Rev Neurosci *2*, 315–324.

Castro-Alamancos, M.A., and Calcagnotto, M.E. (1999). Presynaptic long-term potentiation in corticothalamic synapses. Journal of Neuroscience *19*, 9090–9097.

Ceccarelli, B., Hurlbut, W.P., and Mauro, A. (1973). Turnover of transmitter and synaptic vesicles at the frog neuromuscular junction. J Cell Biol *57*, 499–524.

Chakrabarti, S., and Fombonne, E. (2001). Pervasive developmental disorders in preschool children. Jama *285*, 3093–3099.

Chavez-Noriega, L.E., and Stevens, C.F. (1994). Increased transmitter release at excitatory synapses produced by direct activation of adenylate cyclase in rat hippocampal slices. Journal of Neuroscience *14*, 310–317.

Chen, X., Barg, S., and Almers, W. (2008a). Release of the styryl dyes from single synaptic vesicles in hippocampal neurons. Journal of Neuroscience *28*, 1894–1903.

Chen, X., Winters, C., Azzam, R., Li, X., Galbraith, J.A., Leapman, R.D., and Reese, T.S. (2008b). Organization of the core structure of the postsynaptic density. Proc Natl Acad Sci USA *105*, 4458.

Chen, Y., Bourne, J.N., Pieribone, V.A., and Fitzsimonds, R.M. (2004). The role of actin in the regulation of dendritic spine morphology and bidirectional synaptic plasticity. Neuroreport *15*, 829–832.

Chirillo, M., Bourne, J., Lindsey, L., and Harris, K. (2015). Complexity of dendritic SER increases at enlarging synapses during LTP.

Choi, C.H., Schoenfeld, B.P., Bell, A.J., Hinchey, P., Kollaros, M., Gertner, M.J., Woo, N.H., Tranfaglia, M.R., Bear, M.F., Zukin, R.S., et al. (2011). Pharmacological reversal of synaptic plasticity deficits in the mouse model of fragile X syndrome by group II mGluR antagonist or lithium treatment. Brain Res. *1380*, 106–119.

Chowdhury, S., Shepherd, J.D., Okuno, H., Lyford, G., Petralia, R.S., Plath, N., Kuhl, D., Huganir, R.L., and Worley, P.F. (2006). Arc/Arg3.1 interacts with the endocytic machinery to regulate AMPA receptor trafficking. Neuron *52*, 445–459.

Christie, J.M., and Jahr, C.E. (2006). Multivesicular release at Schaffer collateral-CA1 hippocampal synapses. Journal of Neuroscience *26*, 210–216.

Christie, S.B., Akins, M.R., Schwob, J.E., and Fallon, J.R. (2009). The FXG: a presynaptic fragile X granule expressed in a subset of developing brain circuits. J Neurosci *29*, 1514–1524.

Chuang, S.-C., Zhao, W., Bauchwitz, R., Yan, Q., Bianchi, R., and Wong, R.K.S. (2005). Prolonged epileptiform discharges induced by altered group I metabotropic glutamate receptor-mediated synaptic responses in hippocampal slices of a fragile X mouse model. Journal of Neuroscience *25*, 8048–8055.

Clarke, J.R., Cammarota, M., Gruart, A., Izquierdo, I., and Delgado-García, J.M. (2010). Plastic modifications induced by object recognition memory processing. Proc Natl Acad Sci USA *107*, 2652–2657.

Cochilla, A.J., Angleson, J.K., and Betz, W.J. (1999). Monitoring secretory membrane with FM1-43 fluorescence. Annu. Rev. Neurosci. *22*, 1–10.

Cohen, A.S., and Abraham, W.C. (1996). Facilitation of long-term potentiation by prior activation of metabotropic glutamate receptors. Journal of Neurophysiology *76*, 953–962.

Coleman, M.P., and Freeman, M.R. (2010). Wallerian degeneration, wld(s), and nmnat. Annu. Rev. Neurosci. *33*, 245–267.

Colgin, L.L. (2013). Mechanisms and functions of theta rhythms. Annu. Rev. Neurosci. *36*, 295–312.

Collin, T., Marty, A., and Llano, I. (2005). Presynaptic calcium stores and synaptic transmission. Current Opinion in Neurobiology *15*, 275–281.

Collingridge, G.L., Kehl, S.J., and McLennan, H. (1983). The antagonism of amino acid-induced excitations of rat hippocampal CA1 neurones in vitro. The Journal of Physiology *334*, 19–31.

Collingridge, G.L., Peineau, S., Howland, J.G., and Wang, Y.T. (2010). Long-term depression in the CNS. Nat Rev Neurosci *11*, 459–473.

Comery, T.A., Harris, J.B., Willems, P.J., Oostra, B.A., Irwin, S.A., Weiler, I.J., and Greenough, W.T. (1997). Abnormal dendritic spines in fragile X knockout mice: maturation and pruning deficits. Proc Natl Acad Sci USA *94*, 5401–5404.

Cooney, J.R., Hurlburt, J.L., Selig, D.K., Harris, K.M., and Fiala, J.C. (2002). Endosomal compartments serve multiple hippocampal dendritic spines from a widespread rather than a local store of recycling membrane. Journal of Neuroscience *22*, 2215–2224.

Cooper, L.N., and Bear, M.F. (2012). The BCM theory of synapse modification at 30: interaction of theory with experiment. Nat Rev Neurosci *13*, 798–810.

Cruz-Martín, A., Crespo, M., and Portera-Cailliau, C. (2010). Delayed stabilization of dendritic spines in fragile X mice. Journal of Neuroscience *30*, 7793–7803.

Cui-Wang, T., Hanus, C., Cui, T., Helton, T., Bourne, J.N., Watson, D., Harris, K.M., and Ehlers, M.D. (2012). Local zones of endoplasmic reticulum complexity confine cargo in neuronal dendrites. Cell *148*, 309–321.

Dalva, M.B., McClelland, A.C., and Kayser, M.S. (2007). Cell adhesion molecules: signalling functions at the synapse. Nat Rev Neurosci *8*, 206–220.

Dancause, N., Barbay, S., Frost, S.B., Plautz, E.J., Chen, D., Zoubina, E.V., Stowe, A.M., and Nudo, R.J. (2005). Extensive cortical rewiring after brain injury. Journal of Neuroscience *25*, 10167–10179.

Darcy, K.J., Staras, K., Collinson, L.M., and Goda, Y. (2006). Constitutive sharing of recycling synaptic vesicles between presynaptic boutons. Nat Neurosci *9*, 315–321.

Darian-Smith, C., and Gilbert, C.D. (1994). Axonal sprouting accompanies functional reorganization in adult cat striate cortex. Nature *368*, 737–740.

Darnell, J.C., Van Driesche, S.J., Zhang, C., Hung, K.Y.S., Mele, A., Fraser, C.E., Stone, E.F., Chen, C., Fak, J.J., Chi, S.W., et al. (1975). The smooth endoplasmic reticulum: structure and role in the renewal of axonal membrane and synaptic vesicles by fast axonal transport. Brain Res. *93*, 1–13.

De Paola, V., Arber, S., and Caroni, P. (2003). AMPA receptors regulate dynamic equilibrium of presynaptic terminals in mature hippocampal networks. Nat Neurosci *6*, 491–500.

De Paola, V., Holtmaat, A., Knott, G., Song, S., Wilbrecht, L., Caroni, P., and Svoboda, K. (2006). Cell type-specific structural plasticity of axonal branches and boutons in the adult neocortex. Neuron *49*, 861–875.

De Robertis, E.D., and Bennett, H.S. (1955). Some features of the submicroscopic morphology of synapses in frog and earthworm. J Biophys Biochem Cytol *1*, 47–58.

de Vrij, F.M.S., Levenga, J., van der Linde, H.C., Koekkoek, S.K., De Zeeuw, C.I., Nelson, D.L., Oostra, B.A., and Willemsen, R. (2008). Rescue of behavioral phenotype and neuronal protrusion morphology in Fmr1 KO mice. Neurobiol. Dis. *31*, 127–132.

Debanne, D., Gähwiler, B.H., and Thompson, S.M. (1998). Long-term synaptic plasticity between pairs of individual CA3 pyramidal cells in rat hippocampal slice cultures. The Journal of Physiology *507 (Pt 1)*, 237–247.

del Castillo, J., and Katz, B. (1954). Quantal components of the end-plate potential. The Journal of Physiology *124*, 560–573.

Deller, T., Merten, T., Roth, S.U., Mundel, P., and Frotscher, M. (2000). Actin-associated protein synaptopodin in the rat hippocampal formation: localization in the spine neck and close association with the spine apparatus of principal neurons. J Comp Neurol *418*, 164–181.

Deller, T., Korte, M., Chabanis, S., Drakew, A., Schwegler, H., Stefani, G.G., Zuniga, A., Schwarz, K., Bonhoeffer, T., Zeller, R., et al. (2003). Synaptopodin-deficient mice lack a spine apparatus and show deficits in synaptic plasticity. Proc Natl Acad Sci USA *100*, 10494–10499.

Deng, P.-Y., Sojka, D., and Klyachko, V.A. (2011). Abnormal presynaptic short-term plasticity and information processing in a mouse model of fragile X syndrome. Journal of Neuroscience *31*, 10971–10982.

Desmond, N.L., and Levy, W.B. (1986a). Changes in the numerical density of synaptic contacts with long-term potentiation in the hippocampal dentate gyrus. J Comp Neurol *253*, 466–475.

Desmond, N.L., and Levy, W.B. (1986b). Changes in the postsynaptic density with long-term potentiation in the dentate gyrus. J Comp Neurol *253*, 476–482.

Dinerman, J.L., Dawson, T.M., Schell, M.J., Snowman, A., and Snyder, S.H. (1994). Endothelial Nitric-Oxide Synthase Localized to Hippocampal Pyramidal Cells - Implications for Synaptic Plasticity. Proceedings of the National Academy of Sciences *91*, 4214–4218.

Dityatev, A., Schachner, M., and Sonderegger, P. (2010). The dual role of the extracellular matrix in synaptic plasticity and homeostasis. Nat Rev Neurosci *11*, 735–746.

Dobrunz, L.E., and Stevens, C.F. (1997). Heterogeneity of release probability, facilitation, and depletion at central synapses. Neuron *18*, 995–1008.

Dobrunz, L.E. (2002). Release probability is regulated by the size of the readily releasable vesicle pool at excitatory synapses in hippocampus. Int. J. Dev. Neurosci. *20*, 225–236.

Dolphin, A.C., Errington, M.L., and Bliss, T.V. (1982). Long-term potentiation of the perforant path in vivo is associated with increased glutamate release. Nature *297*, 496–498.

Dölen, G., Osterweil, E., Rao, B.S.S., Smith, G.B., Auerbach, B.D., Chattarji, S., and Bear, M.F. (2007). Correction of fragile X syndrome in mice. Neuron *56*, 955–962.

Droz, B., Rambourg, A., and Koenig, H.L. (1975). The smooth endoplasmic reticulum: structure and role in the renewal of axonal membrane and synaptic vesicles by fast axonal transport. Brain Res. *93*, 1–13.

Dudek, S.M., and Bear, M.F. (1992). Homosynaptic long-term depression in area CA1 of hippocampus and effects of N-methyl-D-aspartate receptor blockade. Proc Natl Acad Sci USA *89*, 4363–4367.

Dumas, T.C. (2005). Late postnatal maturation of excitatory synaptic transmission permits adult-like expression of hippocampal-dependent behaviors. Hippocampus *15*, 562–578.

Dunwiddie, T., and Lynch, G. (1978). Long-term potentiation and depression of synaptic responses in the rat hippocampus: localization and frequency dependency. The Journal of Physiology *276*, 353–367.

Durand, G.M., Kovalchuk, Y., and Konnerth, A. (1996). Long-term potentiation and functional synapse induction in developing hippocampus. Nature *381*, 71–75.

Dustin, M.L. (2012). Signaling at neuro/immune synapses. J. Clin. Invest. *122*, 1149–1155.

Dustin, M.L., and Colman, D.R. (2002). Neural and immunological synaptic relations. Science *298*, 785–789.

Ebashi, S., and Endo, M. (1968). Calcium and muscle contraction. Progress in Biophysics and Molecular Biology *18*, 123–183.

Ehlers, M.D. (2000). Reinsertion or degradation of AMPA receptors determined by activity-dependent endocytic sorting. Neuron *28*, 511–525.

Eichenbaum, H. (2008). Learning & Memory (W. W. Norton & Company, Inc.).

Elsabbagh, M., Divan, G., Koh, Y.-J., Kim, Y.S., Kauchali, S., Marcín, C., Montiel-Nava, C., Patel, V., Paula, C.S., Wang, C., et al. (2012). Global Prevalence of Autism and Other Pervasive Developmental Disorders. Autism Res.

Emptage, N.J., Reid, C.A., and Fine, A. (2001). Calcium stores in hippocampal synaptic boutons mediate short-term plasticity, store-operated Ca2+ entry, and spontaneous transmitter release. Neuron *29*, 197–208.

Emptage, N., Bliss, T.V., and Fine, A. (1999). Single synaptic events evoke NMDA receptor-mediated release of calcium from internal stores in hippocampal dendritic spines. Neuron *22*, 115–124.

Emptage, N.J., Reid, C.A., Fine, A., and Bliss, T.V.P. (2003). Optical quantal analysis reveals a presynaptic component of LTP at hippocampal Schaffer-associational synapses. Neuron *38*, 797–804.

Engert, F., and Bonhoeffer, T. (1999). Dendritic spine changes associated with hippocampal long-term synaptic plasticity. Nature *399*, 66–70.

Enoki, R., Hu, Y.-L., Hamilton, D., and Fine, A. (2009). Expression of long-term plasticity at individual synapses in hippocampus is graded, bidirectional, and mainly presynaptic: optical quantal analysis. Neuron *62*, 242–253.

Fallini, C., Zhang, H., Su, Y., Silani, V., Singer, R.H., Rossoll, W., and Bassell, G.J. (2011). The survival of motor neuron (SMN) protein interacts with the mRNA-binding protein HuD and regulates localization of poly(A) mRNA in primary motor neuron axons. Journal of Neuroscience *31*, 3914–3925.

Fatt, P., and Katz, B. (1950). Some observations on biological noise. Nature *166*, 597–598.

Fatt, P., and Katz, B. (1952). Spontaneous subthreshold activity at motor nerve endings. The Journal of Physiology *117*, 109–128.

Fernández de Sevilla, D., and Buño, W. (2010). The muscarinic long-term enhancement of NMDA and AMPA receptor-mediated transmission at Schaffer collateral synapses develop through different intracellular mechanisms. Journal of Neuroscience *30*, 11032–11042.

Fernández de Sevilla, D., Núñez, A., Borde, M., Malinow, R., and Buño, W. (2008). Cholinergic-mediated IP3-receptor activation induces long-lasting synaptic enhancement in CA1 pyramidal neurons. Journal of Neuroscience *28*, 1469–1478.

Fiala, J.C. (2005). Reconstruct: a free editor for serial section microscopy. J Microsc *218*, 52–61.

Fiala, J.C., and Harris, K.M. (2001a). Cylindrical diameters method for calibrating section thickness in serial electron microscopy. J Microsc *202*, 468–472.

Fiala, J.C., and Harris, K.M. (2001b). Extending unbiased stereology of brain ultrastructure to three-dimensional volumes. J Am Med Inform Assoc *8*, 1–16.

Fiala, J.C., Feinberg, M., Popov, V., and Harris, K.M. (1998). Synaptogenesis via dendritic filopodia in developing hippocampal area CA1. J Neurosci *18*, 8900–8911.

Fiala, J.C., Kirov, S.A., Feinberg, M.D., Petrak, L.J., George, P., Goddard, C.A., and Harris, K.M. (2003). Timing of neuronal and glial ultrastructure disruption during brain slice preparation and recovery in vitro. J Comp Neurol *465*, 90–103.

Fifková, E., Markham, J.A., and Delay, R.J. (1983). Calcium in the spine apparatus of dendritic spines in the dentate molecular layer. Brain Res. *266*, 163–168.

Fitzpatrick, J.S., Hagenston, A.M., Hertle, D.N., Gipson, K.E., Bertetto-D'Angelo, L., and Yeckel, M.F. (2009). Inositol-1,4,5-trisphosphate receptor-mediated Ca2+ waves in pyramidal neuron dendrites propagate through hot spots and cold spots. The Journal of Physiology *587*, 1439–1459.

Florence, S.L., Taub, H.B., and Kaas, J.H. (1998). Large-scale sprouting of cortical connections after peripheral injury in adult macaque monkeys. Science *282*, 1117–1121.

Franks, K.M., and Sejnowski, T.J. (2002). Complexity of calcium signaling in synaptic spines. Bioessays *24*, 1130–1144.

Fredj, N.B., and Burrone, J. (2009). A resting pool of vesicles is responsible for spontaneous vesicle fusion at the synapse. Nat Neurosci *12*, 751–758.

Frei, T., Bohlen und Halbach, von, F., Wille, W., and Schachner, M. (1992). Different extracellular domains of the neural cell adhesion molecule (N-CAM) are involved in different functions. J Cell Biol *118*, 177–194.

Frey, U., and Morris, R.G. (1997). Synaptic tagging and long-term potentiation. Nature *385*, 533–536.

Frey, U., Huang, Y.Y., and Kandel, E.R. (1993). Effects of cAMP simulate a late stage of LTP in hippocampal CA1 neurons. Science *260*, 1661–1664.

Frey, U., Krug, M., Reymann, K.G., and Matthies, H. (1988). Anisomycin, an inhibitor of protein synthesis, blocks late phases of LTP phenomena in the hippocampal CA1 region in vitro. Brain Res. *452*, 57–65.

Fujino, I., Yamada, N., Miyawaki, A., Hasegawa, M., Furuichi, T., and Mikoshiba, K. (1995). Differential expression of type 2 and type 3 inositol 1,4,5-trisphosphate receptor mRNAs in various mouse tissues: in situ hybridization study. Cell Tissue Res. *280*, 201–210.

Fukazawa, Y., Saitoh, Y., Ozawa, F., Ohta, Y., Mizuno, K., and Inokuchi, K. (2003). Hippocampal LTP is accompanied by enhanced F-actin content within

the dendritic spine that is essential for late LTP maintenance in vivo. Neuron *38*, 447–460.

Galeotti, N., Vivoli, E., Bartolini, A., and Ghelardini, C. (2008). A gene-specific cerebral types 1, 2, and 3 RyR protein knockdown induces an antidepressant-like effect in mice. Journal of Neurochemistry *106*, 2385–2394.

Gao, F.B. (1998). Messenger RNAs in dendrites: localization, stability, and implications for neuronal function. Bioessays *20*, 70–78.

Gardiol, A., Racca, C., and Triller, A. (1999). Dendritic and postsynaptic protein synthetic machinery. J Neurosci *19*, 168–179.

Garthwaite, J. (2008). Concepts of neural nitric oxide-mediated transmission. Eur J Neurosci *27*, 2783–2802.

Giese, K.P., Fedorov, N.B., Filipkowski, R.K., and Silva, A.J. (1998). Autophosphorylation at Thr286 of the alpha calcium-calmodulin kinase II in LTP and learning. Science *279*, 870–873.

Giuditta, A., Dettbarn, W.D., and Brzin, M. (1968). Protein synthesis in the isolated giant axon of the squid. Proc Natl Acad Sci USA *59*, 1284–1287.

Gogolla, N., Galimberti, I., and Caroni, P. (2007). Structural plasticity of axon terminals in the adult. Current Opinion in Neurobiology *17*, 516–524.

Golding, N.L., Staff, N.P., and Spruston, N. (2002). Dendritic spikes as a mechanism for cooperative long-term potentiation. Nature *418*, 326–331.

Görlich, D., and Rapoport, T.A. (1993). Protein translocation into proteoliposomes reconstituted from purified components of the endoplasmic reticulum membrane. Cell *75*, 615–630.

Grakoui, A., Bromley, S.K., Sumen, C., Davis, M.M., Shaw, A.S., Allen, P.M., and Dustin, M.L. (1999). The immunological synapse: a molecular machine controlling T cell activation. Science *285*, 221–227.

Granger, A.J., and Nicoll, R.A. (2014). Expression mechanisms underlying long-term potentiation: a postsynaptic view, 10 years on. Philosophical Transactions of the Royal Society B: Biological Sciences *369*, 20130136.

Granseth, B., Odermatt, B., Royle, S.J., and Lagnado, L. (2006). Clathrin-mediated endocytosis is the dominant mechanism of vesicle retrieval at hippocampal synapses. Neuron *51*, 773–786.

Gray, C.M. (1959). Axo-somatic and axo-dendritic synapses of the cerebral cortex: an electron microscope study. J Anatomy *93*, 420–433.

Gray, K., Keating, C., Taffe, J., Brereton, A., Einfeld, S., and Tonge, B. (2012). Trajectory of behavior and emotional problems in autism. Am J Intellect Dev Disabil *117*, 121–133.

Green, E.J., McNaughton, B.L., and Barnes, C.A. (1990). Exploration-dependent modulation of evoked responses in fascia dentata: dissociation of motor, EEG, and sensory factors and evidence for a synaptic efficacy change. J Neurosci *10*, 1455–1471.

Greger, I.H., Khatri, L., and Ziff, E.B. (2002). RNA editing at arg607 controls AMPA receptor exit from the endoplasmic reticulum. Neuron *34*, 759–772.

Grigoryan, G., Korkotian, E., and Segal, M. (2012). Selective facilitation of LTP in the ventral hippocampus by calcium stores. Hippocampus *22*, 1635–1644.

Grigston, J.C., VanDongen, H.M.A., McNamara, J.O., and VanDongen, A.M.J. (2005). Translation of an integral membrane protein in distal dendrites of hippocampal neurons. Eur J Neurosci *21*, 1457–1468.

Grillo, F.W., Song, S., Teles-Grilo Ruivo, L.M., Huang, L., Gao, G., Knott, G.W., Maco, B., Ferretti, V., Thompson, D., Little, G.E., et al. (2013). Increased axonal bouton dynamics in the aging mouse cortex. Proc Natl Acad Sci USA *110*, E1514–E1523.

Grossman, A.W., Elisseou, N.M., McKinney, B.C., and Greenough, W.T. (2006). Hippocampal pyramidal cells in adult Fmr1 knockout mice exhibit an immature-appearing profile of dendritic spines. Brain Res. *1084*, 158–164.

Gruart, A., Muñoz, M.D., and Delgado-García, J.M. (2006). Involvement of the CA3-CA1 synapse in the acquisition of associative learning in behaving mice. Journal of Neuroscience *26*, 1077–1087.

Hagerman, R., Hoem, G., and Hagerman, P. (2010). Fragile X and autism: Intertwined at the molecular level leading to targeted treatments. Mol Autism *1*, 12.

Hanse, E., and Gustafsson, B. (2001). Vesicle release probability and pre-primed pool at glutamatergic synapses in area CA1 of the rat neonatal hippocampus. The Journal of Physiology *531*, 481–493.

Hanson, J.E., and Madison, D.V. (2007). Presynaptic FMR1 genotype influences the degree of synaptic connectivity in a mosaic mouse model of fragile X syndrome. Journal of Neuroscience *27*, 4014–4018.

Hanus, C., and Ehlers, M.D. (2008). Secretory outposts for the local processing of membrane cargo in neuronal dendrites. Traffic *9*, 1437–1445.

Harris, K.M., and Kater, S.B. (1994). Dendritic spines: cellular specializations imparting both stability and flexibility to synaptic function. Annu. Rev. Neurosci. *17*, 341–371.

Harris, K.M., and Stevens, J.K. (1988). Dendritic spines of rat cerebellar Purkinje cells: serial electron microscopy with reference to their biophysical characteristics. J Neurosci *8*, 4455–4469.

Harris, K.M., and Stevens, J.K. (1989). Dendritic spines of CA 1 pyramidal cells in the rat hippocampus: serial electron microscopy with reference to their biophysical characteristics. J Neurosci *9*, 2982–2997.

Harris, K.M., and Sultan, P. (1995). Variation in the number, location and size of synaptic vesicles provides an anatomical basis for the nonuniform probability of release at hippocampal CA1 synapses. Neuropharmacology *34*, 1387–1395.

Harris, K.M., and Teyler, T.J. (1984). Developmental onset of long-term potentiation in area CA1 of the rat hippocampus. The Journal of Physiology *346*, 27–48.

Harris, K.M., and Weinberg, R.J. (2012). Ultrastructure of synapses in the mammalian brain. Cold Spring Harb Perspect Biol *4*, a005587.

Harris, K.M., Perry, E., Bourne, J.N., Feinberg, M., Ostroff, L., and Hurlburt, J. (2006). Uniform serial sectioning for transmission electron microscopy. Journal of Neuroscience *26*, 12101–12103.

Harvey, C.D., Yasuda, R., Zhong, H., and Svoboda, K. (2008). The spread of Ras activity triggered by activation of a single dendritic spine. Science *321*, 136–140.

Harvey, J., and Collingridge, G.L. (1992). Thapsigargin blocks the induction of long-term potentiation in rat hippocampal slices. Neurosci. Lett. *139*, 197–200.

Hatton, D.D., Sideris, J., Skinner, M., Mankowski, J., Bailey, D.B., Roberts, J., and Mirrett, P. (2006). Autistic behavior in children with fragile X syndrome: prevalence, stability, and the impact of FMRP. Am. J. Med. Genet. A *140A*, 1804–1813.

Haucke, V., Neher, E., and Sigrist, S.J. (2011). Protein scaffolds in the coupling of synaptic exocytosis and endocytosis. Nat Rev Neurosci *12*, 127–138.

Hayashi, M.L., Rao, B.S.S., Seo, J.-S., Choi, H.-S., Dolan, B.M., Choi, S.-Y., Chattarji, S., and Tonegawa, S. (2007). Inhibition of p21-activated kinase rescues symptoms of fragile X syndrome in mice. Proc Natl Acad Sci USA *104*, 11489–11494.

Hazelrigg, T. (1998). The destinies and destinations of RNAs. Cell *95*, 451–460.

He, K., Lee, A., Song, L., Kanold, P.O., and Lee, H.-K. (2011). AMPA receptor subunit GluR1 (GluA1) serine-845 site is involved in synaptic depression but not in spine shrinkage associated with chemical long-term depression. Journal of Neurophysiology *105*, 1897–1907.

Hebb, D.O. (1949). The Organization of Behavior (New York: Wiley).

Herpers, B., and Rabouille, C. (2004). mRNA localization and ER-based protein sorting mechanisms dictate the use of transitional endoplasmic reticulum-golgi units involved in gurken transport in Drosophila oocytes. Mol. Biol. Cell *15*, 5306–5317.

Hersh, J.H., Saul, R.A., Committee on Genetics (2011). Health supervision for children with fragile X syndrome. Pediatrics *127*, 994–1006.

Heuser, J.E., and Reese, T.S. (1973). Evidence for recycling of synaptic vesicle membrane during transmitter release at the frog neuromuscular junction. J Cell Biol *57*, 315–344.

Higley, M.J., and Sabatini, B.L. (2012). Calcium signaling in dendritic spines. Cold Spring Harb Perspect Biol *4*, a005686.

Hinton, V.J., Brown, W.T., Wisniewski, K., and Rudelli, R.D. (1991). Analysis of neocortex in three males with the fragile X syndrome. Am. J. Med. Genet. *41*, 289–294.

Hjelmstad, G.O., Nicoll, R.A., and Malenka, R.C. (1997). Synaptic refractory period provides a measure of probability of release in the hippocampus. Neuron *19*, 1309–1318.

Ho, O.H., Delgado, J.Y., and O'Dell, T.J. (2004). Phosphorylation of proteins involved in activity-dependent forms of synaptic plasticity is altered in hippocampal slices maintained in vitro. Journal of Neurochemistry *91*, 1344–1357.

Holbro, N., Grunditz, A., and Oertner, T.G. (2009). Differential distribution of endoplasmic reticulum controls metabotropic signaling and plasticity at hippocampal synapses. Proc Natl Acad Sci USA *106*, 15055–15060.

Holt, C.E., and Schuman, E.M. (2013). The central dogma decentralized: new perspectives on RNA function and local translation in neurons. Neuron *80*, 648–657.

Holtmaat, A., and Svoboda, K. (2009). Experience-dependent structural synaptic plasticity in the mammalian brain. Nat Rev Neurosci *10*, 647–658.

Hopf, F.W., Waters, J., Mehta, S., and Smith, S.J. (2002). Stability and plasticity of developing synapses in hippocampal neuronal cultures. Journal of Neuroscience *22*, 775–781.

Horton, A.C., Rácz, B., Monson, E.E., Lin, A.L., Weinberg, R.J., and Ehlers, M.D. (2005). Polarized secretory trafficking directs cargo for asymmetric dendrite growth and morphogenesis. Neuron *48*, 757–771.

Hosokawa, T., Rusakov, D.A., Bliss, T.V., and Fine, A. (1995). Repeated confocal imaging of individual dendritic spines in the living hippocampal slice:

evidence for changes in length and orientation associated with chemically induced LTP. J Neurosci *15*, 5560–5573.

Hu, G.Y., Hvalby, O., Walaas, S.I., Albert, K.A., Skjeflo, P., Andersen, P., and Greengard, P. (1987). Protein kinase C injection into hippocampal pyramidal cells elicits features of long term potentiation. Nature *328*, 426–429.

Huang, E.P. (1999). Synaptic plasticity: regulated translation in dendrites. Curr Biol *9*, R168–R170.

Huber, K.M., Kayser, M.S., and Bear, M.F. (2000). Role for rapid dendritic protein synthesis in hippocampal mGluR-dependent long-term depression. Science *288*, 1254–1257.

Huber, K.M., Roder, J.C., and Bear, M.F. (2001). Chemical induction of mGluR5- and protein synthesis--dependent long-term depression in hippocampal area CA1. Journal of Neurophysiology *86*, 321–325.

Huber, K.M., Gallagher, S.M., Warren, S.T., and Bear, M.F. (2002). Altered synaptic plasticity in a mouse model of fragile X mental retardation. Proc Natl Acad Sci USA *99*, 7746–7750.

Huganir, R.L., and Nicoll, R.A. (2013). AMPARs and synaptic plasticity: the last 25 years. Neuron *80*, 704–717.

Humeau, Y., Shaban, H., Bissière, S., and Lüthi, A. (2003). Presynaptic induction of heterosynaptic associative plasticity in the mammalian brain. Nature *426*, 841–845.

Hyman, J.M., Wyble, B.P., Goyal, V., Rossi, C.A., and Hasselmo, M.E. (2003). Stimulation in hippocampal region CA1 in behaving rats yields long-term potentiation when delivered to the peak of theta and long-term depression when delivered to the trough. Journal of Neuroscience *23*, 11725–11731.

Irwin, S.A., Patel, B., Idupulapati, M., Harris, J.B., Crisostomo, R.A., Larsen, B.P., Kooy, F., Willems, P.J., Cras, P., Kozlowski, P.B., et al. (2001). Abnormal dendritic spine characteristics in the temporal and visual cortices of patients with fragile-X syndrome: a quantitative examination. Am. J. Med. Genet. *98*, 161–167.

Irwin, S.A., Idupulapati, M., Gilbert, M.E., Harris, J.B., Chakravarti, A.B., Rogers, E.J., Crisostomo, R.A., Larsen, B.P., Mehta, A., Alcantara, C.J., et al. (2002). Dendritic spine and dendritic field characteristics of layer V pyramidal neurons in the visual cortex of fragile-X knockout mice. Am. J. Med. Genet. *111*, 140–146.

Isaac, J.T., Nicoll, R.A., and Malenka, R.C. (1995). Evidence for silent synapses: implications for the expression of LTP. Neuron *15*, 427–434.

Isaacson, R.L., and Wickelgren, W.O. (1962). Hippocampal ablation and passive avoidance. Science *138*, 1104–1106.

Jackson, P.S., Suppes, T., and Harris, K.M. (1993). Stereotypical changes in the pattern and duration of long-term potentiation expressed at postnatal days 11 and 15 in the rat hippocampus. Journal of Neurophysiology *70*, 1412–1419.

Jahr, C.E., and Stevens, C.F. (1987). Glutamate activates multiple single channel conductances in hippocampal neurons. Nature *325*, 522–525.

Jedlicka, P., Schwarzacher, S.W., Winkels, R., Kienzler, F., Frotscher, M., Bramham, C.R., Schultz, C., Bas-Orth, C., and Deller, T. (2009). Impairment of in vivo theta-burst long-term potentiation and network excitability in the dentate gyrus of synaptopodin-deficient mice lacking the spine apparatus and the cisternal organelle. Hippocampus *19*, 130–140.

Jeneson, A., and Squire, L.R. (2012). Working memory, long-term memory, and medial temporal lobe function. Learn. Mem. *19*, 15–25.

Jensen, F.E., and Harris, K.M. (1989). Preservation of neuronal ultrastructure in hippocampal slices using rapid microwave-enhanced fixation. J. Neurosci. Methods *29*, 217–230.

Johnston, D., Williams, S., Jaffe, D., and Gray, R. (1992). NMDA-receptor-independent long-term potentiation. Annu Rev Physiol *54*, 489–505.

Ju, W., Morishita, W., Tsui, J., Gaietta, G., Deerinck, T.J., Adams, S.R., Garner, C.C., Tsien, R.Y., Ellisman, M.H., and Malenka, R.C. (2004). Activity-dependent regulation of dendritic synthesis and trafficking of AMPA receptors. Nat Neurosci *7*, 244–253.

Jung, H., Yoon, B.C., and Holt, C.E. (2012). Axonal mRNA localization and local protein synthesis in nervous system assembly, maintenance and repair. Nat Rev Neurosci *13*, 308–324.

Kacharmina, J.E., Job, C., Crino, P., and Eberwine, J. (2000). Stimulation of glutamate receptor protein synthesis and membrane insertion within isolated neuronal dendrites. Proceedings of the National Academy of Sciences *97*, 11545–11550.

Kang, H., and Schuman, E.M. (1996). A requirement for local protein synthesis in neurotrophin-induced hippocampal synaptic plasticity. Science *273*, 1402–1406.

Kelleher, R.J., and Bear, M.F. (2008). The autistic neuron: troubled translation? Cell *135*, 401–406.

Kelleher, R.J., Govindarajan, A., and Tonegawa, S. (2004a). Translational regulatory mechanisms in persistent forms of synaptic plasticity. Neuron *44*, 59–73.

163

Kelleher, R.J., Govindarajan, A., Jung, H.-Y., Kang, H., and Tonegawa, S. (2004b). Translational control by MAPK signaling in long-term synaptic plasticity and memory. Cell *116*, 467–479.

Kelly, P.T., and Vernon, P. (1985). Changes in the subcellular distribution of calmodulin-kinase II during brain development. Brain Res. *350*, 211–224.

Kemp, A., and Manahan-Vaughan, D. (2004). Hippocampal long-term depression and long-term potentiation encode different aspects of novelty acquisition. Proc Natl Acad Sci USA *101*, 8192–8197.

Kemp, A., and Manahan-Vaughan, D. (2007). Hippocampal long-term depression: master or minion in declarative memory processes? Trends in Neurosciences *30*, 111–118.

Kemp, A., and Manahan-Vaughan, D. (2008). The hippocampal CA1 region and dentate gyrus differentiate between environmental and spatial feature encoding through long-term depression. Cereb. Cortex *18*, 968–977.

Kemp, N., McQueen, J., Faulkes, S., and Bashir, Z.I. (2000). Different forms of LTD in the CA1 region of the hippocampus: role of age and stimulus protocol. Eur J Neurosci *12*, 360–366.

Kennedy, M.B. (2013). Synaptic Signaling in Learning and Memory. Cold Spring Harb Perspect Biol a016824.

Kerchner, G.A., and Nicoll, R.A. (2008). Silent synapses and the emergence of a postsynaptic mechanism for LTP. Nat Rev Neurosci *9*, 813–825.

Kindler, S., and Kreienkamp, H.-J. (2012). Dendritic mRNA targeting and translation. Adv. Exp. Med. Biol. *970*, 285–305.

Kirov, S.A., and Harris, K.M. (1999). Dendrites are more spiny on mature hippocampal neurons when synapses are inactivated. Nat Neurosci *2*, 878–883.

Kirov, S.A., Sorra, K.E., and Harris, K.M. (1999). Slices have more synapses than perfusion-fixed hippocampus from both young and mature rats. J Neurosci *19*, 2876–2886.

Kiryushko, D., Korshunova, I., Berezin, V., and Bock, E. (2006). Neural cell adhesion molecule induces intracellular signaling via multiple mechanisms of Ca2+ homeostasis. Mol. Biol. Cell *17*, 2278–2286.

Klann, E., Chen, S.J., and Sweatt, J.D. (1991). Persistent protein kinase activation in the maintenance phase of long-term potentiation. J. Biol. Chem. *266*, 24253–24256.

Klemmer, P., Meredith, R.M., Holmgren, C.D., Klychnikov, O.I., Stahl-Zeng, J., Loos, M., van der Schors, R.C., Wortel, J., de Wit, H., Spijker, S., et al.

(2011). Proteomics, ultrastructure, and physiology of hippocampal synapses in a fragile X syndrome mouse model reveal presynaptic phenotype. J. Biol. Chem. *286*, 25495–25504.

Klopfenstein, D.R., Kappeler, F., and Hauri, H.P. (1998). A novel direct interaction of endoplasmic reticulum with microtubules. Embo J. *17*, 6168–6177.

Koenig, E. (1967). Synthetic mechanisms in the axon. IV. In vitro incorporation of [3H]precursors into axonal protein and RNA. Journal of Neurochemistry *14*, 437–446.

Koga, K., Liu, M.-G., Qiu, S., Song, Q., O'Den, G., Chen, T., and Zhuo, M. (2015). Impaired presynaptic long-term potentiation in the anterior cingulate cortex of Fmr1 knock-out mice. Journal of Neuroscience *35*, 2033–2043.

Korkotian, E., Frotscher, M., and Segal, M. (2014). Synaptopodin regulates spine plasticity: mediation by calcium stores. Journal of Neuroscience *34*, 11641–11651.

Krueger, D.D., and Bear, M.F. (2011). Toward fulfilling the promise of molecular medicine in fragile X syndrome. Annu Rev Med *62*, 411–429.

Krueger, S.R., Kolar, A., and Fitzsimonds, R.M. (2003). The presynaptic release apparatus is functional in the absence of dendritic contact and highly mobile within isolated axons. Neuron *40*, 945–957.

Krug, M., Lössner, B., and Ott, T. (1984). Anisomycin blocks the late phase of long-term potentiation in the dentate gyrus of freely moving rats. Brain Res. Bull. *13*, 39–42.

Kuhl, D., and Skehel, P. (1998). Dendritic localization of mRNAs. Current Opinion in Neurobiology *8*, 600–606.

Kuo, I.Y., and Ehrlich, B.E. (2015). Signaling in Muscle Contraction. Cold Spring Harb Perspect Biol *7*, a006023.

Kushnir, A., Betzenhauser, M.J., and Marks, A.R. (2010). Ryanodine receptor studies using genetically engineered mice. FEBS Lett. *584*, 1956–1965.

Kuwajima, M., Mendenhall, J.M., Lindsey, L.F., and Harris, K.M. (2013). Automated transmission-mode scanning electron microscopy (tSEM) for large volume analysis at nanoscale resolution. PLoS ONE *8*, e59573.

Kwon, H.-B., and Castillo, P.E. (2008). Long-term potentiation selectively expressed by NMDA receptors at hippocampal mossy fiber synapses. Neuron *57*, 108–120.

Kwon, H.-B., and Sabatini, B.L. (2011). Glutamate induces de novo growth of functional spines in developing cortex. Nature *474*, 100–104.

Landis, D.M., Hall, A.K., Weinstein, L.A., and Reese, T.S. (1988). The organization of cytoplasm at the presynaptic active zone of a central nervous system synapse. Neuron *1*, 201–209.

Larson, J., Wong, D., and Lynch, G. (1986). Patterned Stimulation at the Theta-Frequency Is Optimal for the Induction of Hippocampal Long-Term Potentiation. Brain Res. *368*, 347–350.

Le Duigou, C., and Kullmann, D.M. (2011). Group I mGluR agonist-evoked long-term potentiation in hippocampal oriens interneurons. Journal of Neuroscience *31*, 5777–5781.

Leal, G., Comprido, D., and Duarte, C.B. (2014). BDNF-induced local protein synthesis and synaptic plasticity. Neuropharmacology *76 Pt C*, 639–656.

Lee, H.K., Barbarosie, M., Kameyama, K., Bear, M.F., and Huganir, R.L. (2000). Regulation of distinct AMPA receptor phosphorylation sites during bidirectional synaptic plasticity. Nature *405*, 955–959.

Lee, S.-J.R., Escobedo-Lozoya, Y., Szatmari, E.M., and Yasuda, R. (2009). Activation of CaMKII in single dendritic spines during long-term potentiation. Nature *458*, 299–304.

Lewis, E.M., Barnett, J.F., Freshwater, L., Hoberman, A.M., and Christian, M.S. (2002). Sexual maturation data for Crl Sprague-Dawley rats: criteria and confounding factors. Drug Chem Toxicol *25*, 437–458.

Li, C., Bassell, G.J., and Sasaki, Y. (2009). Fragile X Mental Retardation Protein is Involved in Protein Synthesis-Dependent Collapse of Growth Cones Induced by Semaphorin-3A. Front Neural Circuits *3*, 11.

Li, W., Cui, Y., Kushner, S.A., Brown, R.A.M., Jentsch, J.D., Frankland, P.W., Cannon, T.D., and Silva, A.J. (2005a). The HMG-CoA reductase inhibitor lovastatin reverses the learning and attention deficits in a mouse model of neurofibromatosis type 1. Curr Biol *15*, 1961–1967.

Li, Z., Burrone, J., Tyler, W.J., Hartman, K.N., Albeanu, D.F., and Murthy, V.N. (2005b). Synaptic vesicle recycling studied in transgenic mice expressing synaptopHluorin. Proc Natl Acad Sci USA *102*, 6131–6136.

Liao, J.K. (2002). Isoprenoids as mediators of the biological effects of statins. J. Clin. Invest. *110*, 285–288.

Linden, D.J., and Routtenberg, A. (1989). The role of protein kinase C in long-term potentiation: a testable model. Brain Res. Brain Res. Rev. *14*, 279–296.

Lisman, J. (1989). A mechanism for the Hebb and the anti-Hebb processes underlying learning and memory. Proc Natl Acad Sci USA *86*, 9574–9578.

Lisman, J.E., and Harris, K.M. (1993). Quantal analysis and synaptic anatomy--integrating two views of hippocampal plasticity. Trends in Neurosciences *16*, 141–147.

Lisman, J., Schulman, H., and Cline, H. (2002). The molecular basis of CaMKII function in synaptic and behavioural memory. Nat Rev Neurosci *3*, 175–190.

Llano, I., González, J., Caputo, C., Lai, F.A., Blayney, L.M., Tan, Y.P., and Marty, A. (2000). Presynaptic calcium stores underlie large-amplitude miniature IPSCs and spontaneous calcium transients. Nat Neurosci *3*, 1256–1265.

Lou, X., Fan, F., Messa, M., Raimondi, A., Wu, Y., Looger, L.L., Ferguson, S.M., and De Camilli, P. (2012). Reduced release probability prevents vesicle depletion and transmission failure at dynamin mutant synapses. Proc Natl Acad Sci USA *109*, E515–E523.

Lu, Y.M., Jia, Z., Janus, C., Henderson, J.T., Gerlai, R., Wojtowicz, J.M., and Roder, J.C. (1997). Mice lacking metabotropic glutamate receptor 5 show impaired learning and reduced CA1 long-term potentiation (LTP) but normal CA3 LTP. J Neurosci *17*, 5196–5205.

Lubs, H.A. (1969). A marker X chromosome. Am. J. Hum. Genet. *21*, 231–244.

Lubs, H.A., Stevenson, R.E., and Schwartz, C.E. (2012). Fragile X and X-linked intellectual disability: four decades of discovery. Am. J. Hum. Genet. *90*, 579–590.

Lucić, V., Yang, T., Schweikert, G., Förster, F., and Baumeister, W. (2005). Morphological characterization of molecular complexes present in the synaptic cleft. Structure *13*, 423–434.

Lüscher, C., and Malenka, R.C. (2012). NMDA receptor-dependent long-term potentiation and long-term depression (LTP/LTD). Cold Spring Harb Perspect Biol *4*, a005710–a005710.

Lynch, G., Larson, J., Kelso, S., Barrionuevo, G., and Schottler, F. (1983). Intracellular injections of EGTA block induction of hippocampal long-term potentiation. Nature *305*, 719–721.

MacDermott, A.B., Mayer, M.L., Westbrook, G.L., Smith, S.J., and Barker, J.L. (1986). NMDA-receptor activation increases cytoplasmic calcium concentration in cultured spinal cord neurones. Nature *321*, 519–522.

MacDougall, M.J., and Fine, A. (2014). The expression of long-term potentiation: reconciling the preists and the postivists. Philosophical Transactions of the Royal Society B: Biological Sciences *369*, 20130135.

Magee, J.C., and Johnston, D. (1997). A synaptically controlled, associative signal for Hebbian plasticity in hippocampal neurons. Science *275*, 209–213.

Malenka, R.C., and Nicoll, R.A. (1999). Long-term potentiation--a decade of progress? Science *285*, 1870–1874.

Malenka, R.C., Kauer, J.A., Zucker, R.S., and Nicoll, R.A. (1988). Postsynaptic calcium is sufficient for potentiation of hippocampal synaptic transmission. Science *242*, 81–84.

Malenka, R.C., and Bear, M.F. (2004). LTP and LTD: an embarrassment of riches. Neuron *44*, 5–21.

Maletic-Savatic, M., Malinow, R., and Svoboda, K. (1999). Rapid dendritic morphogenesis in CA1 hippocampal dendrites induced by synaptic activity. Science *283*, 1923–1927.

Malgaroli, A., and Tsien, R.W. (1992). Glutamate-induced long-term potentiation of the frequency of miniature synaptic currents in cultured hippocampal neurons. Nature *357*, 139.

Malinow, R., Schulman, H., and Tsien, R.W. (1989). Inhibition of postsynaptic PKC or CaMKII blocks induction but not expression of LTP. Science *245*, 862–866.

Mammen, A.L., Kameyama, K., Roche, K.W., and Huganir, R.L. (1997). Phosphorylation of the alpha-amino-3-hydroxy-5-methylisoxazole4-propionic acid receptor GluR1 subunit by calcium/calmodulin-dependent kinase II. J. Biol. Chem. *272*, 32528–32533.

Man, H.Y., Lin, J.W., Ju, W.H., Ahmadian, G., Liu, L., Becker, L.E., Sheng, M., and Wang, Y.T. (2000). Regulation of AMPA receptor-mediated synaptic transmission by clathrin-dependent receptor internalization. Neuron *25*, 649–662.

Manahan-Vaughan, D., and Braunewell, K.H. (1999). Novelty acquisition is associated with induction of hippocampal long-term depression. Proc Natl Acad Sci USA *96*, 8739–8744.

Manahan-Vaughan, D., and Braunewell, K.-H. (2005). The metabotropic glutamate receptor, mGluR5, is a key determinant of good and bad spatial learning performance and hippocampal synaptic plasticity. Cereb. Cortex *15*, 1703–1713.

Martin, J.P., and Bell, J. (1943). A PEDIGREE OF MENTAL DEFECT SHOWING SEX-LINKAGE. J Neurol Psychiatry *6*, 154–157.

Martone, M.E., Zhang, Y., Simpliciano, V.M., Carragher, B.O., and Ellisman, M.H. (1993). Three-dimensional visualization of the smooth endoplasmic reticulum in Purkinje cell dendrites. J Neurosci *13*, 4636–4646.

Matlack, K.E., Mothes, W., and Rapoport, T.A. (1998). Protein translocation: tunnel vision. Cell *92*, 381–390.

Matsuo, N., Reijmers, L., and Mayford, M. (2008). Spine-type-specific recruitment of newly synthesized AMPA receptors with learning. Science *319*, 1104–1107.

Matsuzaki, M., Honkura, N., Ellis-Davies, G.C.R., and Kasai, H. (2004). Structural basis of long-term potentiation in single dendritic spines. Nature *429*, 761–766.

Matteoli, M., Coco, S., Schenk, U., and Verderio, C. (2004). Vesicle turnover in developing neurons: how to build a presynaptic terminal. Trends in Cell Biology *14*, 133–140.

Mayer, M.L., Westbrook, G.L., and Guthrie, P.B. (1984). Voltage-dependent block by Mg2+ of NMDA responses in spinal cord neurones. Nature *309*, 261–263.

McCurry, C.L., Shepherd, J.D., Tropea, D., Wang, K.H., Bear, M.F., and Sur, M. (2010). Loss of Arc renders the visual cortex impervious to the effects of sensory experience or deprivation. Nat Neurosci *13*, 450–457.

McCutcheon, J.E., and Marinelli, M. (2009). Age matters. Eur J Neurosci *29*, 997–1014.

McGlade-McCulloh, E., Yamamoto, H., Tan, S.E., Brickey, D.A., and Soderling, T.R. (1993). Phosphorylation and regulation of glutamate receptors by calcium/calmodulin-dependent protein kinase II. Nature *362*, 640–642.

McGraw, C.F., Somlyo, A.V., and Blaustein, M.P. (1980). Localization of calcium in presynaptic nerve terminals. An ultrastructural and electron microprobe analysis. J Cell Biol *85*, 228–241.

McHugh, T.J., Blum, K.I., Tsien, J.Z., Tonegawa, S., and Wilson, M.A. (1996). Impaired hippocampal representation of space in CA1-specific NMDAR1 knockout mice. Cell *87*, 1339–1349.

McKinney, B.C., Grossman, A.W., Elisseou, N.M., and Greenough, W.T. (2005). Dendritic spine abnormalities in the occipital cortex of C57BL/6 Fmr1 knockout mice. Am. J. Med. Genet. B Neuropsychiatr. Genet. *136B*, 98–102.

McKinney, R.A., Capogna, M., Dürr, R., Gähwiler, B.H., and Thompson, S.M. (1999). Miniature synaptic events maintain dendritic spines via AMPA receptor activation. Nat Neurosci *2*, 44–49.

Mellentin, C., Jahnsen, H., and Abraham, W.C. (2007). Priming of long-term potentiation mediated by ryanodine receptor activation in rat hippocampal slices. Neuropharmacology *52*, 118–125.

Meyer, D., Bonhoeffer, T., and Scheuss, V. (2014). Balance and stability of synaptic structures during synaptic plasticity. Neuron *82*, 430–443.

Miesenböck, G., De Angelis, D.A., and Rothman, J.E. (1998). Visualizing secretion and synaptic transmission with pH-sensitive green fluorescent proteins. Nature *394*, 192–195.

Miesenböck, G. (2012). Synapto-pHluorins: genetically encoded reporters of synaptic transmission. Cold Spring Harb Protoc *2012*, 213–217.

Mignery, G.A., Sudhof, T.C., Takei, K., and De Camilli, P. (1989). Putative receptor for inositol 1,4,5-trisphosphate similar to ryanodine receptor. Nature *342*, 192–195.

Miller, S.G., and Kennedy, M.B. (1986). Regulation of brain type II Ca2+/calmodulin-dependent protein kinase by autophosphorylation: a Ca2+-triggered molecular switch. Cell *44*, 861–870.

Min, W.W., Yuskaitis, C.J., Yan, Q., Sikorski, C., Chen, S., Jope, R.S., and Bauchwitz, R.P. (2009). Elevated glycogen synthase kinase-3 activity in Fragile X mice: key metabolic regulator with evidence for treatment potential. Neuropharmacology *56*, 463–472.

Missler, M., Sudhof, T.C., and Biederer, T. (2012). Synaptic cell adhesion. Cold Spring Harb Perspect Biol *4*, a005694.

Morgan, S.L., and Teyler, T.J. (2001). Electrical stimuli patterned after the theta-rhythm induce multiple forms of LTP. Journal of Neurophysiology *86*, 1289–1296.

Morris, R.G. (1989). Synaptic plasticity and learning: selective impairment of learning rats and blockade of long-term potentiation in vivo by the N-methyl-D-aspartate receptor antagonist AP5. J Neurosci *9*, 3040–3057.

Morris, R.G.M., Moser, E.I., Riedel, G., Martin, S.J., Sandin, J., Day, M., and O'Carroll, C. (2003). Elements of a neurobiological theory of the hippocampus: the role of activity-dependent synaptic plasticity in memory. Philosophical Transactions of the Royal Society B: Biological Sciences *358*, 773–786.

Morris, R. (2007). Theories of Hippocampal Function. In The Hippocampus Book, (New York: Oxford University Press), pp. 581–713.

Moser, E., Moser, M.B., and Andersen, P. (1993). Synaptic potentiation in the rat dentate gyrus during exploratory learning. Neuroreport *5*, 317–320.

Moser, M.B., Trommald, M., and Andersen, P. (1994). An increase in dendritic spine density on hippocampal CA1 pyramidal cells following spatial learning in adult rats suggests the formation of new synapses. Proc Natl Acad Sci USA *91*, 12673–12675.

Moult, P.R., Corrêa, S.A.L., Collingridge, G.L., Fitzjohn, S.M., and Bashir, Z.I. (2008). Co-activation of p38 mitogen-activated protein kinase and protein

tyrosine phosphatase underlies metabotropic glutamate receptor-dependent long-term depression. The Journal of Physiology *586*, 2499–2510.

Muddashetty, R.S., Kelić, S., Gross, C., Xu, M., and Bassell, G.J. (2007). Dysregulated metabotropic glutamate receptor-dependent translation of AMPA receptor and postsynaptic density-95 mRNAs at synapses in a mouse model of fragile X syndrome. Journal of Neuroscience *27*, 5338–5348.

Mulkey, R.M., and Malenka, R.C. (1992). Mechanisms underlying induction of homosynaptic long-term depression in area CA1 of the hippocampus. Neuron *9*, 967–975.

Mulkey, R.M., Endo, S., Shenolikar, S., and Malenka, R.C. (1994). Involvement of a calcineurin/inhibitor-1 phosphatase cascade in hippocampal long-term depression. Nature *369*, 486–488.

Mulkey, R.M., Herron, C.E., and Malenka, R.C. (1993). An essential role for protein phosphatases in hippocampal long-term depression. Science *261*, 1051–1055.

Muller, D., Buchs, P.A., and Stoppini, L. (1993). Time course of synaptic development in hippocampal organotypic cultures. Brain Res. Dev. Brain Res. *71*, 93–100.

Mundel, P., Heid, H.W., Mundel, T.M., Krüger, M., Reiser, J., and Kriz, W. (1997). Synaptopodin: an actin-associated protein in telencephalic dendrites and renal podocytes. J Cell Biol *139*, 193–204.

Murthy, V.N., Sejnowski, T.J., and Stevens, C.F. (1997). Heterogeneous release properties of visualized individual hippocampal synapses. Neuron *18*, 599–612.

Murthy, V.N., and De Camilli, P. (2003). Cell biology of the presynaptic terminal. Annu. Rev. Neurosci. *26*, 701–728.

Naber, P.A., Lopes da Silva, F.H., and Witter, M.P. (2001). Reciprocal connections between the entorhinal cortex and hippocampal fields CA1 and the subiculum are in register with the projections from CA1 to the subiculum. Hippocampus *11*, 99–104.

Nagase, T., Ito, K.I., Kato, K., Kaneko, K., Kohda, K., Matsumoto, M., Hoshino, A., Inoue, T., Fujii, S., Kato, H., et al. (2003). Long-term potentiation and long-term depression in hippocampal CA1 neurons of mice lacking the IP(3) type 1 receptor. Neuroscience *117*, 821–830.

Naie, K., and Manahan-Vaughan, D. (2004). Regulation by metabotropic glutamate receptor 5 of LTP in the dentate gyrus of freely moving rats: relevance for learning and memory formation. Cereb. Cortex *14*, 189–198.

Nakamoto, M., Nalavadi, V., Epstein, M.P., Narayanan, U., Bassell, G.J., and Warren, S.T. (2007). Fragile X mental retardation protein deficiency leads to excessive mGluR5-dependent internalization of AMPA receptors. Proceedings of the National Academy of Sciences *104*, 15537–15542.

Nägerl, U.V., Eberhorn, N., Cambridge, S.B., and Bonhoeffer, T. (2004). Bidirectional activity-dependent morphological plasticity in hippocampal neurons. Neuron *44*, 759–767.

Neukomm, L.J., and Freeman, M.R. (2014). Diverse cellular and molecular modes of axon degeneration. Trends in Cell Biology *24*, 515–523.

Nguyen, P.V., and Woo, N.H. (2003). Regulation of hippocampal synaptic plasticity by cyclic AMP-dependent protein kinases. Prog Neurobiol *71*, 401–437.

Nguyen, P.V., Abel, T., and Kandel, E.R. (1994). Requirement of a critical period of transcription for induction of a late phase of LTP. Science *265*, 1104–1107.

Nikonenko, I., Jourdain, P., and Muller, D. (2003). Journal of Neuroscience.

Nimchinsky, E.A., Oberlander, A.M., and Svoboda, K. (2001). Abnormal development of dendritic spines in FMR1 knock-out mice. Journal of Neuroscience *21*, 5139–5146.

Nishiyama, M., Hong, K., Mikoshiba, K., Poo, M.M., and Kato, K. (2000). Calcium stores regulate the polarity and input specificity of synaptic modification. Nature *408*, 584–588.

Nowak, L., Bregestovski, P., Ascher, P., Herbet, A., and Prochiantz, A. (1984). Magnesium gates glutamate-activated channels in mouse central neurones. Nature *307*, 462–465.

Nusser, Z., Lujan, R., Laube, G., Roberts, J.D., Molnar, E., and Somogyi, P. (1998). Cell type and pathway dependence of synaptic AMPA receptor number and variability in the hippocampus. Neuron *21*, 545–559.

O'Dell, T.J., Hawkins, R.D., Kandel, E.R., and Arancio, O. (1991). Tests of the roles of two diffusible substances in long-term potentiation: evidence for nitric oxide as a possible early retrograde messenger. Proc Natl Acad Sci USA *88*, 11285–11289.

Okamoto, K.-I., Nagai, T., Miyawaki, A., and Hayashi, Y. (2004). Rapid and persistent modulation of actin dynamics regulates postsynaptic reorganization underlying bidirectional plasticity. Nat Neurosci *7*, 1104–1112.

Okamoto, K., Bosch, M., and Hayashi, Y. (2009). The roles of CaMKII and F-actin in the structural plasticity of dendritic spines: a potential molecular identity of a synaptic tag? Physiology (Bethesda) *24*, 357–366.

Oliet, S.H., Malenka, R.C., and Nicoll, R.A. (1997). Two distinct forms of long-term depression coexist in CA1 hippocampal pyramidal cells. Neuron *18*, 969–982.

Osterweil, E.K., Chuang, S.-C., Chubykin, A.A., Sidorov, M., Bianchi, R., Wong, R.K.S., and Bear, M.F. (2013). Lovastatin corrects excess protein synthesis and prevents epileptogenesis in a mouse model of fragile x syndrome. Neuron *77*, 243–250.

Osterweil, E.K., Krueger, D.D., Reinhold, K., and Bear, M.F. (2010). Hypersensitivity to mGluR5 and ERK1/2 leads to excessive protein synthesis in the hippocampus of a mouse model of fragile X syndrome. Journal of Neuroscience *30*, 15616–15627.

Ostroff, L.E., Fiala, J.C., Allwardt, B., and Harris, K.M. (2002). Polyribosomes redistribute from dendritic shafts into spines with enlarged synapses during LTP in developing rat hippocampal slices. Neuron *35*, 535–545.

Otani, S., Marshall, C.J., Tate, W.P., Goddard, G.V., and Abraham, W.C. (1989). Maintenance of long-term potentiation in rat dentate gyrus requires protein synthesis but not messenger RNA synthesis immediately post-tetanization. Neuroscience *28*, 519–526.

Ottersen, O.P., and Storm-Mathisen, J. (1984). Glutamate- and GABA-containing neurons in the mouse and rat brain, as demonstrated with a new immunocytochemical technique. J Comp Neurol *229*, 374–392.

Ouyang, Y., Martone, M.E., Deerinck, T.J., Airey, J.A., Sutko, J.L., and Ellisman, M.H. (1997). Differential distribution and subcellular localization of ryanodine receptor isoforms in the chicken cerebellum during development. Brain Res. *775*, 52–62.

Owczarek, S., Kiryushko, D., Larsen, M.H., Kastrup, J.S., Gajhede, M., Sandi, C., Berezin, V., Bock, E., and Soroka, V. (2010). Neuroplastin-55 binds to and signals through the fibroblast growth factor receptor. Faseb J. *24*, 1139–1150.

Owczarek, S., Soroka, V., Kiryushko, D., Larsen, M.H., Yuan, Q., Sandi, C., Berezin, V., and Bock, E. (2011). Neuroplastin-65 and a mimetic peptide derived from its homophilic binding site modulate neuritogenesis and neuronal plasticity. Journal of Neurochemistry *117*, 984–994.

Padamsey, Z., and Emptage, N. (2014). Two sides to long-term potentiation: a view towards reconciliation. Philosophical Transactions of the Royal Society B: Biological Sciences *369*, 20130154.

Padua, R.A., Nagy, J.I., and Geiger, J.D. (1996). Subcellular localization of ryanodine receptors in rat brain. Eur. J. Pharmacol. *298*, 185–189.

Palade, G. (1975). Intracellular aspects of the process of protein synthesis. Science *189*, 867.

Palay, S.L. (1956). Synapses in the central nervous system. J Biophys Biochem Cytol *2*, 193–202.

Palay, S.L., and Palade, G.E. (1955). THE FINE STRUCTURE OF NEURONS. J Biophys Biochem Cytol *1*, 69.

Palmer, M.J., Irving, A.J., Seabrook, G.R., Jane, D.E., and Collingridge, G.L. (1997). The group I mGlu receptor agonist DHPG induces a novel form of LTD in the CA1 region of the hippocampus. Neuropharmacology *36*, 1517–1532.

Park, S., Park, J.M., Kim, S., Kim, J.-A., Shepherd, J.D., Smith-Hicks, C.L., Chowdhury, S., Kaufmann, W., Kuhl, D., Ryazanov, A.G., et al. (2008). Elongation factor 2 and fragile X mental retardation protein control the dynamic translation of Arc/Arg3.1 essential for mGluR-LTD. Neuron *59*, 70–83.

Penn, A.C., Williams, S.R., and Greger, I.H. (2008). Gating motions underlie AMPA receptor secretion from the endoplasmic reticulum. Embo J. *27*, 3056–3068.

Phillips, G.R., Huang, J.K., Wang, Y., Tanaka, H., Shapiro, L., Zhang, W., Shan, W.S., Arndt, K., Frank, M., Gordon, R.E., et al. (2001). The presynaptic particle web: ultrastructure, composition, dissolution, and reconstitution. Neuron *32*, 63–77.

Pierce, J.P., Mayer, T., and McCarthy, J.B. (2001). Evidence for a satellite secretory pathway in neuronal dendritic spines. Curr Biol *11*, 351–355.

Pierce, J.P., van Leyen, K., and McCarthy, J.B. (2000). Translocation machinery for synthesis of integral membrane and secretory proteins in dendritic spines. Nat Neurosci *3*, 311–313.

Pieretti, M., Zhang, F.P., Fu, Y.H., Warren, S.T., Oostra, B.A., Caskey, C.T., and Nelson, D.L. (1991). Absence of expression of the FMR-1 gene in fragile X syndrome. Cell *66*, 817–822.

Popov, V.I., Davies, H.A., Rogachevsky, V.V., Patrushev, I.V., Errington, M.L., Gabbott, P.L.A., Bliss, T.V.P., and Stewart, M.G. (2004). Remodelling of synaptic morphology but unchanged synaptic density during late phase long-term potentiation (LTP): a serial section electron micrograph study in the dentate gyrus in the anaesthetised rat. Neuroscience *128*, 251–262.

Porter, K.R., and Kallman, F.L. (1952). Significance of cell particulates as seen by electron microscopy. Ann. N. Y. Acad. Sci. *54*, 882–891.

Porter, K.R., and Thompson, H.P. (1948). A particulate body associated with epithelial cells cultured from mammary carcinomas of mice of a milkfactor strain. J. Exp. Med. *88*, 15–24.

Porter, K.R., Claude, A., and Fullam, E.F. (1945). A STUDY OF TISSUE CULTURE CELLS BY ELECTRON MICROSCOPY : METHODS AND PRELIMINARY OBSERVATIONS. J. Exp. Med. *81*, 233–246.

Portera-Cailliau, C. (2012). Which comes first in fragile X syndrome, dendritic spine dysgenesis or defects in circuit plasticity? The Neuroscientist : a Review Journal Bringing Neurobiology, Neurology and Psychiatry *18*, 28–44.

Portera-Cailliau, C., Weimer, R.M., De Paola, V., Caroni, P., and Svoboda, K. (2005). Diverse modes of axon elaboration in the developing neocortex. PLoS Biol *3*.

Pozzan, T., Rizzuto, R., Volpe, P., and Meldolesi, J. (1994). Molecular and cellular physiology of intracellular calcium stores. Physiol. Rev. *74*, 595–636.

Preston, A.R., and Eichenbaum, H. (2013). Interplay of hippocampus and prefrontal cortex in memory. Curr Biol *23*, R764–R773.

Qin, M., Kang, J., Burlin, T.V., Jiang, C., and Smith, C.B. (2005). Postadolescent changes in regional cerebral protein synthesis: an in vivo study in the FMR1 null mouse. Journal of Neuroscience *25*, 5087–5095.

Ratnayaka, A., Marra, V., Branco, T., and Staras, K. (2011). Extrasynaptic vesicle recycling in mature hippocampal neurons. Nat Commun *2*, 531.

Ratnayaka, A., Marra, V., Bush, D., Burden, J.J., Branco, T., and Staras, K. (2012). Recruitment of resting vesicles into recycling pools supports NMDA-receptor dependent synaptic potentiation in cultured hippocampal neurons. The Journal of Physiology.

Raymond, C.R., Thompson, V.L., Tate, W.P., and Abraham, W.C. (2000). Metabotropic glutamate receptors trigger homosynaptic protein synthesis to prolong long-term potentiation. J Neurosci *20*, 969–976.

Raymond, C.R., and Redman, S.J. (2002). Different calcium sources are narrowly tuned to the induction of different forms of LTP. Journal of Neurophysiology *88*, 249–255.

Raymond, C.R., and Redman, S.J. (2006). Spatial segregation of neuronal calcium signals encodes different forms of LTP in rat hippocampus. The Journal of Physiology *570*, 97–111.

Regehr, W.G., Carey, M.R., and Best, A.R. (2009). Activity-dependent regulation of synapses by retrograde messengers. Neuron *63*, 154–170.

Rizzoli, S.O., and Betz, W.J. (2005). Synaptic vesicle pools. Nat Rev Neurosci *6*, 57–69.

Rizzoli, S.O., and Jahn, R. (2007). Kiss-and-run, collapse and "readily retrievable" vesicles. Traffic *8*, 1137–1144.

Rose, C.R., and Konnerth, A. (2001). Stores not just for storage. intracellular calcium release and synaptic plasticity. Neuron *31*, 519–522.

Rosenmund, C., and Stevens, C.F. (1996). Definition of the readily releasable pool of vesicles at hippocampal synapses. Neuron *16*, 1197–1207.

Rudelli, R.D., Brown, W.T., Wisniewski, K., Jenkins, E.C., Laure-Kamionowska, M., Connell, F., and Wisniewski, H.M. (1985). Adult fragile X syndrome. Clinico-neuropathologic findings. Acta Neuropathol. *67*, 289–295.

Ruthazer, E.S., Akerman, C.J., and Cline, H.T. (2003). Control of axon branch dynamics by correlated activity in vivo. Science *301*, 66–70.

Ryan, T.A. (2001). Presynaptic imaging techniques. Current Opinion in Neurobiology *11*, 544–549.

Ryan, T.A. (2006). A pre-synaptic to-do list for coupling exocytosis to endocytosis. Curr. Opin. Cell Biol. *18*, 416–421.

Rønn, L.C.B., Dissing, S., Holm, A., Berezin, V., and Bock, E. (2002). Increased intracellular calcium is required for neurite outgrowth induced by a synthetic peptide ligand of NCAM. FEBS Lett. *518*, 60–66.

Sabo, S.L., Gomes, R.A., and McAllister, A.K. (2006). Formation of presynaptic terminals at predefined sites along axons. Journal of Neuroscience *26*, 10813–10825.

Sacktor, T.C., Osten, P., Valsamis, H., Jiang, X., Naik, M.U., and Sublette, E. (1993). Persistent activation of the zeta isoform of protein kinase C in the maintenance of long-term potentiation. Proc Natl Acad Sci USA *90*, 8342–8346.

Sajikumar, S., Li, Q., Abraham, W.C., and Xiao, Z.C. (2009). Priming of short-term potentiation and synaptic tagging/capture mechanisms by ryanodine receptor activation in rat hippocampal CA1. Learn. Mem. *16*, 186.

Sajikumar, S., Navakkode, S., and Frey, J.U. (2005). Protein synthesis-dependent long-term functional plasticity: methods and techniques. Current Opinion in Neurobiology *15*, 607–613.

Sala, C., Roussignol, G., Meldolesi, J., and Fagni, L. (2005). Key role of the postsynaptic density scaffold proteins Shank and Homer in the functional architecture of Ca2+ homeostasis at dendritic spines in hippocampal neurons. Journal of Neuroscience *25*, 4592.

Salin, P.A., Malenka, R.C., and Nicoll, R.A. (1996). Cyclic AMP mediates a presynaptic form of LTP at cerebellar parallel fiber synapses. Neuron *16*, 797–803.

Sandell, J.H., and Masland, R.H. (1988). Photoconversion of some fluorescent markers to a diaminobenzidine product. J. Histochem. Cytochem. *36*, 555–559.

Sarihi, A., Mirnajafi-Zadeh, J., Jiang, B., Sohya, K., Safari, M.-S., Arami, M.K., Yanagawa, Y., and Tsumoto, T. (2012). Cell type-specific, presynaptic LTP of inhibitory synapses on fast-spiking GABAergic neurons in the mouse visual cortex. Journal of Neuroscience *32*, 13189–13199.

Saul, R.A., and Tarleton, J.C. (2012). FMR1-Related Disorders. GeneReviews.

Schikorski, T., and Stevens, C.F. (2001). Morphological correlates of functionally defined synaptic vesicle populations. Nat Neurosci *4*, 391–395.

Schuch, U., Lohse, M.J., and Schachner, M. (1989). Neural cell adhesion molecules influence second messenger systems. Neuron *3*, 13–20.

Schultz, C., and Engelhardt, M. (2014). Anatomy of the hippocampal formation. Front Neurol Neurosci *34*, 6–17.

Schuman, E.M., and Madison, D.V. (1991). A requirement for the intercellular messenger nitric oxide in long-term potentiation. Science *254*, 1503–1506.

Schwartzkroin, P.A., and Wester, K. (1975). Long-lasting facilitation of a synaptic potential following tetanization in the in vitro hippocampal slice. Brain Res. *89*, 107–119.

Scoville, W.B., and Milner, B. (1957). Loss of recent memory after bilateral hippocampal lesions. J. Neurol. Neurosurg. Psychiatr. *20*, 11–21.

Segal, M., and Korkotian, E. (2014). Endoplasmic reticulum calcium stores in dendritic spines. Front Neuroanat *8*, 64.

Segal, M., Kreher, U., Greenberger, V., and Braun, K. (2003). Is fragile X mental retardation protein involved in activity-induced plasticity of dendritic spines? Brain Res. *972*, 9–15.

Seymour-Laurent, K.J., and Barish, M.E. (1995). Inositol 1,4,5-trisphosphate and ryanodine receptor distributions and patterns of acetylcholine- and caffeine-induced calcium release in cultured mouse hippocampal neurons. J Neurosci *15*, 2592–2608.

Shaban, H., Humeau, Y., Herry, C., Cassasus, G., Shigemoto, R., Ciocchi, S., Barbieri, S., van der Putten, H., Kaupmann, K., Bettler, B., et al. (2006). Generalization of amygdala LTP and conditioned fear in the absence of presynaptic inhibition. Nat Neurosci *9*, 1028–1035.

Shapira, M., Zhai, R.G., Dresbach, T., Bresler, T., Torres, V.I., Gundelfinger, E.D., Ziv, N.E., and Garner, C.C. (2003). Unitary assembly of presynaptic active zones from Piccolo-Bassoon transport vesicles. Neuron *38*, 237–252.

Sharp, A.H., McPherson, P.S., Dawson, T.M., Aoki, C., Campbell, K.P., and Snyder, S.H. (1993). Differential immunohistochemical localization of inositol 1,4,5-trisphosphate- and ryanodine-sensitive Ca2+ release channels in rat brain. J Neurosci *13*, 3051–3063.

Sharp, P.E., McNaughton, B.L., and Barnes, C.A. (1989). Exploration-dependent modulation of evoked responses in fascia dentata: Fundamental observations and time course. Psychobiology *17*, 257–269.

Shavelle, R.M., and Strauss, D. (1998). Comparative mortality of persons with autism in California, 1980-1996. J Insur Med *30*, 220–225.

Shepherd, J.D., Rumbaugh, G., Wu, J., Chowdhury, S., Plath, N., Kuhl, D., Huganir, R.L., and Worley, P.F. (2006). Arc/Arg3.1 mediates homeostatic synaptic scaling of AMPA receptors. Neuron *52*, 475–484.

Sheppard, C.A., Simpson, P.B., Sharp, A.H., Nucifora, F.C., Ross, C.A., Lange, G.D., and Russell, J.T. (1997). Comparison of type 2 inositol 1,4,5-trisphosphate receptor distribution and subcellular Ca2+ release sites that support Ca2+ waves in cultured astrocytes. Journal of Neurochemistry *68*, 2317–2327.

Shi, S.H., Hayashi, Y., Petralia, R.S., Zaman, S.H., Wenthold, R.J., Svoboda, K., and Malinow, R. (1999). Rapid spine delivery and redistribution of AMPA receptors after synaptic NMDA receptor activation. Science *284*, 1811–1816.

Shima, Y., Copeland, N.G., Gilbert, D.J., Jenkins, N.A., Chisaka, O., Takeichi, M., and Uemura, T. (2002). Differential expression of the seven-pass transmembrane cadherin genes Celsr1-3 and distribution of the Celsr2 protein during mouse development. Dev. Dyn. *223*, 321–332.

Shima, Y., Kawaguchi, S.-Y., Kosaka, K., Nakayama, M., Hoshino, M., Nabeshima, Y., Hirano, T., and Uemura, T. (2007). Opposing roles in neurite growth control by two seven-pass transmembrane cadherins. Nat Neurosci *10*, 963–969.

Shin, R.-M., Tully, K., Li, Y., Cho, J.-H., Higuchi, M., Suhara, T., and Bolshakov, V.Y. (2010). Hierarchical order of coexisting pre- and postsynaptic forms of long-term potentiation at synapses in amygdala. Proc Natl Acad Sci USA *107*, 19073–19078.

Sidorov, M.S., Auerbach, B.D., and Bear, M.F. (2013). Fragile X mental retardation protein and synaptic plasticity. Mol Brain *6*, 15.

Simonoff, E., Pickles, A., Charman, T., Chandler, S., Loucas, T., and Baird, G. (2008). Psychiatric disorders in children with autism spectrum disorders: prevalence, comorbidity, and associated factors in a population-derived sample. J Am Acad Child Adolesc Psychiatry *47*, 921–929.

Simpson, P.B., Challiss, R.A., and Nahorski, S.R. (1995). Neuronal Ca2+ stores: activation and function. Trends in Neurosciences *18*, 299–306.

Simpson, P.B., Holtzclaw, L.A., Langley, D.B., and Russell, J.T. (1998). Characterization of ryanodine receptors in oligodendrocytes, type 2 astrocytes, and O-2A progenitors. J. Neurosci. Res. *52*, 468–482.

Skrede, K.K., and Malthe-Sørenssen, D. (1981). Increased resting and evoked release of transmitter following repetitive electrical tetanization in hippocampus: a biochemical correlate to long-lasting synaptic potentiation. Brain Res. *208*, 436–441.

Skrede, K.K., and Westgaard, R.H. (1971). The transverse hippocampal slice: a well-defined cortical structure maintained in vitro. Brain Res. *35*, 589–593.

Smith, C.L., Afroz, R., Bassell, G.J., Furneaux, H.M., Perrone-Bizzozero, N.I., and Burry, R.W. (2004). GAP-43 mRNA in growth cones is associated with HuD and ribosomes. J. Neurobiol. *61*, 222–235.

Sobczyk, A., Scheuss, V., and Svoboda, K. (2005). NMDA receptor subunit-dependent [Ca2+] signaling in individual hippocampal dendritic spines. Journal of Neuroscience *25*, 6037–6046.

Sokolov, M.V., Rossokhin, A.V., Astrelin, A.V., Frey, J.U., and Voronin, L.L. (2002). Quantal analysis suggests strong involvement of presynaptic mechanisms during the initial 3 h maintenance of long-term potentiation in rat hippocampal CA1 area in vitro. Brain Res. *957*, 61–75.

Somogyi, P., Halasy, K., Somogyi, J., Storm-Mathisen, J., and Ottersen, O.P. (1986). Quantification of immunogold labelling reveals enrichment of glutamate in mossy and parallel fibre terminals in cat cerebellum. Neuroscience *19*, 1045–1050.

Sorra, K.E., and Harris, K.M. (1993). Occurrence and three-dimensional structure of multiple synapses between individual radiatum axons and their target pyramidal cells in hippocampal area CA1. Journal of Neuroscience *13*, 3736–3748.

Sorra, K.E., and Harris, K.M. (1998). Stability in synapse number and size at 2 hr after long-term potentiation in hippocampal area CA1. J Neurosci *18*, 658–671.

Sorra, K.E., Mishra, A., Kirov, S.A., and Harris, K.M. (2006). Dense core vesicles resemble active-zone transport vesicles and are diminished following

synaptogenesis in mature hippocampal slices. Neuroscience *141*, 2097–2106.

Spacek, J. (1985). Three-dimensional analysis of dendritic spines. II. Spine apparatus and other cytoplasmic components. Anat. Embryol. *171*, 235–243.

Spacek, J., and Harris, K.M. (1997). Three-dimensional organization of smooth endoplasmic reticulum in hippocampal CA1 dendrites and dendritic spines of the immature and mature rat. J Neurosci *17*, 190–203.

Spejo, A.B., and Oliveira, A.L.R. (2014). Synaptic rearrangement following axonal injury: old and new players. Neuropharmacology.

Stanton, M.E. (2000). Multiple memory systems, development and conditioning. Behav Brain Res *110*, 25–37.

Stanton, P.K., Chattarji, S., and Sejnowski, T.J. (1991). 2-Amino-3-phosphonopropionic acid, an inhibitor of glutamate-stimulated phosphoinositide turnover, blocks induction of homosynaptic long-term depression, but not potentiation, in rat hippocampus. Neurosci. Lett. *127*, 61–66.

Stanton, P.K., Winterer, J., Zhang, X.-L., and Müller, W. (2005). Imaging LTP of presynaptic release of FM1-43 from the rapidly recycling vesicle pool of Schaffer collateral-CA1 synapses in rat hippocampal slices. Eur J Neurosci *22*, 2451–2461.

Staras, K., Branco, T., Burden, J.J., Pozo, K., Darcy, K., Marra, V., Ratnayaka, A., and Goda, Y. (2010). A vesicle superpool spans multiple presynaptic terminals in hippocampal neurons. Neuron *66*, 37–44.

Stettler, D.D., Yamahachi, H., Li, W., Denk, W., and Gilbert, C.D. (2006). Axons and synaptic boutons are highly dynamic in adult visual cortex. Neuron *49*, 877–887.

Stevens, C.F., and Wang, Y. (1994). Changes in reliability of synaptic function as a mechanism for plasticity. Nature *371*, 704–707.

Stevens, C.F., and Wang, Y. (1995). Facilitation and depression at single central synapses. Neuron *14*, 795–802.

Steward, O., and Levy, W.B. (1982). Preferential localization of polyribosomes under the base of dendritic spines in granule cells of the dentate gyrus. J Neurosci *2*, 284–291.

Steward, O., and Schuman, E.M. (2001). Protein synthesis at synaptic sites on dendrites. Annu. Rev. Neurosci. *24*, 299–325.

Stewart, M.G., Medvedev, N.I., Popov, V.I., Schoepfer, R., Davies, H.A., Murphy, K., Dallérac, G.M., Kraev, I.V., and Rodríguez, J.J. (2005). Chemically

induced long-term potentiation increases the number of perforated and complex postsynaptic densities but does not alter dendritic spine volume in CA1 of adult mouse hippocampal slices. Eur J Neurosci *21*, 3368–3378.

Storm-Mathisen, J., Leknes, A.K., Bore, A.T., Vaaland, J.L., Edminson, P., Haug, F.M., and Ottersen, O.P. (1983). First visualization of glutamate and GABA in neurones by immunocytochemistry. Nature *301*, 517–520.

Streb, H., Irvine, R.F., Berridge, M.J., and Schulz, I. (1983). Release of Ca2+ from a nonmitochondrial intracellular store in pancreatic acinar cells by inositol-1,4,5-trisphosphate. Nature *306*, 67–69.

Stuart, G.J., and Sakmann, B. (1994). Active propagation of somatic action potentials into neocortical pyramidal cell dendrites. Nature *367*, 69–72.

Sudhof, T.C. (1995). The synaptic vesicle cycle: a cascade of protein-protein interactions. Nature *375*, 645–653.

Sudhof, T.C. (2012). Calcium Control of Neurotransmitter Release. Cold Spring Harb Perspect Biol *4*, a011353–a011353.

Sutherland, G.R. (1977). Fragile sites on human chromosomes: demonstration of their dependence on the type of tissue culture medium. Science *197*, 265–266.

Tabares, L., Ruiz, R., Linares-Clemente, P., Gaffield, M.A., Alvarez de Toledo, G., Fernandez-Chacón, R., and Betz, W.J. (2007). Monitoring synaptic function at the neuromuscular junction of a mouse expressing synaptopHluorin. Journal of Neuroscience *27*, 5422–5430.

Tennyson, V.M. (1970). The fine structure of the axon and growth cone of the dorsal root neuroblast of the rabbit embryo. J Cell Biol *44*, 62–79.

Terasaki, M., Slater, N.T., Fein, A., Schmidek, A., and Reese, T.S. (1994). Continuous network of endoplasmic reticulum in cerebellar Purkinje neurons. Proc Natl Acad Sci USA *91*, 7510–7514.

Thomas, A.M., Bui, N., Graham, D., Perkins, J.R., Yuva-Paylor, L.A., and Paylor, R. (2011). Genetic reduction of group 1 metabotropic glutamate receptors alters select behaviors in a mouse model for fragile X syndrome. Behav Brain Res *223*, 310–321.

Thomas, A.M., Bui, N., Perkins, J.R., Yuva-Paylor, L.A., and Paylor, R. (2012). Group I metabotropic glutamate receptor antagonists alter select behaviors in a mouse model for fragile X syndrome. Psychopharmacology (Berl.) *219*, 47–58.

Tiedge, H., Bloom, F.E., and Richter, D. (1999). RNA, whither goest thou? Science *283*, 186–187.

Till, S.M., Wijetunge, L.S., Seidel, V.G., Harlow, E., Wright, A.K., Bagni, C., Contractor, A., Gillingwater, T.H., and Kind, P.C. (2012). Altered maturation of the primary somatosensory cortex in a mouse model of fragile X syndrome. Hum. Mol. Genet.

Truckenbrodt, S., and Rizzoli, S.O. (2014). Spontaneous vesicle recycling in the synaptic bouton. Front Cell Neurosci *8*, 409.

Tsien, J.Z., Chen, D.F., Gerber, D., Tom, C., Mercer, E.H., Anderson, D.J., Mayford, M., Kandel, E.R., and Tonegawa, S. (1996a). Subregion- and cell type-restricted gene knockout in mouse brain. Cell *87*, 1317–1326.

Tsien, J.Z., Huerta, P.T., and Tonegawa, S. (1996b). The essential role of hippocampal CA1 NMDA receptor-dependent synaptic plasticity in spatial memory. Cell *87*, 1327–1338.

Tsvetkov, E., Carlezon, W.A., Benes, F.M., Kandel, E.R., and Bolshakov, V.Y. (2002). Fear conditioning occludes LTP-induced presynaptic enhancement of synaptic transmission in the cortical pathway to the lateral amygdala. Neuron *34*, 289–300.

Tuchman, R., Cuccaro, M., and Alessandri, M. (2010). Autism and epilepsy: historical perspective. Brain Dev. *32*, 709–718.

Unni, V.K., Zakharenko, S.S., Zablow, L., DeCostanzo, A.J., and Siegelbaum, S.A. (2004). Calcium release from presynaptic ryanodine-sensitive stores is required for long-term depression at hippocampal CA3-CA3 pyramidal neuron synapses. Journal of Neuroscience *24*, 9612–9622.

Van Harreveld, A., and Fifková, E. (1975). Swelling of dendritic spines in the fascia dentata after stimulation of the perforant fibers as a mechanism of post-tetanic potentiation. Exp. Neurol. *49*, 736–749.

Vaughan, C.J. (2003). Prevention of stroke and dementia with statins: Effects beyond lipid lowering. Am. J. Cardiol. *91*, 23B–29B.

Vedrenne, C., Klopfenstein, D.R., and Hauri, H.-P. (2005). Phosphorylation controls CLIMP-63-mediated anchoring of the endoplasmic reticulum to microtubules. Mol. Biol. Cell *16*, 1928–1937.

Verkerk, A.J., Pieretti, M., Sutcliffe, J.S., Fu, Y.H., Kuhl, D.P., Pizzuti, A., Reiner, O., Richards, S., Victoria, M.F., and Zhang, F.P. (1991). Identification of a gene (FMR-1) containing a CGG repeat coincident with a breakpoint cluster region exhibiting length variation in fragile X syndrome. Cell *65*, 905–914.

Verkhratsky, A., and Shmigol, A. (1996). Calcium-induced calcium release in neurones. Cell Calcium *19*, 1–14.

Vlachos, A., Ikenberg, B., Lenz, M., Becker, D., Reifenberg, K., Bas-Orth, C., and Deller, T. (2013). Synaptopodin regulates denervation-induced homeostatic synaptic plasticity. Proc Natl Acad Sci USA *110*, 8242–8247.

Vlachos, A., Korkotian, E., Schonfeld, E., Copanaki, E., Deller, T., and Segal, M. (2009). Synaptopodin regulates plasticity of dendritic spines in hippocampal neurons. Journal of Neuroscience *29*, 1017–1033.

Vlachos, A., Maggio, N., and Segal, M. (2008). Lack of correlation between synaptopodin expression and the ability to induce LTP in the rat dorsal and ventral hippocampus. Hippocampus *18*, 1–4.

Walton, P.D., Airey, J.A., Sutko, J.L., Beck, C.F., Mignery, G.A., Sudhof, T.C., Deerinck, T.J., and Ellisman, M.H. (1991). Ryanodine and inositol trisphosphate receptors coexist in avian cerebellar Purkinje neurons. J Cell Biol *113*, 1145–1157.

Wang, J.H., and Kelly, P.T. (1997). Attenuation of paired-pulse facilitation associated with synaptic potentiation mediated by postsynaptic mechanisms. Journal of Neurophysiology *78*, 2707–2716.

Wang, L., and Leslie, D.L. (2010). Health care expenditures for children with autism spectrum disorders in Medicaid. J Am Acad Child Adolesc Psychiatry *49*, 1165–1171.

Wang, X.-S., Peng, C.-Z., Cai, W.-J., Xia, J., Jin, D., Dai, Y., Luo, X.-G., Klyachko, V.A., and Deng, P.-Y. (2014). Activity-dependent regulation of release probability at excitatory hippocampal synapses: a crucial role of fragile X mental retardation protein in neurotransmission. Eur J Neurosci *39*, 1602–1612.

Wang, Y., Wu, J., Rowan, M.J., and Anwyl, R. (1996). Ryanodine produces a low frequency stimulation-induced NMDA receptor-independent long-term potentiation in the rat dentate gyrus in vitro. The Journal of Physiology *495 (Pt 3)*, 755–767.

Ward, B., McGuinness, L., Akerman, C.J., Fine, A., Bliss, T.V.P., and Emptage, N.J. (2006). State-dependent mechanisms of LTP expression revealed by optical quantal analysis. Neuron *52*, 649–661.

Weber, A., Herz, R., and Reiss, I. (1966). Study of kinetics of calcium transport by isolated fragmented sarcoplasmic reticulum. Biochemische Zeitschrift *345*, 329–369.

Westphal, V., Rizzoli, S.O., Lauterbach, M.A., Kamin, D., Jahn, R., and Hell, S.W. (2008). Video-rate far-field optical nanoscopy dissects synaptic vesicle movement. Science *320*, 246–249.

Whitlock, J.R., Heynen, A.J., Shuler, M.G., and Bear, M.F. (2006). Learning induces long-term potentiation in the hippocampus. Science *313*, 1093–1097.

Whittingham, T.S., Lust, W.D., Christakis, D.A., and Passonneau, J.V. (1984). Metabolic stability of hippocampal slice preparations during prolonged incubation. Journal of Neurochemistry *43*, 689–696.

Wiegert, J.S., Hofmann, F., Bading, H., and Bengtson, C.P. (2009). A transcription-dependent increase in miniature EPSC frequency accompanies late-phase plasticity in cultured hippocampal neurons. BMC Neurosci *10*, 124.

Wijetunge, L.S., Angibaud, J., Frick, A., Kind, P.C., and Nägerl, U.V. (2014). Stimulated emission depletion (STED) microscopy reveals nanoscale defects in the developmental trajectory of dendritic spine morphogenesis in a mouse model of fragile X syndrome. J Neurosci *34*, 6405–6412.

Wikström, M.A., Matthews, P., Roberts, D., Collingridge, G.L., and Bortolotto, Z.A. (2003). Parallel kinase cascades are involved in the induction of LTP at hippocampal CA1 synapses. Neuropharmacology *45*, 828–836.

Wisniewski, K.E., Segan, S.M., Miezejeski, C.M., Sersen, E.A., and Rudelli, R.D. (1991). The Fra(X) syndrome: neurological, electrophysiological, and neuropathological abnormalities. Am. J. Med. Genet. *38*, 476–480.

Woolley, C.S., Gould, E., Frankfurt, M., and McEwen, B.S. (1990). Naturally occurring fluctuation in dendritic spine density on adult hippocampal pyramidal neurons. J Neurosci *10*, 4035–4039.

Xiao, M.Y., Zhou, Q., and Nicoll, R.A. (2001). Metabotropic glutamate receptor activation causes a rapid redistribution of AMPA receptors. Neuropharmacology *41*, 664–671.

Xu, J., Zhu, Y., Contractor, A., and Heinemann, S.F. (2009). mGluR5 has a critical role in inhibitory learning. Journal of Neuroscience *29*, 3676–3684.

Yamada, K.M., Spooner, B.S., and Wessells, N.K. (1971). J Cell Biol *49*, 614.

Yamazaki, M., Matsuo, R., Fukazawa, Y., Ozawa, F., and Inokuchi, K. (2001). Regulated expression of an actin-associated protein, synaptopodin, during long-term potentiation. Journal of Neurochemistry *79*, 192–199.

Yan, Q.J., Asafo-Adjei, P.K., Arnold, H.M., Brown, R.E., and Bauchwitz, R.P. (2004). A phenotypic and molecular characterization of the fmr1-tm1Cgr fragile X mouse. Genes Brain Behav. *3*, 337–359.

Yan, Q.J., Rammal, M., Tranfaglia, M., and Bauchwitz, R.P. (2005). Suppression of two major Fragile X Syndrome mouse model phenotypes by the mGluR5 antagonist MPEP. Neuropharmacology *49*, 1053–1066.

Yang, Y., and Calakos, N. (2013). Presynaptic long-term plasticity. Front Synaptic Neurosci 5, 8.

Yao, C.-K., Lin, Y.Q., Ly, C.V., Ohyama, T., Haueter, C.M., Moiseenkova-Bell, V.Y., Wensel, T.G., and Bellen, H.J. (2009). A synaptic vesicle-associated Ca2+ channel promotes endocytosis and couples exocytosis to endocytosis. Cell 138, 947–960.

Yasuda, H., Barth, A.L., Stellwagen, D., and Malenka, R.C. (2003). A developmental switch in the signaling cascades for LTP induction. Nat Neurosci 6, 15–16.

Yuste, R., and Bonhoeffer, T. (2001). Morphological changes in dendritic spines associated with long-term synaptic plasticity. Annu. Rev. Neurosci. 24, 1071–1089.

Yuste, R., and Denk, W. (1995). Dendritic spines as basic functional units of neuronal integration. Nature 375, 682–684.

Yuste, R., Majewska, A., Cash, S.S., and Denk, W. (1999). Mechanisms of calcium influx into hippocampal spines: heterogeneity among spines, coincidence detection by NMDA receptors, and optical quantal analysis. J Neurosci 19, 1976–1987.

Zakharenko, S.S., Zablow, L., and Siegelbaum, S.A. (2001). Visualization of changes in presynaptic function during long-term synaptic plasticity. Nat Neurosci 4, 711–717.

Zakharenko, S.S., Patterson, S.L., Dragatsis, I., Zeitlin, S.O., Siegelbaum, S.A., Kandel, E.R., and Morozov, A. (2003). Presynaptic BDNF required for a presynaptic but not postsynaptic component of LTP at hippocampal CA1-CA3 synapses. Neuron 39, 975–990.

Zelená, J. (1970). Ribosome-like particles in myelinated axons of the rat. Brain Res. 24, 359–363.

Zhai, R.G., Vardinon-Friedman, H., Cases-Langhoff, C., Becker, B., Gundelfinger, E.D., Ziv, N.E., and Garner, C.C. (2001). Assembling the presynaptic active zone: a characterization of an active one precursor vesicle. Neuron 29, 131.

Zhang, H., Xing, L., Rossoll, W., Wichterle, H., Singer, R.H., and Bassell, G.J. (2006). Multiprotein complexes of the survival of motor neuron protein SMN with Gemins traffic to neuronal processes and growth cones of motor neurons. Journal of Neuroscience 26, 8622–8632.

Zhang, X.-L., Pöschel, B., Faul, C., Upreti, C., Stanton, P.K., and Mundel, P. (2013). Essential role for synaptopodin in dendritic spine plasticity of the developing hippocampus. Journal of Neuroscience 33, 12510–12518.

Zhang, Y.-P., Holbro, N., and Oertner, T.G. (2008). Optical induction of plasticity at single synapses reveals input-specific accumulation of alphaCaMKII. Proc Natl Acad Sci USA *105*, 12039–12044.

Zhou, Q., Homma, K.J., and Poo, M.-M. (2004). Shrinkage of dendritic spines associated with long-term depression of hippocampal synapses. Neuron *44*, 749–757.

Zhu, J.J., Qin, Y., Zhao, M., van Aelst, L., and Malinow, R. (2002). Ras and Rap control AMPA receptor trafficking during synaptic plasticity. Cell *110*, 443–455.

Zhukareva, V., Chernevskaya, N., Pimenta, A., Nowycky, M., and Levitt, P. (1997). Limbic system-associated membrane protein (LAMP) induces neurite outgrowth and intracellular Ca2+ increase in primary fetal neurons. Mol Cell Neurosci *10*, 43–55.

Ziv, N.E., and Garner, C.C. (2004). Cellular and molecular mechanisms of presynaptic assembly. Nat Rev Neurosci *5*, 385–399.

Zoghbi, H.Y., and Bear, M.F. (2012). Synaptic dysfunction in neurodevelopmental disorders associated with autism and intellectual disabilities. Cold Spring Harb Perspect Biol *4*.

Zuber, B., Nikonenko, I., Klauser, P., Muller, D., and Dubochet, J. (2005). The mammalian central nervous synaptic cleft contains a high density of periodically organized complexes. Proc Natl Acad Sci USA *102*, 19192–19197.